

**ADVANCED TOOLS FOR CHARACTERIZING HMA  
FATIGUE RESISTANCE**

A Thesis

by

JAMES JEFFERIES LAWRENCE

Submitted to the Office of Graduate Studies of  
Texas A&M University  
in partial fulfillment of the requirements for the degree of

MASTER OF SCIENCE

December 2009

Major Subject: Civil Engineering

**ADVANCED TOOLS FOR CHARACTERIZING HMA  
FATIGUE RESISTANCE**

A Thesis

by

JAMES JEFFERIES LAWRENCE

Submitted to the Office of Graduate Studies of  
Texas A&M University  
in partial fulfillment of the requirements for the degree of

MASTER OF SCIENCE

Approved by:

Chair of Committee,	Amy Epps Martin
Committee Members,	Robert L. Lytton
	Charles J. Glover
Head of Department,	John Niedzwecki

December 2009

Major Subject: Civil Engineering

## ABSTRACT

Advanced Tools for Characterizing HMA Fatigue Resistance.

(December 2009)

James Jefferies Lawrence, B.S., Utah State University

Chair of Advisory Committee: Dr. Amy Epps Martin

Accurately and efficiently characterizing the material properties of hot mix asphalt (HMA) is critical to the design and development of pavements that can experience repeated loading for long periods of time and resist fatigue cracking. The Calibrated Mechanistic with Surface Energy (CMSE) method of design to preclude this primary type of distress requires that the HMA material be tested using the Relaxation Modulus (RM) and Repeated Direct Tension (RDT) tests to determine the material properties required for accurate calculations.

The RM test requires considerable time to complete and provides results with relatively high variability. Further research has led to the development of the Viscoelastic Characterization (VEC) test, from which the RM master curve can be developed. Material properties from the RM master curve can be easily determined and applied in the CMSE method.

The modified repeated direct tension (RDT\*) test removes rest periods and unwanted healing from the RDT test. The RDT\* test also allows the dissipated pseudo strain energy (DPSE) to be separated into permanent deformation and fatigue cracking

energies. The rate of change in DPSE associated with fatigue can then be applied in the CMSE method.

Data sets for these tests are extensive and time consuming to analyze. Microsoft Excel spreadsheet macros were developed to reduce the time required for analysis from an estimated 10 hours to approximately 8 minutes.

Testing of 14 different samples showed that the VEC and RDT\* tests still required some adjustments in order to get accurate results. The rate of loading in the VEC test must be reduced to allow sufficient testing time to obtain the required data. The RDT\* test requires a decrease in the controlling strain levels from 80  $\mu\epsilon$  and 350  $\mu\epsilon$  to 20  $\mu\epsilon$  and 175  $\mu\epsilon$  for the undamaged and damaged portions of the test, respectively.

Testing of a sample using the new VEC and RDT\* test recommendations showed that the recommended changes provided better results. Samples were undamaged where required and damaged portions of the test ran to completion without causing compression or sample failure. Material properties can be accurately determined and applied in the CMSE method.

## **DEDICATION**

This thesis is first dedicated to my wife, Melinda and our children, Isaac James, David Everett, and Joshua Michael who were willing to follow their husband and father on a wild adventure to pursue his dreams. Second to my son, Michael Oran and mother, Sharol Lawrence both of whose untimely passing helped me to see that life is short and is best spent with family, friends, and searching for the things in life that makes one truly happy.

## ACKNOWLEDGEMENTS

I would like to thank my committee chair, Dr. Epps Martin, for her patience with a student who had to relearn how to be a student. Her guidance, direction, and council helped me to gain confidence in my ability to complete this task. She never gave up on me and helped me to find the funding necessary to finish this project. She is a true friend.

I would also like to thank my committee members, Dr. Lytton, who helped me to tie what I have learned in the workforce with what I have learned in the classroom, and Dr. Glover, who has taught me to look deeper and find the true source of a problem along with the solution.

I would like to thank Jeff Perry and David Zeig for all of their help with preparing the samples and running the required tests. Their dedication to accuracy made a significant impact.

Thanks to Nick Sweet, Brandon Jamison, Justin Clark, Jason Snider, and Joel Miller for their untiring and dedicated work on aggregate collection, sieving, and sample fabrication. I would also like to thank them for their help with laboratory testing.

I also appreciate Rong Luo and Xue Luo who spent a great deal of time developing the VEC and RDT\* tests. They spent a lot of time getting me up to speed and helping me out whenever I got stuck and made significant contributions to the development of the analysis spreadsheets.

I would like to acknowledge the faculty and staff in both Civil Engineering and TTI. Without them, there are several things I would not have finished, nor would I have known where to start.

Thank you to Dr. Spencer Guthrie and Dr. Dan Zollinger who encouraged me to come to Texas A&M in the first place. Their guidance and kindness has meant a great deal to me.

I am especially grateful to my little family: Melinda, Isaac, David and Josh. It has been a hard move, but they have taken it well and have stuck by me, even when their dad came home frustrated and overwhelmed. They have made this burden light.

In addition to my family, I have to mention my mother and father. They allowed me to do what was best for me and my family, even though it was a difficult time for them and for me. Though my mother faced an overwhelming struggle with a cancer that would ultimately take her life, she never discouraged me from coming here and never asked me to stay home.

Finally, I would like to thank my Heavenly Father, who asked me to build a ship, showed me how to build it, and gave me strength to continue even when others thought it couldn't be done.

## TABLE OF CONTENTS

	Page
ABSTRACT .....	iii
DEDICATION .....	v
ACKNOWLEDGEMENTS .....	vi
TABLE OF CONTENTS .....	viii
LIST OF FIGURES.....	x
LIST OF TABLES .....	xii
INTRODUCTION.....	1
CMSE FATIGUE ANALYSIS .....	3
Fatigue Testing Methods.....	3
CMSE Fatigue Analysis Equations .....	4
CMSE Required Fatigue Tests .....	19
CMSE Summary .....	27
RECENT FATIGUE TESTING DEVELOPMENTS.....	29
Viscoelastic Characterization Test (VEC) .....	29
Modified Repeated Direct Tension Test (RDT*).....	42
REVISED CMSE (CMSE*).....	66
Application of VEC Test Results .....	66
Application of RDT* Test Results .....	66
Calculation of Crack Density .....	67
CMSE* Summary .....	69



	Page
TEST ANALYSIS MACRO DEVELOPMENT .....	71
VEC Analysis Macro .....	71
RDT* Analysis Macro .....	84
ANALYSIS OF VEC AND RDT* TESTING METHODS .....	94
Material Selection and Preparation .....	94
VEC Test Analysis .....	100
RDT* Test Analysis .....	110
Test Method Analysis Summary .....	120
IMPLEMENTATION OF TEST RECOMMENDATIONS .....	122
Material Selection and Preparation .....	122
Implementation of VEC Test Recommendations.....	125
Implementation of RDT* Test Recommendations.....	128
Implementation of Recommendations Summary .....	131
CONCLUSION .....	133
VEC Test.....	133
RDT* Test.....	135
Future Research.....	137
REFERENCES.....	138
APPENDIX A .....	142
VITA .....	162

## LIST OF FIGURES

FIGURE		Page
1	Common Fatigue Testing Methods.....	4
2	CMSE Material Characterization Tests. Adapted from Walibita (7).....	6
3	CMSE Method of Fatigue Analysis.....	28
4	CMSE* Adjusted Material Characterization Tests.....	30
5	VEC and RDT* Test Setup.....	31
6	Strain Response and Stress Input from the RDT* Test. Adapted from Luo et al. (20).....	46
7	DPSE Integration Bands. Adapted from Luo et al. (20).....	50
8	CMSE* Method of Fatigue Analysis.....	70
9	Calculated Variables from Raw Data of VEC Master Spreadsheet.....	76
10	RM Master Curve Worksheet from VEC Master Spreadsheet.....	78
11	RM Master Curve.....	79
12	Phase Angle Master Curve Worksheet from VEC Master Spreadsheet.....	81
13	VEC Analysis Macro – Part One.....	82
14	VEC Analysis Macro – Part Two.....	83
15	RDT* Analysis Macro.....	92
16	Super Gyrotory Compactor (SGC).....	99
17	Typical Applied Stresses During VEC Test.....	101
18	50°F (10°C) Average Strain Response from VEC Test.....	102

FIGURE	Page
19	VEC Test Indicating LVDT Noise..... 104
20	VEC Test Exceeding 100 $\mu\epsilon$ .....105
21	VEC Test Insufficient Sample Tightening..... 106
22	VEC Test Average Microstrains Recorded for Same Sample at Three Different Testing Temperatures..... 108
23	Typical RDT* Test Applied Stress and Resulting Strain..... 111
24	Drifting LVDT's in RDT* Test.....112
25	RDT* Test 80 $\mu\epsilon$ to 350 $\mu\epsilon$ Transition..... 113
26	RDT* Test Noisy LVDT and Effects on Average.....114
27	RDT* Test Soft Side LVDT Placement and Results.....116
28	RDT* Test Sample Damage During 80 $\mu\epsilon$ Cycles..... 117
29	VEC Test Results with Implemented Recommendations..... 126
30	Applied Stress from VEC Test with Implemented Recommendations..... 127
31	RM Master Curve from VEC Test with Implemented Recommendations..... 128
32	20 $\mu\epsilon$ Response from RDT* Test with Implemented Recommendations..... 129
33	175 $\mu\epsilon$ Response from RDT* Test with Implemented Recommendations..... 131

## LIST OF TABLES

TABLE		Page
1	Design Shear Strain, $\gamma$ . Adapted from Walibita (7).....	13
2	Pavement Section Characteristics used by Walibita (7).....	13
3	Fatigue Calibration Constants (13).....	18
4	VEC Test Data.....	32
5	RDT* Test Data.....	44
6	DPSE Integration Bands. Adapted from Luo et al. (20).....	51
7	RDT* Data Import Correlations.....	88
8	TxDOT Type C Master Gradation Bands (% Passing by Weight or Volume) (21).....	95
9	LRD Mix Aggregate Gradation Blend.....	96
10	LRD Mix Adjusted Aggregate Gradation Based on Wet-Sieve Analysis...97	
11	Binder Content, $G_{mm}$ , and Air Voids for LRD Mix Samples.....	98
12	$E_l$ and $m$ Values from VEC Test.....	103
13	Two Sided t-Test Results for 80 $\mu\epsilon$ RDT* Test.....	118
14	VEC and RDT* Test Issues and Recommendations.....	121
15	TxDOT Type D Master Gradation Bands (% Passing by Weight or Volume) (21).....	122
16	CHS Mix Aggregate Gradation Blend.....	123
17	CHS Mix Adjusted Aggregate Gradation Based on Wet-Sieve Analysis. 124	
18	Two Sided t-Test Results for the 20 $\mu\epsilon$ RDT* Test.....	130

## INTRODUCTION

Hot mix asphalt concrete (HMA) is a complex material with complex properties. The US Department of Transportation has reported that as of 2007 there are 2,635,471 miles of paved roads in the United States. Approximately 98% of these roads have a flexible pavement surface (1). With over \$10 billion spent each year on restoration and rehabilitation of our roads (2), it is vital that new and more effective methods of testing and designing HMA pavements be developed. Researchers are continuously trying to revisit and refine testing methods and procedures in order to get a correct representation of how HMA behaves under different conditions. Fatigue resistance is one of several characteristics used to describe the performance of HMA. Fatigue resistance is a measure of the ability to resist cracking under repeated loading. Tests have been developed for this material characteristic in order to determine how HMA will behave in both the field and laboratory. As testing methods have advanced, so have the prediction models. A greater effort is being made to provide a more mechanistic approach to design where in the past an empirical approach was used. The advancements made in testing have attempted to improve on the strengths and weaknesses associated with their predecessors. New methods continue to be developed in order to provide better and more realistic results which are representative of what is occurring under field conditions.

---

This thesis follows the style of *Transportation Research Record*.

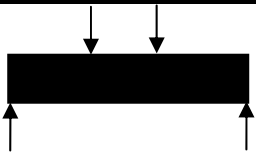
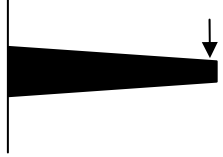
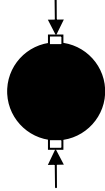
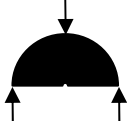
This study will discuss the investigation of new methods of evaluating the fatigue resistance of HMA. A review of fatigue testing methods will be discussed. More particular attention will be given to the testing and evaluation associated with the Calibrated Mechanistic Surface Energy (CMSE) and Revised CMSE (CMSE\*) methods. Data analysis procedures for fatigue tests associated with these methods will be included and discussed. Microsoft Excel macro's developed for the analysis of the data obtained from the CMSE\* test methods will also be included. An evaluation of CMSE\* testing methods will be conducted in order to determine the quality and sensitivity of the tests on laboratory mixed and laboratory compacted (LMLC) samples. Recommendations for improvements will be made. Finally, a summary of the results will be made as well as a discussion regarding the need for further research.

## **CMSE FATIGUE ANALYSIS**

The CMSE fatigue analysis method requires several material properties in order to provide an accurate evaluation. Several fatigue testing methods have been developed in order to determine these properties. These tests have developed over time into direct tension testing methods. Some of these tests will be summarized. The CMSE fatigue analysis equations will also be reviewed and outlined.

### **FATIGUE TESTING METHODS**

Several fatigue tests have been developed in order to determine the material properties necessary for the evaluation of the fatigue resistance of HMA. These tests can generally be categorized as simple flexure, indirect tension or direct tension tests (3). Each type of test has strengths and weaknesses. Over time, these tests have evolved and developed into improved and more reliable methods. FIGURE 1 provides a summary of some of the more familiar fatigue tests that are regularly used as well as some comments regarding drawbacks associated with each.

Test Name	Loading Diagram	Loading Type	Comments
Flexural Bending Beam Test		Flexure Test	<ul style="list-style-type: none"> <li>• Considerable time required for testing (3).</li> <li>• Variability in results (3).</li> </ul>
Cantilevered Beam Test		Flexure Test	<ul style="list-style-type: none"> <li>• Considerable time required for testing (3).</li> <li>• Variability in results (3).</li> <li>• Difficult sample preparation (3).</li> </ul>
Diametral Test		Indirect Tension Test	<ul style="list-style-type: none"> <li>• Simple to conduct (4).</li> <li>• Healing not accounted for (5).</li> <li>• Samples experience permanent deformation during testing (6, 4).</li> </ul>
Semi-Circular Bending Test		Indirect Tension and Flexure Test	<ul style="list-style-type: none"> <li>• Simple to conduct (4).</li> <li>• Healing not accounted for.</li> </ul>

**FIGURE 1.** Common Fatigue Testing Methods.

Data from these tests is then analyzed and adjusted to determine the fatigue life of field pavements. Using test methods that more closely mimic the response of the pavement in the field allow for more accurate results that are repeatable for several types of pavements under several different conditions.

### **CMSE FATIGUE ANALYSIS EQUATIONS**


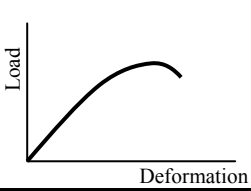

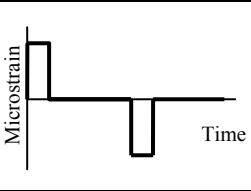

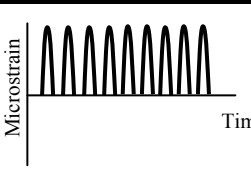
A testing and evaluation method has been developed that makes use of direct tension testing methods in order to determine critical material properties of HMA. This method of fatigue analysis was developed at Texas A&M and is known as the Calibrated Mechanistic with Surface Energy (CMSE) method (7). A study performed by Lubinda



Walibita (7) compared the CMSE method with the Mechanistic Empirical (ME) method, the Mechanistic-Empirical Pavement Design Guide (MEPDG) method, and the Calibrated Mechanistic (CM) method. The ME method uses flexural bending beam test for fatigue analysis while the MEPDG uses the Dynamic Shear Rheometer (DSR) test and the Dynamic Modulus (DM) test (which is a compression test). The CM method uses the same testing as the CMSE without determining and including surface energy. Walubita's (7) study indicated that while the CMSE analysis method was more time consuming than the others, testing was relatively simple to perform and the results provided much less variability than the others. The required tests include the tensile strength (TS), relaxation modulus (RM) test, and the repeated direct tension (RDT) tests which are summarized in FIGURE 2 and which will be briefly described in subsequent sections.

### **Calculation of Number of Loads to Failure**

In order to define the fatigue equation for the CMSE method, it is first necessary to understand that HMA has not only fracture properties, but also healing properties.

Test Name	Loading Diagram	Loading Configuration
Tensile Strength Test		
Relaxation Modulus Test		
Repeated Direct Tension Test		

**FIGURE 2.** CMSE Material Characterization Tests. Adapted from Walibita (7).

Healing is defined as the closure of the fracture surfaces and is related to the surface energy of the material. As fracture occurs, energy is stored on the fracture surface. In the healing process, some of this energy is released. The dissipated energy associated with the coalescence of microcracks and propagation of macrocracks is called dissipated pseudo strain energy (DPSE) and is a representation of the damage experienced in a viscoelastic material (7). The CMSE fatigue equation calculates the number of loads to failure ( $N_f$ ) by including both crack initiation ( $N_i$ ) and crack propagation ( $N_p$ ) as is shown in Equation 1 (7). All of the following CMSE equations require that the input variables be in metric units.

$$N_f = 2 * (SF_{ag})(SF_h)(N_i + N_p) \quad (1)$$

The factor of 2 accounts for the anisotropy of the material, and  $SF_{ag}$  and  $SF_h$  are shift factors associated with aging and healing respectively.

### Calculation of Number of Loads to Crack Initiation

Paris' Law fracture coefficients,  $n$  and  $A$ , in combination with the rate of accumulation of DPSE,  $b$ , are used to calculate the number of loads necessary for crack initiation as shown in Equation 2 through Equation 7 (7).

$$N_i = \left( \frac{C_{\max}^{(1+2n)}}{A} \right) \left( \left[ \frac{4\pi A_c}{b} \right]^n \right) (C_D)^n \quad (2)$$

$$n = \frac{1}{m_t} \quad (3)$$

$$A = \frac{k}{\sigma_t^2 I_i} \left( \left[ \frac{D_1^{(1-m_t)} E_t}{\Delta G_f} \right]^{\left( \frac{1}{m_t} \left[ \frac{1}{(n_{BD}+1)} \right] \right)} \int_0^{\Delta t} w^n(t) dt \right) \quad (4)$$

$$I_i = \frac{2}{(1 + n_{BD})} \quad (5)$$

$$D_1 = \left( \frac{1}{E_t} \right) \left( \frac{\text{Sin}[m_t \pi]}{m_t \pi} \right) \quad (6)$$

$$\int_0^{\Delta t} w^n(t) dt = \int_0^{\Delta t} \left( \text{Sin}^{2n} \left[ \frac{\pi}{\Delta t} \right] \right) dt = 0.5042 - 0.1744 \ln(n) \quad (7)$$

where:

$C_{max}$  = Maximum microcrack length (mm)

$A, n$  = Paris' Law fracture coefficients

$A_c$  = Cross-sectional area of the sample (m<sup>2</sup>)

$b$  = Rate of accumulation of DPSE

$C_D$  = Crack density (cracks/mm<sup>2</sup>)

$m$  = slope of the log relaxation modulus versus log time

$k$  = Material coefficient (~0.33) (7)

$\sigma_t$  = Maximum HMA tensile strength (kPa)

$I_i$  = Dimensionless stress integral factor in crack failure zone (1-2)

$D_1$  = Creep compliance at 1.0 s (MPa<sup>-1</sup>)

$E_t$  = Elastic modulus from relaxation modulus master-curve (MPa)

$\Delta G_f$  = Fracture or dewetting surface energy (ergs/cm<sup>2</sup>)

$n_{BD}$  = Brittle-ductile factor material coefficient (0-1)

$t$  = Time (s)

$\int_0^{\Delta t} w^n(t) dt$  = Load pulse shape factor (0-1)

Material testing is used to determine  $b$ ,  $m$ ,  $E_t$ , and  $\sigma_t$  which will be discussed later.

$\Delta G_f$  is also determined through material testing using the Wilhelmy Plate (WP) test but

will not be discussed as part of this study. Further information with respect to this testing can be found in the work performed by Walubita (7).

The variable  $n$  is simply the inverse of the stress relaxation rate,  $m$ , which is considered a reasonable correlation when  $m$  is obtained from a strain controlled repeated direct tension test (8, 9, 10, 11).

The value used for crack density,  $C_D$ , was obtained from a study performed by Marek and Herrin (12). They found that by using an average microcrack length of 0.015 inches (0.381 mm), the calculated average number of microcracks per unit cross sectional area for most HMA pavements was approximately 1495 cracks/inch<sup>2</sup> (2.317 cracks/mm<sup>2</sup>).

$C_{max}$  represents the maximum microcrack length that the HMA can experience before macrocracks are initiated and begin propagation. Walubita's study used a value of 0.3 inches (7.5 mm) which originated from work performed by Lytton et al. (13).

The material coefficient,  $k$ , relates the fracture process zone to strain energy and tensile strength. Walubita (7) indicated that this value can be measured; however it doesn't vary significantly with respect to microcrack length, therefore, a value of 0.33 was used based on work performed by Lytton et al. (13).

The brittle-ductile factor,  $n_{BD}$ , is an age related adjustment factor that accounts for the brittleness of the HMA in terms of stress-strain relationships. A perfectly plastic material would be represented with an  $n_{BD}$  value of 0.0 while a brittle material would have an  $n_{BD}$  value of 1.0. As HMA ages it becomes more brittle. Walubita (7) used an  $n_{BD}$  value of 0.0 for the unaged materials with values of 0.5 and 0.75 for 3 month and 6

month laboratory aged samples, respectively. Laboratory aging took place at 140°F (60°C).

The integration of  $w_n(t)$  with respect to time provides a description of the shape of the input load pulse. The RDT test uses a Haversine shaped input load form which integrates into the simple logarithmic function shown in Equation 7 and is only affected by Paris' Law fracture coefficient,  $n$ .

As a result of replacing many of the variables with the assumed constant values as described above, the equation was simplified and reduced to the form shown in Equations 8 and 9, which only require  $A$ ,  $n$ ,  $b$ ,  $m$ ,  $\Delta G_f$ ,  $E_t$  at  $t = 1.0$  s ( $E_1$ ), and  $\sigma_t$ .  $A_c$  in Equation 2 is eliminated in Equation 9 by using a radius of approximately 2 inches (51 mm) to calculate the cross-sectional area of the sample.

$$N_i = 1 \times 10^{-5} \left( \frac{0.0075^{(1+2n)}}{A} \right) \left( [2.366 \times 10^5 b^{-1}]^n \right) \quad (8)$$

$$A = 0.165 \sigma_t^{-2} [0.5042 - (0.1744 \text{Ln}(n))] \left[ \frac{E_1^m}{\Delta G_f} \left( \frac{\text{Sin}(m_t \pi)}{m_t \pi} \right)^{(1-m_t)} \right] \quad (9)$$

### Calculation of Number of Loads to Crack Propagation

Crack propagation is also calculated using Paris' Law fracture coefficients as shown in Equations 10 through 12.

$$N_p = \left( \frac{d^{\left(1-\frac{n}{2}\right)}}{[A(2r)^n (SG)^n (1-nq)]} \right) \left( 1 - \left[ \frac{C_{\max}}{d} \right]^{(1-nq)} \right) \left( \frac{1}{\gamma} \right)^n \quad (10)$$

$$S = \frac{(1-\nu)}{(1-2\nu)} \quad (11)$$

$$G = \frac{E_t}{2(1+\nu)} \quad (12)$$

where:

- $A, n$  = Paris' Law fracture coefficients
- $r, q$  = Regression constants for stress intensity factor (~4.40, 1.18)
- $S$  = Shear coefficient
- $G$  = Shear modulus, (MPa)
- $d$  = HMA layer thickness, (mm)
- $C_{\max}$  = Maximum microcrack length (mm)
- $\gamma$  = Maximum design shear strain at the edge of a loaded tire (mm/mm)  
(Calculated from  $G, S$ , and the tire pressure)
- $\nu$  = Poisson's ration
- $E_t$  = Elastic modulus from relaxation modulus master-curve (MPa)

The calculation of crack propagation includes the HMA thickness,  $d$ , because fatigue cracks must extend or propagate through the HMA layer to the surface for failure to occur.

The regression constants  $r$  and  $q$  are a function of the stress intensity distribution near the microcrack tip. Walubita (7) used values of 4.40 and 1.18 for  $r$  and  $q$  respectively, which were based on finite element method analysis work done by Lytton et al (13).

The maximum design shear strain,  $\gamma$ , is a failure load response parameter which can be simply calculated using tire pressure,  $\sigma_p$ , the shear modulus,  $G$ , and the shear coefficient,  $S$  as in Equation 13. This calculated value is a close approximation if the material is assumed linear elastic. However,  $\gamma$  can also be calculated using a layered linear-elastic or visco-elastic model. Walubita (7) opted to calculate these values using FEM and ELSYMS5 software analysis for five pavement sections located in both wet-warm and dry-cold environments (13). The design shear strains are listed in TABLE 1 with the corresponding pavement sections shown in TABLE 2.

$$\gamma = \frac{\sigma_p}{G \times S} \quad (13)$$



**TABLE 1.** Design Shear Strain,  $\gamma$ . Adapted from Walibita (7).

<b>Pavement Section</b>	<b>Wet-Warm Environment</b>	<b>Dry-Cold Environment</b>
1	1.56E-02	1.51E-02
2	1.98E-02	1.89E-02
3	1.91E-02	1.86E-02
4	2.06E-02	1.96E-02
5	1.14E-02	1.46E-02

**TABLE 2.** Pavement Section Characteristics used by Walibita (7).

<b>Pavement Section No.</b>	<b>HMA</b>	<b>Base</b>	<b>Subbase</b>	<b>Subgrade</b>	<b>ESAL's</b>	<b>Percent Trucks</b>
1	150 mm 3447 MPa $\nu = 0.33$	350 mm 414 MPa $\nu = 0.40$	N/A	63 MPa $\nu = 0.45$	5.00E+06	25%
2	50 mm 3447 MPa $\nu = 0.33$	250 mm 414 MPa $\nu = 0.40$	150 mm 241 MPa $\nu = 0.35$	85 MPa $\nu = 0.45$	1.40E+06	24%
3	50 mm 3447 MPa $\nu = 0.33$	150 mm 345 MPa $\nu = 0.40$	127 mm 207 MPa $\nu = 0.40$	69 MPa $\nu = 0.45$	4.00E+05	11%
4	50 mm 3447 MPa $\nu = 0.33$	175 mm 3447 MPa $\nu = 0.35$	200 mm 165 MPa $\nu = 0.40$	66 MPa $\nu = 0.45$	7.20E+06	13%
5	100 mm 3447 MPa $\nu = 0.33$	350 mm 1034 MPa $\nu = 0.35$	N/A	103 MPa $\nu = 0.45$	1.08E+07	15%

Poisson's ratio,  $\nu$ , was assumed to be 0.33 for all HMA pavement layers. The  $S$  and  $G$  values are calculated using  $\nu$  and  $E_t$ .  $E_t$  and  $C_{max}$  are the same as used in the crack initiation equations (Equations 2 through 7).

As with the crack initiation equation (Equation 2), the crack propagation equation (Equation 10) was reduced by inserting assumed and calculated values into the Equations 10 through 13 (7). The result is shown in Equation 14.

$$N_p = 1 \times 10^3 \gamma^{-n} \left( \frac{d^{\left(\frac{1-n}{2}\right)}}{\left[ (1-1.18n) A \left( \frac{4.397 E_1 (1-\nu)}{(1+\nu)(1-2\nu)} \right)^n \right]} \right) \left( 1 - [0.0075 d^{-1}]^{(1-1.18n)} \right) \quad (14)$$

### Calculation of Shift Factors

Because of the effects of anisotropy, aging, and healing within a HMA under field conditions, it is also necessary to calculate and include shift factors in the original fatigue equation. The shift factor due to anisotropy ( $SF_a$ ) was assumed to be 2. This is due to the fact that, generally speaking, the elastic modulus in the vertical direction ( $E_z$ ) is greater than the horizontal elastic modulus ( $E_x$ ) by approximately 1.5 times. Equation 15 shows the relationship between  $E_z$  and  $E_x$  used for the CMSE method (7).

$$SF_a = \left( \frac{E_z}{E_x} \right)^{1.75} \quad (15)$$

With the above defined relationship between  $E_z$  and  $E_x$ , it can be seen that  $SF_a$  is approximately 2.

With varying traffic loadings and changes in temperature, HMA will experience periods of healing. Healing, or the closing of fractures within the HMA, improves the fatigue performance of the pavement. The CMSE method accounts for healing by including a healing shift factor ( $SF_h$ ) which is calculated using traffic rest periods and variations between laboratory and field temperatures (7). Equations 16 through 22 are the equations used to calculate the  $SF_h$  value.

$$SF_h = 1 + g_5 \left( \frac{\Delta t_r}{a_{TSF}} \right)^{g_6} \quad (16)$$

$$\Delta t_r = \frac{31.536 \times 10^6 P_{DL}}{80kN \text{ Traffic ESALs}} \quad (17)$$

$$g_5 = a(h_0)^{g_6} \quad (18)$$

$$h_0 = h_2 + \left( \frac{h_1 - h_2}{1 + \left[ \left( \frac{h_1 - h_2}{h_\beta} \right) \left( \frac{\Delta t C_{sr}}{a_{TSF}} \right) \right]} \right) \quad (19)$$

$$h_1 = \left( \frac{C_1}{[\Delta G_h^{LW} E_c] \left( \frac{1}{m_c} \right)} \right) \quad (20)$$

$$h_2 = \left( \left[ C_2 \left( \frac{\Delta G_h^{AB}}{E_c} \right) \right] \left( \frac{1}{m_c} \right) + C_3 \right) \quad (21)$$

$$h_\beta = C_4 \left( \frac{\Delta G_h^{AB}}{\Delta G_h^{LW}} \right) \left( \frac{C_5}{m_c} \right) \quad (22)$$

where:

$SF_h$	=	Shift factor due to healing (ranging from 1 to 10)
$\Delta t_r$	=	Rest period between major traffic loads under field conditions(s)
$\Delta t$	=	Loading time (s)
$a_{TSF}$	=	Temperature shift factor for field conditions (~1.0)
$C_{sr}$	=	Square rest period factor (~1.0)
$a, g_5, g_6$	=	Fatigue field calibration constants
$h_0, h_1, h_2, h_\beta$	=	Healing indices
$P_{DL}$	=	Pavement design life in years
$ESALs$	=	Equivalent single axle loads for the pavement design period
$C_1$ through $C_5$	=	Healing constants
$E_c$	=	Elastic relaxation modulus from compression relaxation modulus (RM) master-curve
$m_c$	=	Slope of the compression RM master-curve

$$\Delta G_h^i = \text{Surface energy due to healing or dewetting (ergs/cm}^2\text{)}$$

The equation for  $\Delta t_r$  includes both the pavement design life ( $P_{DL}$ ) and the traffic loading (ESALs). The factor of  $31.536 \times 10^6$  equals the number of seconds in one 365 day calendar year.

The temperature shift factor,  $a_{TSF}$ , accounts for differences between lab and field temperature conditions. This value can vary, however Walubita (7) used a value of 1.0 in order to simplify the calculations.

The square rest period factor,  $C_{sr}$ , accounts for the shape of the rest period in the strain wave used for the RDT test. Because the rest period used in Walubita's study was square shaped, a value of 1.0 was used (7).

The field calibration constants and healing indices are dependent upon material properties and climate conditions. While each of these values can be calculated, reasonable values of  $g_5$  and  $g_6$  were found in a study performed by Lytton et al. (13). These fatigue calibration constants as shown in TABLE 3 were determined from extensive research based on back calculation of asphalt moduli from falling weight deflectometer tests and do not vary significantly. Repetitive calculation of these values was avoided by using the values determined by Lytton et al. (13) to reduce calculations to Equations 16 and 17.

**TABLE 3.** Fatigue Calibration Constants (13).

Coefficient	Climatic Zone			
	Wet-Cold	Wet-Warm	Dry-Cold	Dry-Warm
$g_5$	0.037	0.097	0.056	0.051
$g_6$	0.261	0.843	0.642	0.466

The shift factor due to aging ( $SF_{ag}$ ) is a function of the data found from the binder dynamic shear rheometer (DSR) master-curve as shown in Equations 23 through 25.

$$SF_{ag} = u \left( \left( \frac{m' @ t_i}{m' @ t_0} \right) \left( \frac{DSR_{f(1)} @ t_0}{DSR_{f(1)} @ t_i} \right) \right)^w \quad (23)$$

$$DSR_f = \left[ \frac{G'}{\eta' / G'} \right] \quad (24)$$

$$DSR_f(\omega) = DSR_{f(1)}(\omega)^{m'} \quad (25)$$

where:

$SF_{ag}$  = Shift factor due to binder oxidative aging

$u, w$  = Material regression constants

$m'$  = Slope of the binder  $DSR_f(\omega)$  master-curve within a reduced frequency range of 1 E-06 to 1 E+02 rad/s at 68°F (20°C)

$\omega$  = Reduced angular frequency (rad/s)

$G', \eta'$  = Elastic dynamic shear modulus (MPa) and dynamic viscosity (Pa-s)

The value ranges from 0 to 1 with a value of 1 associated with no binder aging, thus having no effect on the total number of loads to failure.

## **CMSE REQUIRED FATIGUE TESTS**

Three different tensile fatigue tests are used to determine several of the material properties used in the CMSE design method. These include the Tensile Strength (TS) test, the Relaxation Modulus (RM) test, and the Repeated Direct Tension (RDT) test.

### **Tensile Strength Test (TS)**

The material properties used in Equations 2 through 25 are determined from laboratory testing. The TS test is used to determine the maximum HMA tensile strength of the sample,  $\sigma_t$ , which is a required value for calculating Paris' Law fracture coefficient,  $A$ . The TS test is also used to obtain the HMA strain at the maximum loading. A percentage of the strain at maximum loading is used to set the controlled strain limits for the Relaxation Modulus and Repeated Direct Tension tests.

The TS test, as described by Walubita (7), is performed by applying a continuously increasing load to a four inch (102 mm) diameter cylindrical HMA sample at a deformation rate of 0.05 inches/min (1.27 mm/min) until the sample fails. It is a relatively quick test, taking only about two minutes to complete. Three vertically applied linear variable displacement transducers (LVDT's) measure the deformation of the HMA sample which is tested and preconditioned at 68°F (20°C). Loading and deformation data is recorded at a rate of once per every 0.1 s. The tensile strength is

then determined by dividing the maximum load by the cross-sectional area as in Equation 26.

$$\sigma_t = \frac{P_{\max}}{\pi r^2} \quad (26)$$

where:

- $\sigma_t$  = Tensile strength, psi (MPa)
- $P_{\max}$  = Maximum tensile load, lbs (N)
- $r$  = Radius of HMA sample, in (mm)

The strain at maximum load is determined by averaging the three vertical LVDT displacement readings and dividing by the LVDT guide spacing as in Equation 27.

$$\varepsilon_t = \frac{(LVDT_1 + LVDT_2 + LVDT_3)}{3 \times L} \quad (27)$$

where:

- $\varepsilon_t$  = Tensile strain at maximum load
- $LVDT_{1-3}$  = Recorded axial displacements, in (mm)
- $L$  = Vertical LVDT guide spacing, in (mm)



While this test is relatively quick and easy to perform, it results in a sample that is damaged to failure and cannot be used for any further tension testing.

### **Relaxation Modulus Test (RM)**

The RM test is used to determine the elastic modulus,  $E_t$ , the tensile relaxation rate,  $m_t$ , and the temperature correction factor  $a_T$ . The RM test is a strain controlled test and is performed by applying a constant strain in tension for a specified period of time followed by a rest period. The rest period allows the sample to relax or recover the elastic deformation it experiences under loading. The test can also be performed in compression in order to determine  $E_c$  and  $m_c$ . However, these values are not required for the final calculations and will not be included in this study. Walubita (7) applied a constant tensile strain of 200 microstrains for a period of 60 seconds followed by a rest period of 600 seconds. A 200 microstrain compressive strain was then applied for another 60 seconds, followed by a 600 second rest period. The 200 microstrain loading was chosen for its ability to provide significant and useful data while not causing significant damage to the sample. This value also approximated 20% of the strain at maximum loading from the TS test. Samples were tested at 50°F (10°C), 68°F (20°C), and 86°F (30°C) with loading and deformation data being collected every 0.5 seconds. As with the TS test, three vertically applied LVDT's measured the deformation of the HMA sample.

The elastic modulus was calculated by dividing the time dependant stress by the strain, as in Equation 28.

$$E(t) = \frac{\sigma(t)}{\varepsilon} = \frac{P(t)}{\pi r^2 \times \varepsilon} \quad (28)$$

where:

- $E(t)$  = Elastic modulus, psi (MPa)  
 $\sigma(t)$  = Time dependant stress, psi (MPa)  
 $\varepsilon$  = Constant strain  
 $P(t)$  = Time dependant load, lbs (N)  
 $r$  = Radius of HMA sample, in (mm)

With  $E(t)$  determined for three temperature levels, the data is then reduced to 68°F (20°C) using time-temperature superposition, to form a time dependant relaxation modulus master curve. From the resulting master curve,  $m$  and  $E_t$  are easily determined. As a result of this analysis,  $a_T$  factors are also determined with  $a_T$  at 68°F (20°C) equal to 1.0.

A recent evaluation of the RM test at Texas A&M (14) found that while this test was a good test and relatively sound, it was difficult to control the deformation in the samples so as to not cause damage. In addition, the test required approximately 25 minutes of testing per sample for each of the required temperatures.

### Repeated Direct Tension Test (RDT)

The RDT test is used in combination with results from the RM test to determine the rate of fracture damage accumulation or the rate of accumulation of dissipated pseudo strain energy,  $b$ . Dissipated pseudo strain energy (DPSE) is used to describe the total accumulated fracture damage in an HMA sample. This is used rather than the actual measured strain energy because it eliminates the time dependant linear viscoelastic effects and nonlinearity of the material (15). The RDT test, as conducted by Walubita (7), is a strain controlled test. The same cylindrical samples used for the RM test are subjected to a haversine shaped load pulse with amplitude of 350 microstrains. The haversine shaped load pulse mimics the loading that occurs in the field under commercial vehicles on interstate highways. The test is performed for 1000 cycles at a frequency of 1 Hz. The actual loading time is set at 0.1 seconds with a 0.9 second rest period. The 0.9 second rest period allows for the relaxation of the material and includes some healing between loads. The test is run at a temperature of  $86 \pm 0.5^\circ\text{F}$  ( $30 \pm 0.5^\circ\text{C}$ ). As with the TS and RM tests, deformation data is collected through three, equally spaced, vertical LVDT's which are glued to the sample. Time, load, and deformation data is collected every 0.005 seconds. The total test time takes 20 minutes to complete.

Dissipated pseudo strain energy (DPSE) and  $b$  are calculated using  $E_t$  and  $m_t$  from the RM test in combination with the results from the RDT test. Because Walubita (7) performed the RDT test at  $86^\circ\text{F}$  ( $30^\circ\text{C}$ ), the data first has to be normalized to  $68^\circ\text{F}$  ( $20^\circ\text{C}$ ). Once this is completed, the pseudo strain under damaged conditions can then be calculated as outlined in Equations 29 through 34.

$$DPSE = \sum(\varepsilon_R^d(t) \times \sigma_m^d(t)) \quad (29)$$

$$\varepsilon_R^d(t) = \psi(t) \left[ \frac{\sigma_c^d(t)}{E_R} \right] \quad (30)$$

$$\psi(t) = \frac{\sigma_{c(1)}^u(t)}{\sigma_{m(1)}^u(t)} \quad (31)$$

$$\sigma_c^u(t) \neq \sigma_m^u(t), \sigma_c^d(t) \neq \sigma_m^d(t) \quad (32)$$

$$\sigma_{c(1)}^u(t) = \sigma_{c(1)}^d(t) \neq \sigma_{c(2...N)}^d(t), \sigma_{m(1)}^u(t) = \sigma_{m(1)}^d(t) \neq \sigma_{m(2...N)}^d(t) \quad (33)$$

$$\sigma_c(t) = \int_0^t E(t - \tau) \frac{\partial \varepsilon(\tau)}{\partial \tau} d\tau \quad (34)$$

where:

$DPSE$	=	Dissipated pseudo strain energy, ft-lbs/in <sup>3</sup> (J/m <sup>3</sup> )
$\sigma_{c(1)}^u(t)$	=	Calculated undamaged tensile stress at first RDT load cycle, psi (kPa)
$\sigma_c^d(t)$	=	Calculated damaged tensile stress at any RDT load cycle, psi (kPa)
$\tau$	=	Loading time history (0.0s to 0.1s)
$E(t - \tau)$	=	Undamaged tensile relaxation modulus, psi (kPa)
$\varepsilon(\tau)$	=	Measured strain at previous time, $\tau$ , in/in (mm/mm)
$\varepsilon_R^d(t)$	=	Calculated pseudo strain under damaged conditions, in/in (mm/mm)
$E_R$	=	Reference modulus for undamaged material, psi (kPa)
$\psi(t)$	=	Dimensionless nonlinearity correction factor

$\sigma_{m(1)}^u(t)$  = Measured undamaged tensile stress from first load cycle, psi (kPa)

$\sigma_m^d(t)$  = Measured damaged tensile stress, psi (kPa)

$E_R$  is determined from the data obtained during the first cycle of the RDT test.

During this first cycle it is assumed that the sample is undamaged.

$\psi(t)$  is used to account for the nonlinearity of the undamaged viscoelastic material and is a ratio of the measured and calculated stresses obtained during the first cycle of the RDT test.  $\psi(t)$  causes the DPSE to be zero during the first RDT cycle. This coincides with the assumption that no fatigue damage is done during this cycle.

The integral in Equation 34 is the general relationship for most linear viscoelastic materials. It is compatible with the changing boundary conditions that are seen with damage growth during transient loading (9, 15). This equation can be rewritten in a simple numeric-integration form as shown in Equation 35.

$$\sigma_c(t_{i+1}) = \sum_{k=0}^{i+1} (C_k \Delta\tau [E_\infty + E_1 (t_{i+1} - t_k)^{-m}]) \quad (35)$$

where:

$t_{i+1}, t_k$  = Present and previous time, respectively (s)

$\Delta\tau$  = Time increment (0.005 s)

$C_k$  = Mean slope of a segment of the Haversine input strain waveform

If  $E_\infty$  is assumed to be zero and  $E_t$ ,  $m_t$ , and  $a_T$  from the RM test are used to represent the undamaged conditions, then Equation 35 can be rewritten as:

$$\sigma_c(t_{i+1}) = \Delta\tau E_t \sum_{k=0}^{k=i+1} \left( C_k \left( \frac{(t_{i+1}-t_k)}{a_T} \right)^{-m_t} \right) \quad (36)$$

Once calculated, DPSE is plotted against the log of the number of load cycles,  $N$ . This plot is fitted with the linear logarithmic function shown in Equation 37.

$$W_R = a + b \log(N) \quad (37)$$

where:

$W_R$  = Dissipated pseudo strain energy, ft-lbs/in<sup>3</sup> (J/m<sup>3</sup>)

$a$  = DPSE at the first load cycle

$b$  = Rate of fracture damage accumulation

$N$  = Load cycle

This  $b$  value can then be used in the CMSE equation to determine the loads to crack initiation value,  $N_i$ .

While the RDT test is an effective method of determining the DPSE associated with damage in HMA, it neglects to account for the compressive stress required to bring the sample back to the initial zero strain level. Material properties are different under tension and compression and this should be accounted for. The RDT test also includes a

0.9 second rest period between cycles. This introduces healing into the test which can cause the  $b$  value to be slightly different than the actual material property.

### **CMSE SUMMARY**

The CMSE method is an effective tool for calculating the number of loads to fatigue failure for an HMA pavement. Walubita has shown that it is the best method for limiting variability and developing more accurate results when compared to the ME, CM, and MEPDG methods (7). It makes use of several shift factors that account for anisotropy, healing, and aging. It also includes fracture mechanics to describe the process of crack initiation and crack propagation in an HMA. A flowchart summarizing this method is shown in FIGURE 3.

Testing for the CMSE method is relatively simple. However, it can be time consuming both in testing and data analysis. These testing methods also appear to provide highly variable results, with the RM test causing damage to the samples and the RDT test introducing healing, which is undesirable.

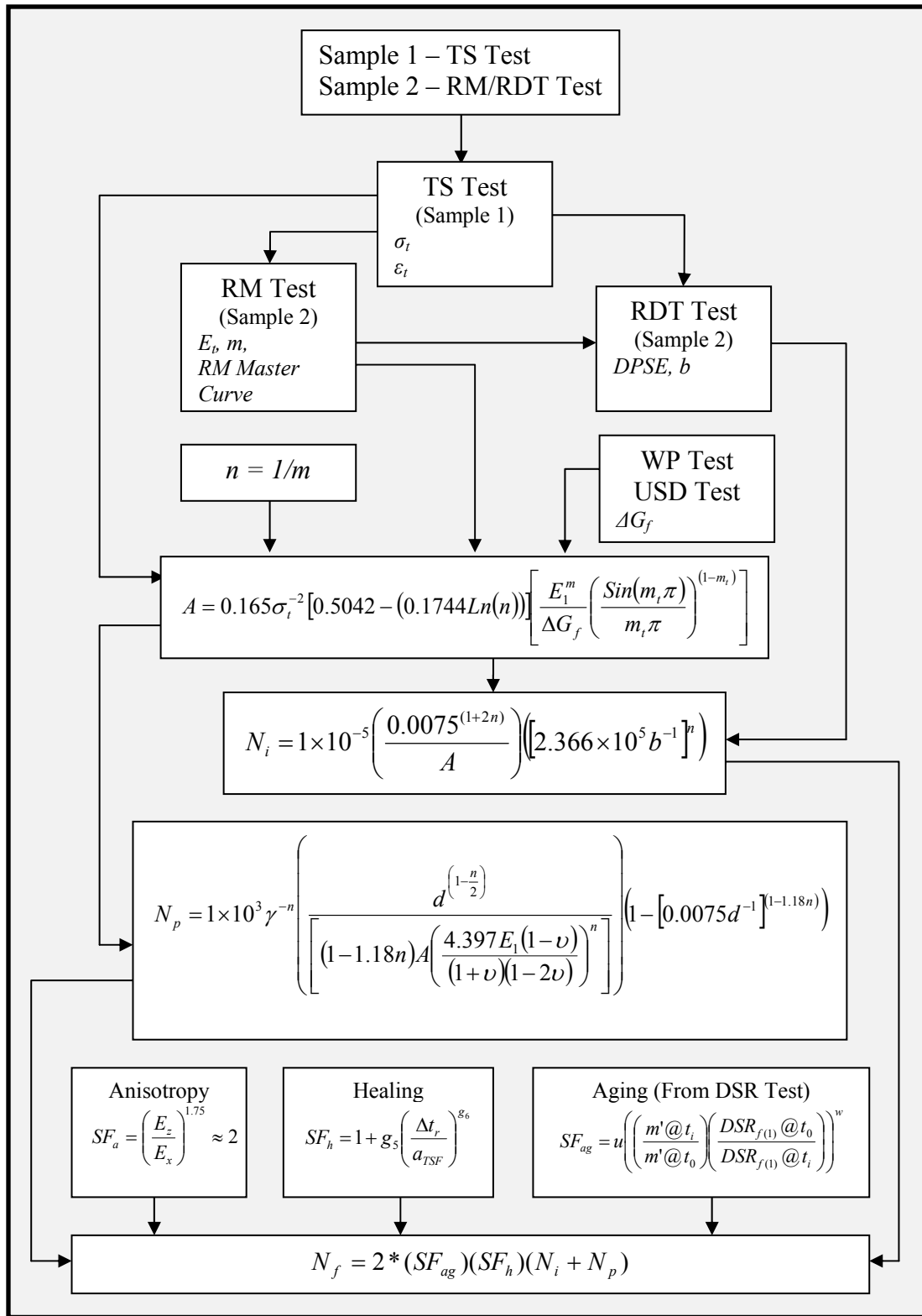


FIGURE 3. CMSE Method of Fatigue Analysis.



## **RECENT FATIGUE TESTING DEVELOPMENTS**


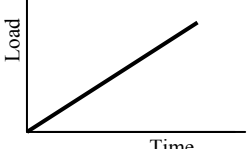

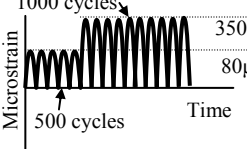
Two new tests have been developed to replace some of the time consuming and highly variable tests used in the CMSE method. These include the Viscoelastic Characterization (VEC) test and the Modified Repeated Direct Tension (RDT\*) test.

### **VISCOELASTIC CHARACTERIZATION TEST (VEC)**

In order to remedy the problems associated with the RM test a new test, called the Viscoelastic Characterization (VEC) test, was developed (14). This new test method models the viscoelastic characteristics of a mix more efficiently while not causing damage to the sample (FIGURE 4). Time dependent stress and strains determined from this test are used to calculate the relaxation modulus and the relaxation rate.

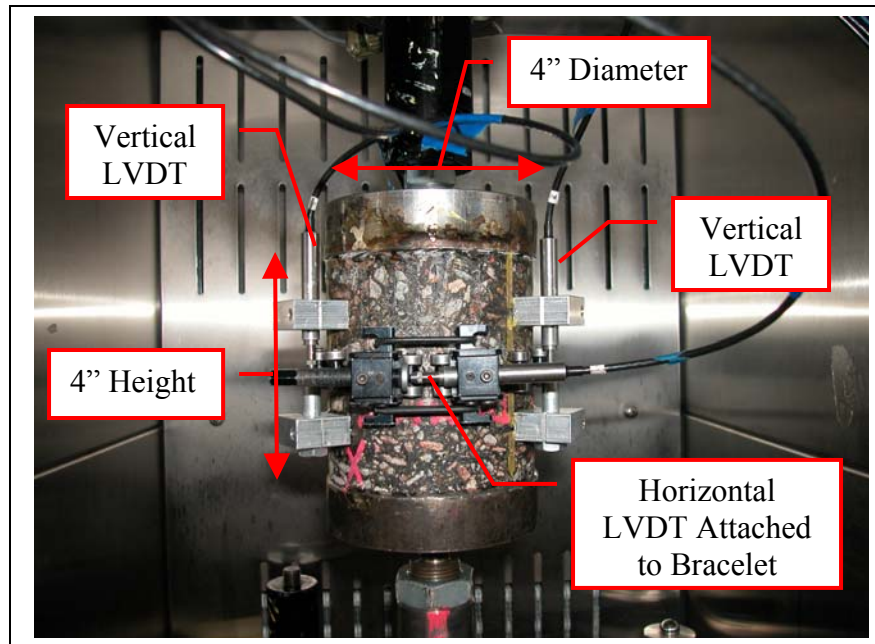
#### **Test Setup and Procedures**

Typical sample size for this test is 4 inches (102 mm) in diameter by 4 inches (102 mm) in height. When using a LMLC sample an initial 6 inch (152 mm) diameter

Test Name	Loading Diagram	Loading Configuration
Viscoelastic Characterization Test		
Modified Repeated Direct Tension Test		

**FIGURE 4.** CMSE\* Adjusted Material Characterization Tests.

by 6 inch (152 mm) height sample is fabricated. This sample is then cored and trimmed to a 4 inch (102 mm) diameter by 4 inch (102 mm) height. This is done to reduce inconsistencies in air void distribution throughout the sample. Bulk specific gravities and air void contents are measured. 4 inch (102 mm) diameter platens are affixed to the sample using a 2 ton (18 kN) epoxy. After allowing sufficient drying time, three LVDT's are attached equidistant and vertically around the sample. The sample is fitted with an LVDT bracelet in order to measure deformations that occur horizontally during the test. The testing setup is shown in FIGURE 5.



**FIGURE 5.** VEC and RDT\* Test Setup.

The test is performed at three different temperatures of 50°F (10°C), 68°F (20°C) and 86°F (30°C). The sample is preconditioned at 50°F (10°C) for approximately 2 hours or until the sample has reached uniform temperature throughout. A monotonically increasing tensile load is applied at a rate of 0.01 inches per minute (0.254 mm/min) and continues until the strain level reaches approximately 100  $\mu\epsilon$ . This value must be carefully and closely monitored due to the rapid nature of the test. The test typically runs for approximately 20 seconds. Throughout the test, load readings from the testing device and displacement readings from the LVDT's are recorded every 0.01 seconds. Once the test is completed for 50°F (10°C), the sample is reconditioned and retested for 68°F (20°C) and 86°F (30°C).

## Test Data

A typical but truncated data set obtained from the VEC test is shown in TABLE

4. For this particular test, units were recorded in English units, but can be recorded in Metric units as well.

**TABLE 4.** VEC Test Data.

Time	Axial Displacement	Axial Force	Axial Ext. Disp.	Input 9	Input 11	Input 10
(sec)	(in)	(lbf)	(in)	(in)	(in)	(in)
39.26	-1.49258	143.30	1.725E-03	2.672E-03	1.146E-03	3.450E-04
39.27	-1.49260	142.88	1.722E-03	2.672E-03	1.172E-03	3.430E-04
39.28	-1.49259	143.51	1.724E-03	2.672E-03	1.153E-03	3.459E-04
39.29	-1.49258	143.27	1.723E-03	2.671E-03	1.149E-03	3.403E-04
39.30	-1.49258	143.23	1.724E-03	2.673E-03	1.179E-03	3.450E-04
39.31	-1.49254	143.43	1.723E-03	2.673E-03	1.148E-03	3.417E-04

The first column indicates the cumulative time of the test and recorded time at each data collection point. The Axial Displacement and Axial Force columns indicate the displacement experienced by the machine and the force applied by the machine to the sample. Axial Ext. Disp., Input 9, Input 11, and Input 10 are the displacements recorded as experienced by the three vertical and one horizontal LVDT's placed on the samples. All recorded data begins with a base value and must be reduced to indicate an actual starting time, load, and displacement of zero. The initial time, load, and displacement values are subtracted from each subsequent reading in order to determine the actual loads and displacements experienced by the sample. With the load and

displacement data reduced, stress and strain values can be calculated using the samples 4 inch (102 mm) diameter to calculate the cross sectional area of the sample and using the 2 inch (51 mm) gauge lengths of the LVDT's respectively.

### **Data Analysis and Resulting Material Properties**

In order to use the VEC test data in CMSE Equations 2 through 25 the relaxation modulus and phase angle master curves must be developed.

#### ***Relaxation Modulus Calculation and Master Curve Development***

The relaxation modulus,  $E(t)$ , is determined by applying a constant strain,  $\varepsilon_0$ , to a material and recording the stress as it changes with time,  $\sigma(t)$ . The resulting stress is divided by the constant strain as seen in Equation 38.

$$E(t) = \frac{\sigma(t)}{\varepsilon_0} \quad (38)$$

Luo and Lytton (14) provided the following explanation of how to determine the relaxation modulus using data obtained from the VEC test. For a linearly viscoelastic material the stress-strain relationships shown in Equation 39 can be derived using the Boltzmann superposition principle (16).

$$\sigma(t) = \int_0^t E(t-\tau) \frac{\partial \varepsilon(\tau)}{\partial \tau} d\tau \quad (39)$$

where:

$\varepsilon(t)$  = time-dependent strain

$\sigma(t)$  = time-dependent stress

$E(t)$  = relaxation modulus

$\tau$  = a dummy variable which is less than or equal to  $t$

The equation for  $\sigma(t)$  is expressed in a convolution form that represents a mathematical operation on two functions with the following property:

$$\int_{-\infty}^{\infty} f(\tau) \cdot g(t-\tau) d\tau = \int_{-\infty}^{\infty} f(t-\tau) \cdot g(\tau) d\tau = f(t) * g(t) \quad (40)$$

where:

$f(t)$  and  $g(t)$  are two separate functions.

The Laplace transform of a convolution  $f(t) * g(t)$  is found using the convolution theorem:

$$\mathcal{L}\{f(t) * g(t)\} = \mathcal{L}\{f(t)\} \cdot \mathcal{L}\{g(t)\} \quad (41)$$

where the Laplace transform of a function  $f(t)$  is defined in Equation 42 for all real numbers as:

$$\mathcal{L}\{f(t)\} = \int_{0^-}^{\infty} e^{-st} f(t) dt \quad (42)$$

Using a Laplace transform and convolution theorem on Equation 39 produces the following equation with the transform variable,  $s$ .

$$\bar{\sigma}(s) = s\bar{E}(s)\bar{\varepsilon}(s) \quad (43)$$

From Equation 38, the Laplace transform of the relaxation modulus is determined as:

$$\bar{E}(s) = \frac{\bar{\sigma}(s)}{s\bar{\varepsilon}(s)} \quad (44)$$

The relaxation modulus can then be calculated by applying the inverse Laplace transform:

$$E(t) = \mathcal{L}^{-1} \left\{ \frac{\bar{\sigma}(s)}{s\bar{\varepsilon}(s)} \right\} \quad (45)$$

The stress and strain data obtained from the VEC test is modeled using Equations 46 and 47.

$$\sigma(t) = a_{\sigma} (1 - e^{-b_{\sigma} t}) \quad (46)$$

$$\varepsilon(t) = a_{\varepsilon} (1 - e^{-b_{\varepsilon} t}) \quad (47)$$

where:

$$\begin{aligned} e &= \text{the base of the natural logarithm} \\ a_{\sigma}, b_{\sigma}, a_{\varepsilon}, b_{\varepsilon} &= \text{fitting parameters} \end{aligned}$$

These fitting parameters can be determined by minimizing the error between measured and calculated values using the SOLVER application in the Microsoft Excel program.

By applying Laplace transforms to Equations 46 and 47, the Laplace transforms for the stress and strain models can be obtained as shown in Equations 48 and 49 as represented by  $\bar{\sigma}(s)$  and  $\bar{\varepsilon}(s)$ .



$$\bar{\sigma}(s) = \frac{a_{\sigma} b_{\sigma}}{s(s + b_{\sigma})} \quad (48)$$

$$\bar{\varepsilon}(s) = \frac{a_{\varepsilon} b_{\varepsilon}}{s(s + b_{\varepsilon})} \quad (49)$$

Using Equation 45, the relaxation modulus can then be determined as:

$$E(t) = \mathcal{L}^{-1} \left\{ \frac{\bar{\sigma}(s)}{\bar{\varepsilon}(s)} \right\} = \mathcal{L}^{-1} \left\{ \frac{\frac{a_{\sigma} b_{\sigma}}{s(s + b_{\sigma})}}{s \cdot \frac{a_{\varepsilon} b_{\varepsilon}}{s(s + b_{\varepsilon})}} \right\} = \frac{a_{\sigma}}{a_{\varepsilon}} \left( 1 + \frac{b_{\sigma} - b_{\varepsilon}}{b_{\varepsilon}} \cdot e^{-b_{\sigma} t} \right) \quad (50)$$

The process is completed for the data sets obtained from the 50°F (10°C), 68°F (20°C), and 86°F (30°C) VEC tests. Once  $E(t)$  is determined for all three temperature levels, the data is then reduced using time temperature superposition to 68°F (20°C) in order to form the time dependant relaxation modulus master curve.

### ***Phase Angle Calculation and Master Curve Development***

When a viscoelastic material is loaded in a sinusoidal fashion the strain response lags behind the applied stress by a phase angle,  $\varphi$  (14). Luo and Lytton also outlined the process for developing the master curve associated with this phase angle using the VEC test (14). The phase angle for a material can be determined by dividing the imaginary part of the complex modulus by the real part as shown in Equations 51 and 52.

$$E^*(\omega) = E_1 + iE_2 \quad (51)$$

$$\tan \varphi = \frac{E_2}{E_1} \quad (52)$$

where:

$E^*(\omega)$  = Complex modulus

$\omega$  = Loading frequency

$E_1$  = Storage modulus

$E_2$  = Loss modulus

Once the relaxation modulus is known, the complex modulus can be obtained if the viscoelastic material is subjected to a steady sinusoidal load and has an oscillatory strain in the form of:

$$\varepsilon(t) = \varepsilon_0 e^{i\omega t} = \varepsilon_0 (\cos \omega t + i \sin \omega t) \quad (53)$$

The complex modulus is calculated by using Equation 54 (17).

$$E^*(\omega) = i\omega \mathcal{L} \{E(t)\}_{s=i\omega} \quad (54)$$

By substituting Equation 50 into Equation 54 and simplifying, the real and imaginary parts of the complex modulus can be determined as shown in Equation 55.

$$\begin{aligned}
E^*(\omega) &= i\omega \mathcal{L}\{E(t)\}_{s=i\omega} \\
&= i\omega \left\{ \frac{\overline{\sigma}(s)}{s\overline{\varepsilon}(s)} \right\}_{s=i\omega} \\
&= i\omega \left\{ \frac{\frac{a_\sigma b_\sigma}{s(s+b_\sigma)}}{s \cdot \frac{a_\varepsilon b_\varepsilon}{s(s+b_\varepsilon)}} \right\}_{s=i\omega} \\
&= i\omega \frac{\frac{a_\sigma b_\sigma}{i\omega(i\omega+b_\sigma)}}{\frac{a_\varepsilon b_\varepsilon}{(i\omega+b_\varepsilon)}} \\
&= \frac{a_\sigma b_\sigma (\omega^2 + b_\varepsilon b_\sigma)}{a_\varepsilon b_\varepsilon (\omega^2 + b_\sigma^2)} + \frac{a_\sigma b_\sigma \omega (b_\sigma - b_\varepsilon)}{a_\varepsilon b_\varepsilon (\omega^2 + b_\sigma^2)} i
\end{aligned} \tag{55}$$

Thus the real part of  $E^*$  becomes:

$$E_1 = \frac{a_\sigma b_\sigma (\omega^2 + b_\varepsilon b_\sigma)}{a_\varepsilon b_\varepsilon (\omega^2 + b_\sigma^2)} \tag{56}$$

and the imaginary part becomes:

$$E_2 = \frac{a_\sigma b_\sigma \omega (b_\sigma - b_\varepsilon)}{a_\varepsilon b_\varepsilon (\omega^2 + b_\sigma^2)} \quad (57)$$

With the phase angle as:

$$\varphi = \arctan\left(\frac{E_2}{E_1}\right) \quad (58)$$

Time-temperature superposition principle is then used to construct the phase angle master curve. Luo and Lytton used the Williams-Landel-Ferry (WLF) formulation (18) as shown in Equation 59 to determine the appropriate temperature shift factors,  $a_\varphi(T)$ .

$$\log a_\varphi(T) = -\frac{C_1(T - T_r)}{C_2 + (T - T_r)} \quad (59)$$

where:

$T_r$  = Reference temperature

$C_1$  and  $C_2$  = Constants

Once the first shift factors were determined, the phase angle master curve was then fitted with the mathematical function shown in Equation 60. The original function

was developed by Bahia et al. (19) and was modified by Luo and Lytton (14) for their study.

$$\varphi = \frac{\varphi_m}{\left\{ 1 + \left[ \frac{\log \left( \frac{\omega_m}{\omega \cdot 10^{\frac{C_1(T-T_r)}{C_2+(T-T_r)}}} \right)}{R_\varphi} \right]^2 \right\}^{\frac{m}{2}}} \quad (60)$$

where:

$\varphi_m$  = Maximum phase angle, in degrees

$\omega_m$  = Frequency where  $\varphi_m$  occurs, in rad/sec

$R_\varphi, m$  = Fitting parameters

The SOLVER application in Microsoft Excel is used to find the best fit values of  $\varphi_m$ ,  $\omega_m$ ,  $R_\varphi$ ,  $m$ ,  $C_1$ , and  $C_2$ . From the phase angle master curve the tensile phase angle can be determined for any frequency.

With the relaxation modulus and phase angle master curves developed, the resulting  $E_t$ ,  $m$ , and  $\varphi$  values can then be determined and used in the CMSE calculations.

## **MODIFIED REPEATED DIRECT TENSION TEST (RDT\*)**

The RDT test was modified by Luo et al. (20) to account for the effects of compressive stresses required to bring the sample back to zero strain and to remove the effects of healing. This new test was renamed the Modified Repeated Direct-Tension (RDT\*) test. This modified test replaced the haversine loading pattern found in the RDT test with the haversine loading shown in FIGURE 4. The 0.9 second rest period between load cycles was removed and a preliminary series of 500 cycles at a lower strain level was introduced to determine the undamaged material properties.

### **Test Setup and Procedures**

Sample preparation for the RDT\* test is the same as that discussed in the VEC test method and as shown in FIGURE 5 with the exception of the LVDT bracelet for horizontal displacement measurements, which is not needed for the RDT\* data analysis. Typical sample size for this test is 4 inches (102 mm) in diameter by 4 inches (102 mm) in height. When using a LMLC sample an initial 6 inch (152 mm) diameter by 6 inch (152 mm) height sample is fabricated. This sample is then cored and trimmed to a 4 inch (102 mm) diameter by 4 inch (102 mm) height. This is done to reduce inconsistencies in air void distribution throughout the sample. Bulk specific gravities and air void contents are measured. 4 inch (102 mm) diameter platens are affixed to the sample using a 2 ton (18 kN) epoxy. After allowing sufficient drying time, three LVDT's are attached equidistant and vertically around the sample.

The sample is preconditioned and tested at 68°F (20°C). The test is run in displacement control mode with load and deformation data collected every 0.005 seconds. The sample is exposed to a haversine loading with a maximum vertical strain level of 80  $\mu\epsilon$  for 500 cycles at a frequency of 1 Hz. For 2 inch (51 mm) LVDT spacing, 80  $\mu\epsilon$  is a change in LVDT length of approximately 0.00016 inches (0.004064 mm). No rest period is given between cycles. This portion of the test can be used to calculate the undamaged viscoelastic phase angle and the relaxation modulus of the material. At the completion of the 500 cycles at 80  $\mu\epsilon$ , a 1000 cycle haversine loading is applied at a frequency of 1 Hz with a maximum strain level of 350  $\mu\epsilon$ . For 2 inch (51 mm) LVDT spacing, 350  $\mu\epsilon$  is a change in LVDT length of approximately 0.0007 inches (0.01778 mm). Though visible cracks may not be apparent, at the completion of the test the sample is damaged and cannot be retested.

### **Test Data**

A typical but truncated data set obtained from the RDT\* test is shown in TABLE 5.

**TABLE 5.** RDT\* Test Data.

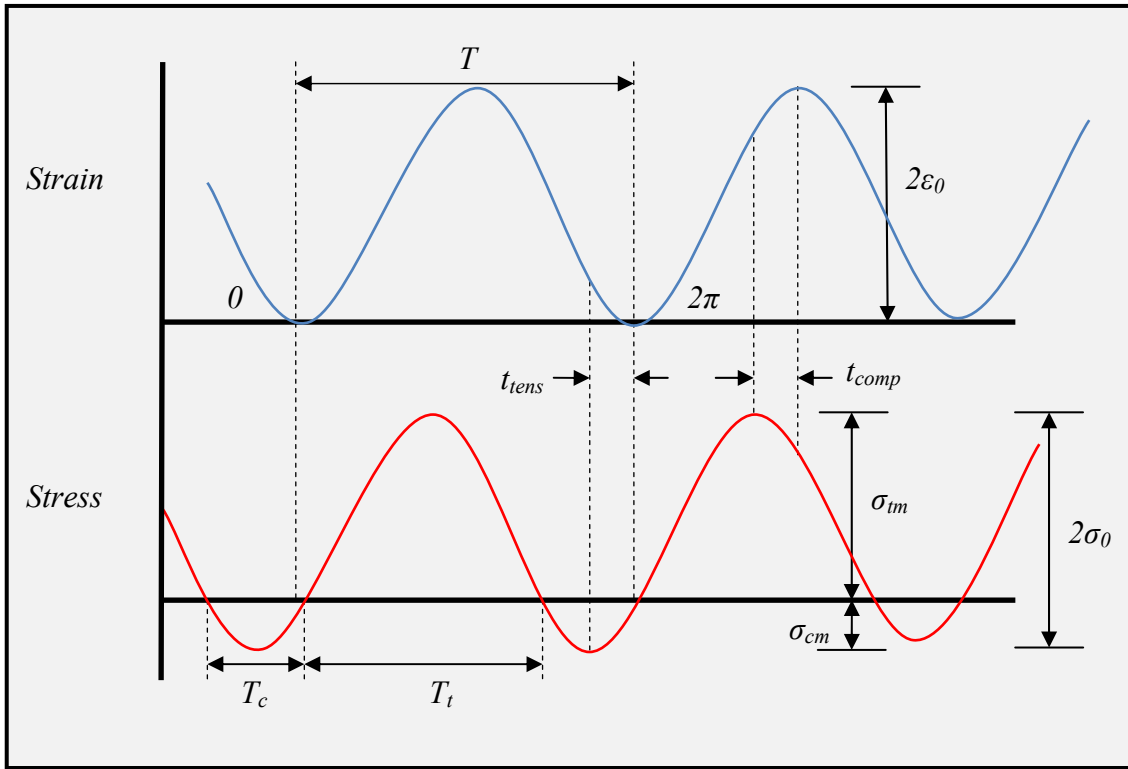
Time	Axial Displacement	Axial Force	Axial Ext. Disp	Input 10	Input 11	Axial Count
(Sec)	(in)	(lbf)	(in)	(in)	(in)	(segments)
491.48	-1.49318	314.97	1.900E-03	3.011E-03	2.927E-03	904
491.48	-1.49319	321.86	1.901E-03	3.012E-03	2.908E-03	904
491.49	-1.49315	327.73	1.904E-03	3.014E-03	2.901E-03	904
491.49	-1.49308	334.07	1.906E-03	3.016E-03	2.924E-03	904
491.50	-1.49310	343.40	1.907E-03	3.016E-03	2.936E-03	904
491.50	-1.49310	350.60	1.908E-03	3.018E-03	2.929E-03	904

The first column indicates the cumulative time of the test and recorded time at each data collection point. The Axial Displacement and Axial Force columns indicate the displacement experienced by the machine and the force applied by the machine to the sample. Axial Ext. Disp., Input 10, and Input 11 are the displacements recorded as experienced by the three vertical LVDT's placed on the samples. Axial Count represents the number of cycles with two counts per cycle. All recorded data begins with a base value and must be reduced to indicate an actual starting time, load, and displacement of zero. The initial time, load, and displacement values are subtracted from each subsequent reading in order to determine the actual loads and displacements experienced by the sample. With the load and displacement data reduced, stress and strain values can be calculated using the samples 4 inch (102 mm) diameter to calculate the cross sectional area of the sample and using the 2 inch (51 mm) gauge lengths of the LVDT's, respectively.



### Data Analysis and Resulting Material Properties

The RDT\* method, as developed by Luo et al. (20), separates the tension and compression components of the test and calculates their related material properties separately. In order to understand some of the variables used in the following equations, it is helpful to show an illustration of the stress response and strain input produced by the test. In FIGURE 6,  $T$  represents the period of the strain wave with a beginning and ending time of 0 and  $2\pi$ , respectively.  $T_c$  is the portion of the stress period corresponding to compressive stresses being applied to the sample.  $T_t$  represents the portion of the stress period corresponding to tensile stress application. In viscoelastic materials the strain lags behind the stress. In this case, the strain lags behind the strain for a time denoted as  $t_{lag}$  with a corresponding phase angle, called the lag angle, of  $\phi_l$ . Also the material responds differently when in tension than it does in compression. To account for these differences in response, the variables  $t_{tens}$  and  $t_{comp}$  (with corresponding lag angles of  $\phi_t$  and  $\phi_c$ ) are used to represent the tensile and compressive lag times, respectively.  $\sigma_{tm}$  is the maximum tensile stress, while  $\sigma_{cm}$  is the maximum compressive stress applied to the sample for each phase. The amplitudes of the input and response waves are identified by  $\sigma_0$  and  $\varepsilon_0$ , respectively.



**FIGURE 6.** Strain Response and Stress Input from the RDT\* Test. Adapted from Luo et al. (20).

Using the equations for wave motion, the lag angle can be determined using Equations 61 through 63.

$$\varepsilon(t) = \varepsilon_0 \sin(2\pi ft + \varphi_l) \quad (61)$$

$$T = \frac{1}{f} \quad (62)$$

Setting  $\varepsilon(t) = 0$  and solving for  $\varphi_l$  gives:

$$\varphi_l = \frac{2\pi t}{T} \quad (63)$$

where:

$f$  = frequency

Recognizing that the wave forms are different for tension and compression, Luo et al. (20) separated and expanded the individual waves in order to develop the equations for the tension and compression stress and strain waves independently. In order to correctly characterize the tensile stress wave function correctly a vertical shift factor,  $\sigma_{st}$ , was introduced. The equations for the tension and compression waves and their respective stress amplitudes,  $\sigma_{0c}$  and  $\sigma_{0t}$ , are found in Equations 64 through 70.

$$\text{Compression wave: } \sigma_c = \sigma_{0c} [1 - \cos(\omega t)] - \sigma_{cm} \quad (64)$$

$$\sigma_{0c} = \frac{\sigma_{cm}}{1 - \sin \left[ \pi \left( \frac{1}{2} - \frac{T_c}{T} \right) \right]} \quad (65)$$

$$\varepsilon = \varepsilon_0 [1 - \cos(\omega t - \varphi_c)] \quad (66)$$

$$\text{Tension wave: } \sigma_t = \sigma_{0t} [1 - \cos(\omega t)] - \sigma_{st} \quad (67)$$

$$\sigma_{0t} = \frac{\sigma_{tm}}{1 - \sin\left[\pi\left(\frac{1}{2} - \frac{T_t}{T}\right)\right]} \quad (68)$$

$$\sigma_{st} = \frac{\sigma_{tm} \left[1 + \sin\left[\pi\left(\frac{1}{2} - \frac{T_t}{T}\right)\right]\right]}{1 - \sin\left[\pi\left(\frac{1}{2} - \frac{T_t}{T}\right)\right]} \quad (69)$$

$$\varepsilon = \varepsilon_0 [1 - \cos(\omega t - \varphi_t)] \quad (70)$$

With the establishment of the wave form equations shown in Equations 64 through 70, pseudo strain energy and DPSE can be calculated.

### ***Calculation of DPSE and b***

Pseudo strain energy is calculated using Equations 66 and 70 with modifications to account for the viscoelastic behavior and reductions in the modulus of the material as in Equations 71 and 72.

In compression: 
$$\varepsilon^R = \frac{E_{VE,c}}{E_{Nc}} \varepsilon_0 [1 - \cos(\omega t - \varphi_c + \varphi_{VE,c})] \quad (71)$$

In tension: 
$$\varepsilon^R = \frac{E_{VE,t}}{E_{Nt}} \varepsilon_0 [1 - \cos(\omega t - \varphi_t + \varphi_{VE,t})] \quad (72)$$

where:

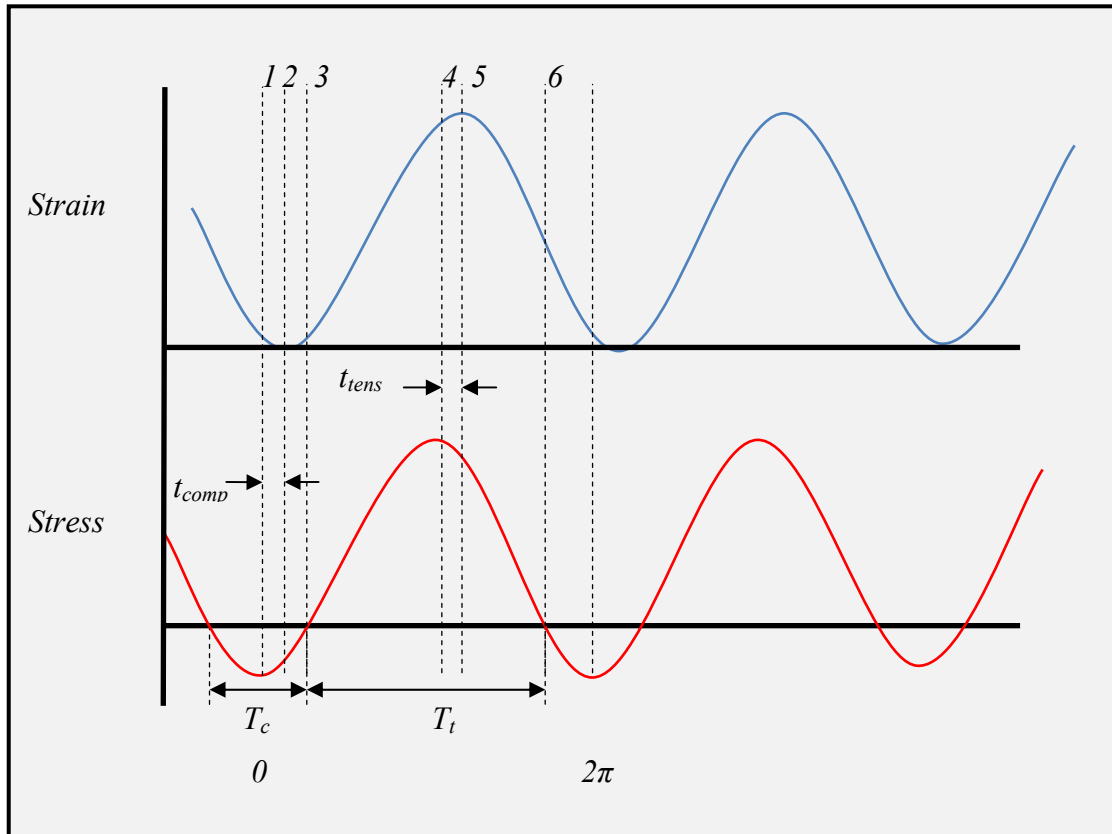
- $\varepsilon^R$  = pseudo strain
- $E_{VE,c}$  = compressive modulus of undamaged viscoelastic material
- $E_{Nc}$  = compressive modulus of load cycle N
- $\varphi_{VE,c}$  = compressive phase angle of undamaged viscoelastic material
- $E_{VE,t}$  = tensile modulus of undamaged viscoelastic material
- $E_{Nt}$  = tensile modulus of load cycle N
- $\varphi_{VE,t}$  = tensile phase angle of undamaged viscoelastic material

$E_{VE}$  and  $\varphi_{VE}$  are the undamaged material properties of the material and are assumed to be constant. The ratio of  $E_{VE}$  to  $E_N$  accounts for the reduction in stiffness of the material that occurs over time under repeated loading. The addition of  $\varphi_{VE}$  eliminates the time dependant viscoelastic behavior of the material and ensures that the energy associated with this behavior is not included in the calculation of DPSE.

DPSE, denoted as  $W_R$  by Luo et al. (20), can be calculated by substituting Equations 71 and 72 into Equation 73 for each of the respective compressive and tensile phases for a cycle of time  $t$ , which varies from 0 to  $\pi/2\omega$ .

$$W_R = \int_0^{\frac{\pi}{2\omega}} \sigma(t) \frac{d\varepsilon^R(t)}{dt} dt \quad (73)$$

Luo et al. (20) divided this integration into six specific bands which designate differing phase angles and stresses as shown in FIGURE 7. The limits associated with these bands are summarized in TABLE 6.



**FIGURE 7.** DPSE Integration Bands. Adapted from Luo et al. (20).

**TABLE 6.** DPSE Integration Bands. Adapted from Luo et al. (20).

Band No.	Stress Direction	Lower limit	Upper limit
1	Compression	0	$\phi_c/\omega$
2	Compression	$\phi_c/\omega$	$T_c/2$
3	Tension	$T_c/2$	$\pi/\omega$
4	Tension	$\pi/\omega$	$\pi/\omega + \phi_t/\omega$
5	Tension	$\pi/\omega + \phi_t/\omega$	$\pi/\omega + T_t/2$
6	Compression	$\pi/\omega + T_t/2$	$2\pi/\omega$

By substituting the appropriate tension or compression equation from Equations 71 and 72 into Equation 73 and applying the appropriate lower and upper limits defined in TABLE 6, the DPSE can be determined for each of the bands. Luo et al. (20) denotes the DPSE for each band as  $W_{R1}$  through  $W_{R6}$ . These integration results for the individual bands can then be summed to provide the total DPSE for the loading cycle. In the following equations,  $W_{R,i}$  represents the general equation used to calculate the DPSE for each of the bands.

$$W_R = W_{R,1} + W_{R,2} + W_{R,3} + W_{R,4} + W_{R,5} + W_{R,6} \quad (74)$$

$$\sigma_0 = \frac{E_N}{\left( \frac{E_N}{E_{VE}} \right)} \varepsilon_0 \quad (75)$$

$$\begin{aligned}
W_{R,i} &= \int_l^u \sigma_0 \varepsilon_0 \omega [1 - \cos(\omega t)] \cdot \sin[\omega t - (\varphi - \varphi_{VE})] dt - \int_l^u \sigma_s \varepsilon_0 \omega \sin[\omega t - (\varphi - \varphi_{VE})] dt \\
&= \sigma_0 \varepsilon_0 \omega \int_l^u [\sin[\omega t - (\varphi - \varphi_{VE})] - \sin[\omega t - (\varphi - \varphi_{VE})] \cos(\omega t)] dt \\
&\quad - \sigma_s \varepsilon_0 \omega \int_l^u \sin[\omega t - (\varphi - \varphi_{VE})] dt \\
&= \sigma_0 \varepsilon_0 \omega \cos(\varphi - \varphi_{VE}) \int_l^u [\sin(\omega t) - \sin(\omega t) \cos(\omega t)] dt \\
&\quad + \sigma_0 \varepsilon_0 \sin(\varphi - \varphi_{VE}) \int_l^u [-\cos(\omega t) + \cos^2(\omega t)] dt \\
&\quad - \sigma_s \varepsilon_0 \omega \cos(\varphi - \varphi_{VE}) \int_l^u \sin(\omega t) dt + \sigma_s \varepsilon_0 \omega \sin(\varphi - \varphi_{VE}) \int_l^u \cos(\omega t) dt \\
&= \varepsilon_0 \omega \cos(\varphi - \varphi_{VE}) \left[ \sigma_0 \left( -\frac{1}{\omega} \cos(\omega t) - \frac{1}{2\omega} \sin^2(\omega t) \right) \Big|_{t=l}^{t=u} - \sigma_s \left( -\frac{1}{\omega} \cos(\omega t) \right) \Big|_{t=l}^{t=u} \right] \\
&\quad + \varepsilon_0 \omega \sin(\varphi - \varphi_{VE}) \left[ \sigma_0 \left( -\sin(\omega t) + \frac{t}{2} + \frac{\sin(2\omega t)}{4\omega} \right) \Big|_{t=l}^{t=u} + \sigma_s \left( \frac{1}{\omega} \sin(\omega t) \right) \Big|_{t=l}^{t=u} \right]
\end{aligned} \tag{76}$$

where:

$u$  = Upper limit of integration

$l$  = Lower limit of integration

By collecting like terms of  $\varepsilon_0 \omega \sin \varphi$  and  $\varepsilon_0 \omega \cos \varphi$ , the DPSE can be separated into dissipated energy that causes fracture damage ( $W_{R1,i}$ ) and the dissipated energy that causes permanent plastic deformation ( $W_{R2,i}$ ), respectively. Luo et al. (20) uses this to further reduce the equations to:



$$W_{R1,i} = A_{Ri} \varepsilon_0 \omega \sin(\varphi - \varphi_{VE}) \quad (77)$$

$$W_{R2,i} = B_{Ri} \varepsilon_0 \omega \cos(\varphi - \varphi_{VE}) \quad (78)$$

$$A_{Ri} = \left[ \frac{\frac{E_N}{E_{VE}} \varepsilon_0 \left( -\frac{1}{\omega} \cos(\omega t) - \frac{1}{2\omega} \sin^2(\omega t) \right)_{t=l}^{t=u} - \frac{E_N}{E_{VE}} \varepsilon_s \left( -\frac{1}{\omega} \cos(\omega t) \right)_{t=l}^{t=u}}{\left( \frac{E_N}{E_{VE}} \right)} \right] \quad (79)$$

$$B_{Ri} = \left[ \frac{\frac{E_N}{E_{VE}} \varepsilon_0 \left( -\sin(\omega t) + \frac{t}{2} + \frac{\sin(2\omega t)}{4\omega} \right)_{t=l}^{t=u} + \frac{E_N}{E_{VE}} \varepsilon_s \left( \frac{1}{\omega} \sin(\omega t) \right)_{t=l}^{t=u}}{\left( \frac{E_N}{E_{VE}} \right)} \right] \quad (80)$$

where:

$$\varepsilon_s = \text{Compressive strain amplitude}$$

Substituting in the integration limits from TABLE 6 and the corresponding tensile or compressive lag and viscoelastic phase angles into Equations 79 and 80, Luo et al. (20) determined the equations for  $A_{Ri}$  and  $B_{Ri}$  for each of the six bands. By including all of the  $A_{Ri}$  and  $B_{Ri}$  terms for each band and collecting like terms,  $W_{R1}$  and  $W_{R2}$  can be defined as:

$$W_{R1} = (A_{R1} + A_{R2} + A_{R6}) \varepsilon_0 \omega \sin(\varphi_c - \varphi_{VE}) + (A_{R3} + A_{R4} + A_{R5}) \varepsilon_0 \omega \sin(\varphi_l - \varphi_{VE}) \quad (81)$$

$$W_{R2} = (B_{R1} + B_{R2} + B_{R6}) \varepsilon_0 \omega \cos(\varphi_c - \varphi_{VE}) + (B_{R3} + B_{R4} + B_{R5}) \varepsilon_0 \omega \cos(\varphi_l - \varphi_{VE}) \quad (82)$$

Finally, the total DPSE is defined as:

$$DPSE = W_{R1} + W_{R2} \quad (83)$$

Because the CMSE equations deal strictly with fatigue, the  $b$  value to be used in the equations is that portion associated with  $W_{R1}$ .  $W_{R2}$  is related to permanent plastic deformation and is therefore dropped out. DPSE associated with  $W_{R1}$  is plotted against the log of the number of load cycles,  $N$ . This plot is fitted with the linear logarithmic function shown in Equation 84.

$$W_{R1} = a + b \log(N) \quad (84)$$

where:

$W_{R1}$  = Dissipated pseudo strain energy associated with fatigue damage ( $J/m^3$ )

$a$  = DPSE at the first load cycle

$b$  = Rate of fracture damage accumulation

$N$  = Load cycle

This  $b$  value can then be used in the CMSE equation to determine the loads to crack initiation value,  $N_i$ .

### ***Calculation of Average Crack Radius***

With the data obtained from the VEC and RDT\* tests and with the analysis completed in order to determine  $E_t$ ,  $m$ ,  $W_{RI}$ , and  $b$ , calculations can then be made to determine Paris' Law fracture coefficients  $A$  and  $n$ . Luo et al. (20) developed a new method of calculating  $A$  which makes direct use of the average crack radius,  $\bar{c}(N)$ , for the given sample. However, this value must first be calculated and was outlined by Luo et al. (20) as follows.

The stress,  $\sigma'$ , that a sample experiences is generally calculated by dividing the applied load,  $L$ , by the cross-sectional area,  $A_0$  as in Equation 85.

$$\sigma' = \frac{L}{A_0} \quad (85)$$

However, once the sample experiences fracture damage and begins to crack, the actual stress in the sample changes. This is due to the change in cross-sectional area from the original value of  $A_0$  to value of  $A$ , which is the original area less the area of the cracks.

This new stress is calculated as:

$$\sigma = \frac{L}{A} \quad (86)$$

therefore,

$$\sigma' A_0 = \sigma A \quad (87)$$

If  $M$  is defined as the number of cracks found throughout any given cross section, then the damaged cross-sectional area can be calculated as:

$$A = A_0 - \pi M \bar{c}(N)^2 \quad (88)$$

The area ratio is then:

$$\frac{A}{A_0} = 1 - \pi \frac{M}{A_0} \bar{c}(N)^2 \quad (89)$$

If the variable  $x$  is defined as the ratio of the stress free volume (or volume of cracks in a sample) per total volume to the cracked area per total cross-sectional area, then:

$$2\pi^2 \left( \frac{M}{A} \right) \frac{\bar{c}(N)^3}{\bar{t}} x = \pi \left( \frac{M}{A_0} \right) \bar{c}(N)^2 \quad (90)$$

$$\text{and, } x = \frac{\bar{t}}{2\pi \bar{c}(N)} \quad (91)$$

where:

$\bar{t}$  : Mean film thickness

The total strain of the cylindrical samples contains three parts as shown in Equations 92 through 96.

$$E = E_1 + E_2 + E_3 \quad (92)$$

$$E = \frac{1}{2}(\sigma\varepsilon) \left( \frac{\pi D^2 \bar{t}}{4} \right) = \frac{1}{2}(E(N)\varepsilon^2) \left( \frac{\pi D^2 \bar{t}}{4} \right) \quad (93)$$

$$E_1 = \frac{1}{2}(\sigma\varepsilon) \left( \frac{\pi D^2 \bar{t}}{4} \right) = \frac{1}{2}(E_0\varepsilon^2) \left( \frac{\pi D^2 \bar{t}}{4} \right) \quad (94)$$

$$E_2 = -\frac{1}{2}(\sigma\varepsilon) \left( 2\pi^2 \bar{c}(N)^3 \right) = -\frac{1}{2}(E_0\varepsilon^2) \left( 2\pi^2 \bar{c}(N)^3 \right) \quad (95)$$

$$E_3 = \Gamma \left( 2\pi \bar{c}(N)^2 \right) \quad (96)$$

where:

$E$  = Total strain energy

$E_1$  = Energy of intact material

$E_2$  = Energy released by crack growth to the present radius,  $\bar{c}(N)$

$E_3$  = Energy stored on newly cracked surface

- $E(N)$  = Modulus for load cycle  $N$   
 $E_0$  = Original modulus  
 $D$  = Diameter of HMAC sample  
 $\Gamma$  = Surface energy,  $\Gamma = \frac{1}{2} \Delta G_f^c$

Substituting Equations 93 through 96 into Equation 92 and simplifying gives:

$$\frac{E(N)}{E_0} = 1 - 2\pi^2 \left( \frac{M}{A} \right) \frac{\bar{c}(N)^3}{\bar{t}} \left( 1 - \frac{E_0 \Delta G_f^c}{\pi \sigma^2 c(N)} \right) \quad (97)$$

with:

$$\left( 1 - \frac{E_0 \Delta G_f^c}{\pi \sigma^2 c(N)} \right) \approx 1 \quad (98)$$

therefore Equation 97 can be rewritten as:

$$\frac{E(N)}{E_0} = 1 - 2\pi^2 \left( \frac{M}{A} \right) \frac{\bar{c}(N)^3}{\bar{t}} \quad (99)$$

Combining Equations 87, 89, 90, 91, and 99 gives:

$$\left(1 - \frac{E(N)}{E_0}\right) \frac{\bar{t}}{2\pi \bar{c}(N)} = 1 - \frac{\sigma'}{\sigma} \quad (100)$$

In the previous section  $W_{R1}$  was calculated as the DPSE associated with fatigue cracking. Because of its association with cracking  $W_{R1}$ , and not  $W_{R2}$ , should be used in the calculation of the crack radius. If at any particular point in time, a single stress amplitude,  $\sigma'$ , and a single phase angle,  $\varphi$ , are used to calculate  $W_{R1}$ , and assuming undamaged conditions, Equation 81 can be rewritten as:

$$W_{R1} = \sum_{i=1}^{i=6} A_i \sigma' \varepsilon_0 \sin \varphi \quad (101)$$

Rewriting  $W_{R1}$  in Equation 101 with the actual stress  $\sigma$  and the original phase angle,  $\varphi_0$ , gives:

$$W_{R1} = \sum_{i=1}^{i=6} A_i \sigma \varepsilon_0 \sin \varphi_0 \quad (102)$$

Combining Equations 101 with 102 gives:

$$\frac{\sigma'}{\sigma} = \frac{\sin \varphi_0}{\sin \varphi} \quad (103)$$

If Equation 103 is then substituted into Equation 100 then:

$$\left(1 - \frac{E(N)}{E_0}\right) \frac{\bar{t}}{2\pi \bar{c}(N)} = 1 - \frac{\sin \varphi_0}{\sin \varphi} \quad (104)$$

The average crack radius is then calculated by:

$$\bar{c}(N) = \frac{\bar{t} \left(1 - \frac{E(N)}{E_0}\right)}{2\pi \left(1 - \frac{\sin \varphi_0}{\sin \varphi}\right)} \quad (105)$$

### ***Calculation of Paris' Law Fracture Coefficients, A and n***

The calculation of  $A$  and  $n$  require the material properties calculated from both the VEC and RDT\* tests. The calculation of  $n$  does not change from that shown in Equation 3. However, with the ability to calculate the average crack radius, the calculation of  $A$  can be determined without testing for and calculating  $\Delta G_f$  as described by Luo et al. (20) and as follows:

With the determination of the average crack radius from Equation 105,  $A$  can be determined from Paris' Law of Fracture Mechanics as shown in Equations 106 and 107.



$$\frac{d\bar{c}(N)}{dN} = A(J_R)^n \quad (106)$$

$$J_R = \frac{\partial W_R}{\partial(c.s.a.)} = \frac{\frac{\partial W_R}{\partial N}}{\frac{\partial(c.s.a.)}{\partial N}} \quad (107)$$

where:

$J_R$  = J-Integral

$c.s.a.$  = Crack surface area

The crack surface area (c.s.a.) can be defined by:

$$c.s.a. = A_0 \left( 2\pi \bar{c}(N) \left( \frac{M}{A_0} \right) \right) \quad (108)$$

where:

$M/A_0$  =  $C_D$  = Crack density

$2\pi \bar{c}(N) (M/A_0)$  = Crack surface area per unit area

Substituting Equation 108 into Equation 106, Paris' Law is rewritten as shown in Equation 109. Again, only  $W_{RI}$  is used due to its relationship to cracking.

$$\frac{d\bar{c}(N)}{dN} = A \left( \frac{\frac{\partial W_{R1}}{\partial N}}{A_0 4\pi \left(\frac{M}{A_0}\right) c(N) \left(\frac{d\bar{c}(N)}{dN}\right)} \right)^n \quad (109)$$

Collecting like variables and rewriting Equation 109 gives:

$$\bar{c}(N)^{\frac{n}{n+1}} \frac{d\bar{c}(N)}{dN} = A^{\frac{1}{n+1}} \left( \frac{\frac{\partial W_{R1}}{\partial N}}{A_0 4\pi \left(\frac{M}{A_0}\right)} \right)^{\frac{n}{n+1}} \quad (110)$$

Both sides of Equation 110 are integrated with average crack radius limits ranging from zero to the maximum crack size and load cycles from zero to  $N_i$ .

$$\bar{c}(N)^{\frac{2n+1}{n+1}} = \left(\frac{2n+1}{n+1}\right) A^{\frac{1}{n+1}} \int_{N=0}^{N=N_i} \left( \frac{\frac{\partial W_{R1}}{\partial N}}{4\pi A_0 \left(\frac{M}{A_0}\right)} \right)^{\frac{n}{n+1}} dN \quad (111)$$

Taking the derivative of Equation 84 with respect to  $N$  gives Equation 112.

$$\frac{\partial W_{R1}}{\partial N} = 0.4343 \frac{b}{N} \quad (112)$$

This is then substituted into the remaining integral in Equation 111 and simplified as in Equation 113.

$$\begin{aligned} \int_{N=0}^{N=N_i} \left( \frac{\frac{\partial W_{R1}}{\partial N}}{4\pi A_0 \left( \frac{M}{A_0} \right)} \right)^{\frac{n}{n+1}} dN &= \int_{N=0}^{N=N_i} \left( \frac{1}{4\pi A_0 \left( \frac{M}{A_0} \right)} \frac{0.4343b}{N} \right)^{\frac{n}{n+1}} dN \\ &= \left( \frac{0.4343b}{4\pi A_0 \left( \frac{M}{A_0} \right)} \right)^{\frac{n}{n+1}} \int_{N=0}^{N=N_i} N^{-\frac{n}{n+1}} dN \\ &= \left( \frac{0.4343b}{4\pi A_0 \left( \frac{M}{A_0} \right)} \right)^{\frac{n}{n+1}} (n+1) N^{\frac{1}{n+1}} \end{aligned} \quad (113)$$

Substituting Equation 113 into Equation 111, and solving for  $\bar{c}(N)$ , gives:

$$\bar{c}(N) = (2n+1)^{\frac{n+1}{2n+1}} A^{\frac{1}{2n+1}} \left( \frac{0.4343b}{4\pi A_0 \left( \frac{M}{A_0} \right)} \right)^{\frac{n}{2n+1}} N^{\frac{1}{2n+1}} \quad (114)$$

Then, assuming that,

$$\log \bar{c}(N) = d + e \log N \quad (115)$$

And taking the log of both sides of Equation 114,

$$\log \bar{c}(N) = \log \left( (2n+1)^{\frac{n+1}{2n+1}} A^{\frac{1}{2n+1}} \left( \frac{0.4343b}{4\pi A_0 \left( \frac{M}{A_0} \right)} \right)^{\frac{n}{2n+1}} \right) + \frac{1}{2n+1} \log N \quad (116)$$

Equation 116 is rearranged to the form found in 115 giving:

$$d = \frac{1}{2n+1} \log \left( (2n+1)^{n+1} \left( \frac{A}{M^n} \right) \left( \frac{0.4343b}{4\pi} \right)^n \right) \quad (117)$$

Solving Equation 117 for  $A$  gives:

$$A = M^n \left( \frac{10^{d(2n+1)}}{(2n+1)^{n+1} \left( \frac{0.4343b}{4\pi} \right)^n} \right) \quad (118)$$

By taking Equation 105, substituting in the material properties associated with various values of  $N$ , and fitting the results with Equation 115, the values for  $d$  and  $e$  can be determined.  $M$  is then determined by,

$$M = A_0 C_D \quad (119)$$

Knowing the value of  $n$  from Equation 3, the value of  $A$  can then be calculated. These newly calculated values which result from the VEC and RDT\* tests can now be applied to the CMSE equations.

## REVISED CMSE (CMSE\*)

With the new advances made with the VEC and RDT\* tests, some of the testing and analysis used for the CMSE method can be replaced and updated.

### APPLICATION OF VEC TEST RESULTS

As mentioned in the Recent Fatigue Testing Developments section, the VEC test can successfully replace the RM test and provides more reliable, less variable results in a shorter amount of time. With the VEC test, values for  $E_t$ ,  $m_b$ , and  $\phi_t$  can be determined. These values can be directly input into Equation 14 for determining  $N_p$ . They can also be used to calculate Paris' Law fracture coefficients  $n$  and  $A$  by direct placement into Equations 3 and 9, respectively. These values are then used in Equation 8 to calculate  $N_i$ . However, in the following section it will be shown that the use of Equation 9 to calculate  $A$  has been eliminated due to the new analysis methods and calculations associated with the RDT\* test. The RDT\* testing and analysis also makes use of the material characteristics obtained from the VEC test.

### APPLICATION OF RDT\* TEST RESULTS

The RDT\* test now replaces the original RDT test and removes the variability introduced by unwanted healing during short rest periods. By using the data obtained from the VEC test, the correct value of  $b$  can be determined. It has also been shown that a new method of calculating  $A$  can be used when using the RDT\* test data. The new

method of calculating  $A$  is shown in Equation 118. Data obtained from the TS test was previously used to determine  $A$  by applying  $\sigma_t$  to Equation 9. Other than its use in determining testing limits for the RM and RDT tests, this is the only place in the CMSE method that used TS data. However, by using the VEC and RDT\* test data and Equation 118 to calculate  $A$ , the TS test can be eliminated from the process as well as Equation 9. With  $A$  and  $b$  calculated from the RDT\* test results and  $n$  determined from VEC test results, Equation 8 can be solved for  $N_i$ .

### **CALCULATION OF CRACK DENSITY**

In order to eliminate Equation 9 and make use of Equation 118 for solving  $A$ , a  $C_D$  value must either be assumed, as was done by Walubita (7), or calculated.

As used in Equation 88, the area of air voids in a sample cross-section ( $AV$ ) can be defined as shown in Equation 120.

$$AV = \pi M \bar{c} (N)^2 \quad (120)$$

For a cylindrical sample, the percent of  $AV$  is the ratio of the volume of air to the total volume of the sample, as in Equation 121. This is also the ratio of  $AV$  to  $A_0$ .

$$\%AV = \frac{Vol.Air}{TotalVolume} = \frac{h \times AV}{h \times A_0} = \frac{AV}{A_0} \quad (121)$$

where:

$h$  = Height of a given sample

If the average initial crack radius is defined as  $\bar{c}_0$ , then, assuming all air voids are microcracks within the sample:

$$AV = \pi M \bar{c}_0^2 \quad (122)$$

And with a total cross-sectional area of:

$$A_0 = \pi r^2 \quad (123)$$

Then:

$$\%AV = \frac{\pi M \bar{c}_0^2}{\pi r^2} = \frac{M \bar{c}_0^2}{r^2} \quad (124)$$

Solving for  $M$ :

$$M = \frac{\%AV r^2}{\bar{c}_0^2} \quad (125)$$

If the  $\%AV$  of a sample and the sample radius are know, then  $M$ , and thus  $C_D$ , can be easily determined by substituting Equation 105, at the first load cycle, into Equation 125.



$M$  can then be used to calculate  $A$ . By rearranging Equation 119,  $C_D$  can be determined as:

$$C_D = \frac{M}{A_0} \quad (126)$$

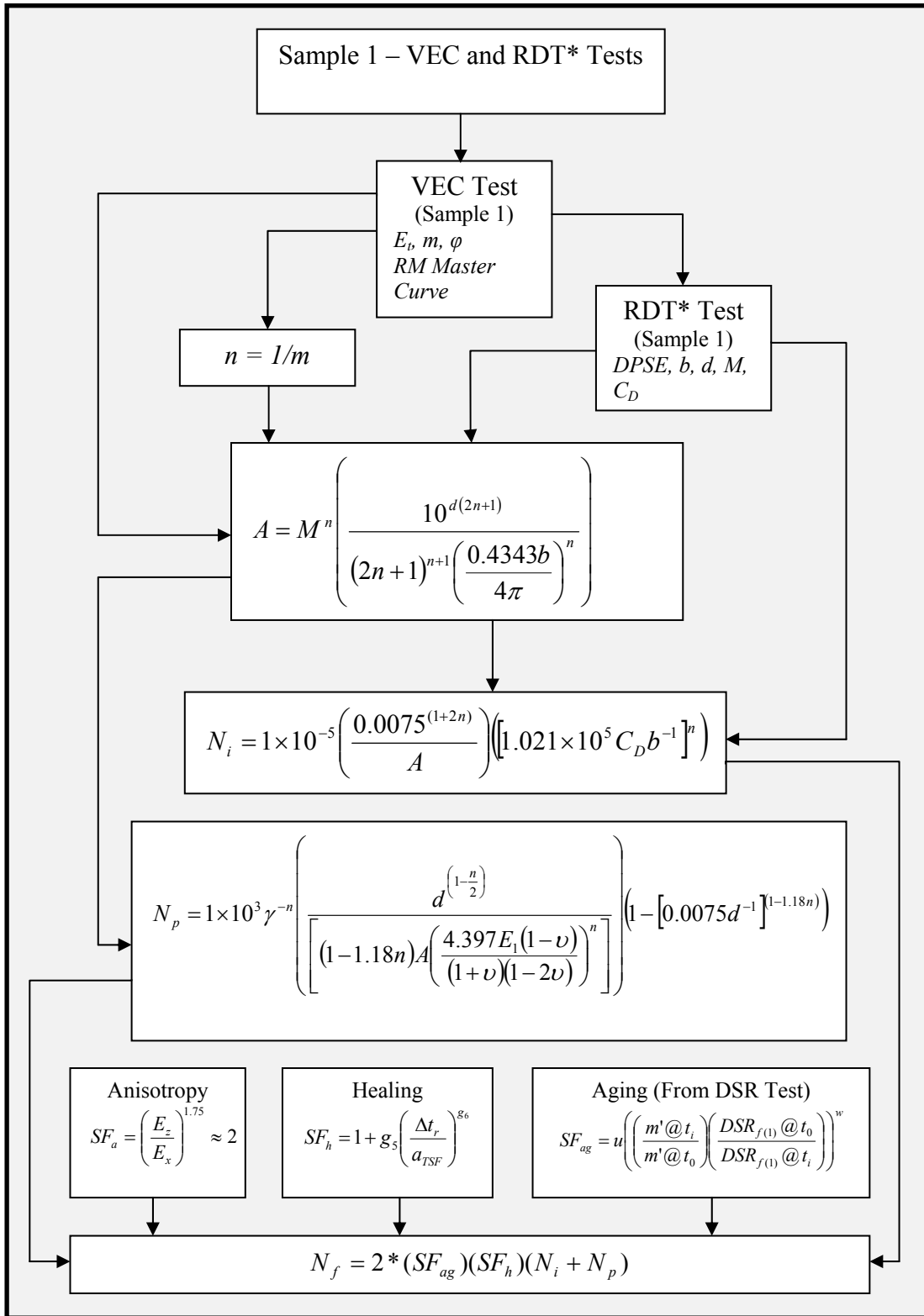
With  $C_D$  determined,  $N_i$  from Equation 2 can be determined using a calculated rather than assumed value. For a 4 inch (152 mm) diameter sample, Equation 8 can be rewritten as:

$$N_i = 1 \times 10^{-5} \left( \frac{0.0075^{(1+2n)}}{A} \right) \left( [1.021 \times 10^5 C_D b^{-1}]^n \right) \quad (127)$$

### **CMSE\* SUMMARY**

With the development of the VEC and RDT\* tests, the CMSE method has been improved and refined to provide more accurate and reliable results. While there is still considerable data analysis and evaluation to be done, the highly variable and unreliable results obtained from the RM test have been eliminated. The RDT test has been adjusted to eliminate variability in results caused by healing that occurs during the 0.9 second rest period. In addition, a new method of calculating Paris' Law fracture coefficients,  $A$  and  $n$ , has been developed. This new method eliminates the need for determining  $\Delta G_f(20)$ .

A summary of the CMSE\* can be seen in FIGURE 8.



**FIGURE 8.** CMSE\* Method of Fatigue Analysis.

## TEST ANALYSIS MACRO DEVELOPMENT

Analysis of the data obtained from the VEC and RDT\* test is extensive. Raw data is provided as load and displacement values. For each data point recorded, loads and displacements must be converted to their respective stresses and strains from which further calculations can be made to determine the material properties of the sample. While spreadsheet applications, such as Microsoft EXCEL, make the repetitive calculations relatively quickly and effectively, the need to find the applicable data then copy, paste, and transfer it from one spreadsheet to the next extends the analysis of both the VEC and RDT\* data to an estimated 10 hours. In order to minimize the time required for the analysis of VEC and RDT\* test data, Microsoft Excel macros were developed. The following sections describe the process associated with each macro as well as its contributions. In addition, suggestions for further development of the macros are also offered.

### VEC ANALYSIS MACRO

The final goal of the VEC test data analysis is to provide the relaxation modulus master curve and the phase angle master curve from which  $E_t$ ,  $m$ , and  $\varphi$  can be determined. In order to accomplish this task, a master spreadsheet was constructed that contains the equations necessary to complete the analysis. This VEC analysis spreadsheet is organized into four specific sections.

The first section includes individual worksheets for 50°F (10°C), 68°F (20°C), and 86°F (30°C) testing temperatures. These worksheets contain the raw data from the VEC test as well as the formulas necessary to calculate the measured strain from each of the LVDT's, the measured stress applied to the sample, and the average measured strain. They also contain formulas for Equations 46 and 47 in order to determine the calculated stress and calculated strain, respectively. Two columns are used to calculate the error between the measured and calculated stress and strain. It is in these worksheets that the fitting parameters,  $a_\sigma$ ,  $b_\sigma$ ,  $a_\epsilon$ , and  $b_\epsilon$ , for Equations 46 and 47 are determined. For the purposes of this document, this set of worksheets is defined as the raw data worksheets.

The next section is referred to as the calculations worksheets, which also contain worksheets for 50°F (10°C), 68°F (20°C), and 86°F (30°C) testing temperatures. This set of worksheets contain the formulas for calculating  $E(t)$ ,  $E_1$ ,  $E_2$ , and  $\phi$  from Equations 50 and 56 through 58 corresponding to the VEC test recorded time. In order to make these calculations, links to the values of  $a_\sigma$ ,  $b_\sigma$ ,  $a_\epsilon$ , and  $b_\epsilon$  contained in the raw data worksheets are included.

The third section is used to calculate and graph the RM master curve. This worksheet contains the calculated values of  $E(t)$  for 50°F (10°C), 68°F (20°C), and 86°F (30°C) determined from the calculations worksheets.  $a_T$  factors are determined for 50°F (10°C) and 86°F (30°C) with  $a_T$  at 68°F (20°C) equal to 1.0. The master curve is created as  $E(t)$  values are shifted to 68°F (20°C) by changing  $a_T$ ,  $E_1$ , and  $m$  from Equations 128 and 129 while minimizing the sum of the error between the calculated values of  $E(t)$  and those predicted by Equation 128.

$$E(t) = E_1 \xi^{-m} \quad (128)$$

where:

$$\xi = \frac{t}{a_T} \quad (129)$$

The fourth section is used to calculate and graph the phase angle master curve. This worksheet contains the calculated values of  $\varphi(\omega)$  for 50°F (10°C), 68°F (20°C), and 86°F (30°C) determined from the calculations worksheets. Log  $a_\varphi(T)$  factors are determined according to Equation 59 for 50°F (10°C) and 86°F (30°C) with log  $a_\varphi(T)$  at 68°F (20°C) equal to zero. The phase angle master curve is created as was done with the RM master curve where  $\varphi(\omega)$  values are shifted to 68°F (20°C) by changing  $\varphi_m$ ,  $\omega_m$ ,  $C_1$ ,  $C_2$ ,  $R_\varphi$ , and  $m$  from Equations 59 and 60 while minimizing the sum of the error between the calculated values of  $\varphi(\omega)$  and those predicted by Equation 60.

With the master spreadsheet organized, macros were developed to import, transfer, and calculate data where necessary.

### **VEC Analysis Macro Process Description**

Several different automated processes were required to simplify the VEC analysis. In order to best accomplish this task, the VEC analysis macro was divided into five smaller subroutines. These subroutines were then compiled into the overall VEC analysis macro. Subroutines were named based on the functions they performed. For

the VEC analysis macro, the subroutines were called Import, Variables, Transfer, EMasterCurve, and PhaseMasterCurve.

### ***Import Subroutine***

The purpose of the Import subroutine is to import data from the raw data files into the raw data section of the master spreadsheet. The process is repeated for each of the three testing temperatures.

In order to ensure that the data included in the analysis is only from the current test, the subroutine clears any old data contained in the raw data columns. The user is then asked to provide the file path and name for the 50°F (10°C) raw data file. The subroutine opens this file and copies all of its contents. This data is imported into the raw data columns of the 50°F (10°C) raw data worksheet. The raw data file is then closed by the subroutine in order to avoid changes being made to the original data. The raw data spreadsheets contain several formulas which must be applied to each row of imported data. Because it is unknown whether or not the previous data file analyzed was longer or shorter than the current one, the subroutine determines the location of the final row of recently imported data. It then locates the final row of formulas. The formula columns are then extended or deleted to correspond with the final row of the raw data columns.

The process is repeated for the 68°F (20°C) and 86°F (30°C) raw data.

### ***Variable Subroutine***

With the raw data imported and the formulas put in place for each row, the variables  $a_\sigma$ ,  $b_\sigma$ ,  $a_\epsilon$ , and  $b_\epsilon$  can be calculated for each temperature. Data from the beginning of each VEC test tends to be highly variable. This portion of the data is truncated from the analysis at different points depending on the temperature at which the sample is tested. For 50°F (10°C), the first 5 seconds of data is not used. 3 seconds and 2 seconds were removed from the beginning of the 68°F (20°C) and 86°F (30°C) analysis, respectively. The following description is for the 50°F (10°C) process, however the same process applies to the 68°F (20°C) and 86°F (30°C) data, but using their respective time truncations.

The Variable subroutine was written to first find the row representing the point at which the test reaches 5 seconds. This row number is then recoded as  $t5sec$ . The last row of data is also found and its respective row number is also recorded as  $tEnd$ .

The columns containing the error between calculated and measured stress and strain are summed from row  $t5sec$  to row  $tEnd$  and recorded at the top of the spreadsheet, as seen in FIGURE 9. The Pearson Correlation is also determined for the measured and calculated strain and stress columns from row  $t5sec$  to row  $tEnd$  in order to provide the user with a statistical check on the accuracy of the calculations.

	S	T	U	V	W	X	Y	Z
1			Stress			Axial Strain		
2			$a_\sigma =$	2.09059463		$a_\epsilon =$	8.41E+05	
3			$b_\sigma =$	0.012454465		$b_\epsilon =$	4.45E-06	
4			Sum of Error =	0.003337569		Sum of Error =	29923.70886	
5			Correlation	0.999910765		Correlation	0.994742929	
6			t = 5 sec @	\$L\$552		t = 5 sec @	\$L\$552	
7								
8								

**FIGURE 9.** Calculated Variables from Raw Data of VEC Master Spreadsheet.

With the sum of the error and Pearson Correlation fields in place, the subroutine opens the SOLVER application in Excel in order to solve for the fitting parameters  $a_\sigma$ ,  $b_\sigma$ ,  $a_\epsilon$ , and  $b_\epsilon$ . SOLVER is set to minimize the sum of the error by changing the values of the fitting parameters. SOLVER is run by the subroutine individually for the stress and strain variables. At the completion of each run, the user is asked to either accept or reject the solution provided.

The process is then repeated for the 68°F (20°C) and 86°F (30°C) data.

### ***Transfer Subroutine***

With values for  $a_\sigma$ ,  $b_\sigma$ ,  $a_\epsilon$ , and  $b_\epsilon$  determined for each temperature, the recorded testing times now have to be transferred to the calculations worksheets where values for  $E(t)$ ,  $E_1$ ,  $E_2$ , and  $\phi$  are calculated. This simple subroutine clears the columns



where time data from previous sample analysis may exist. Then the time columns from the raw data worksheets, which have been normalized to a starting time of zero, are copied and inserted into the calculations worksheets. The subroutine then determines the location of the final row of inserted time data, locates the final row of formulas, and extends or deletes rows of the formula columns to correspond with the final row of the time column. Calculations are made based on previously entered formulas and links to the  $a_{\sigma}$ ,  $b_{\sigma}$ ,  $a_{\varepsilon}$ , and  $b_{\varepsilon}$  values from the 50°F (10°C), 68°F (20°C), and 86°F (30°C) raw data worksheets.

### ***EMasterCurve Subroutine***

To create a RM master curve for the current data, previous values of temperature, time, and  $E(t)$  are first removed by the subroutine. The time and corresponding  $E(t)$  values from the 50°F (10°C) calculations worksheets are copied and inserted into the RM master curve worksheet, beginning with the time value equal to five seconds. In order to properly insert the 68°F (20°C) time and  $E(t)$  values, the final row of the 50°F (10°C) data is located and the value is stored as the variable *LastRow10*. The 68°F (20°C) time and  $E(t)$  values are then copied from their respective calculations worksheet and inserted into the RM master curve worksheet beginning at row *LastRow10* + 1. The last row number of this new set of data is recorded as *LastRow20*. The process is repeated for the 86°F (30°C) data with the last row number recorded as *LastRow30*.

Formula cells are extended or deleted as described in previous sections. However, because each temperature will have a different value of  $a_T$  for calculating the

time-temperature superposition shifted  $E(t)$ , the formulas must be adjusted. Using *LastRow10*, *LastRow20*, and *LastRow30* to locate the beginning and end of each temperature data range, the formulas are adjusted to use the appropriate values of  $a_T$ , which are located at the top of the spreadsheet as seen in FIGURE 10. For convenience in calculations, the base 10 log of  $a_T$  is used.

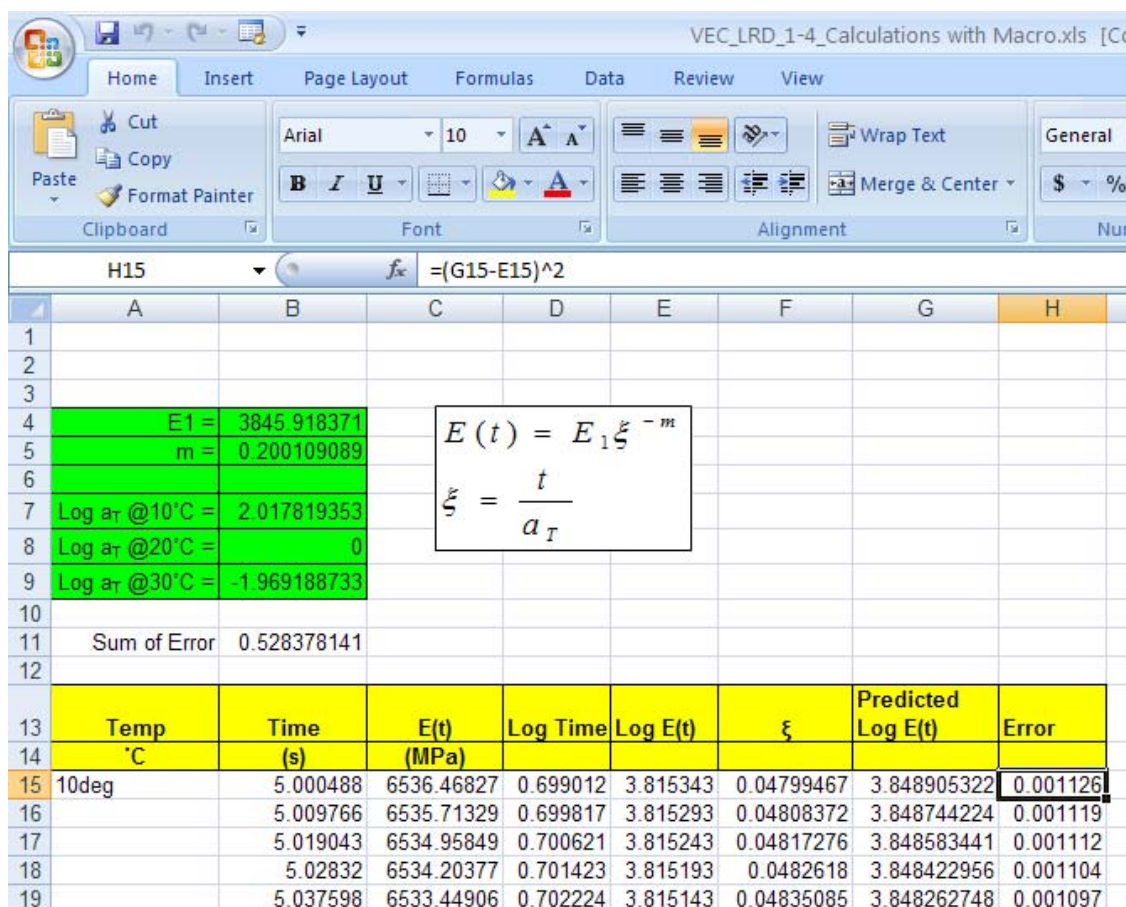
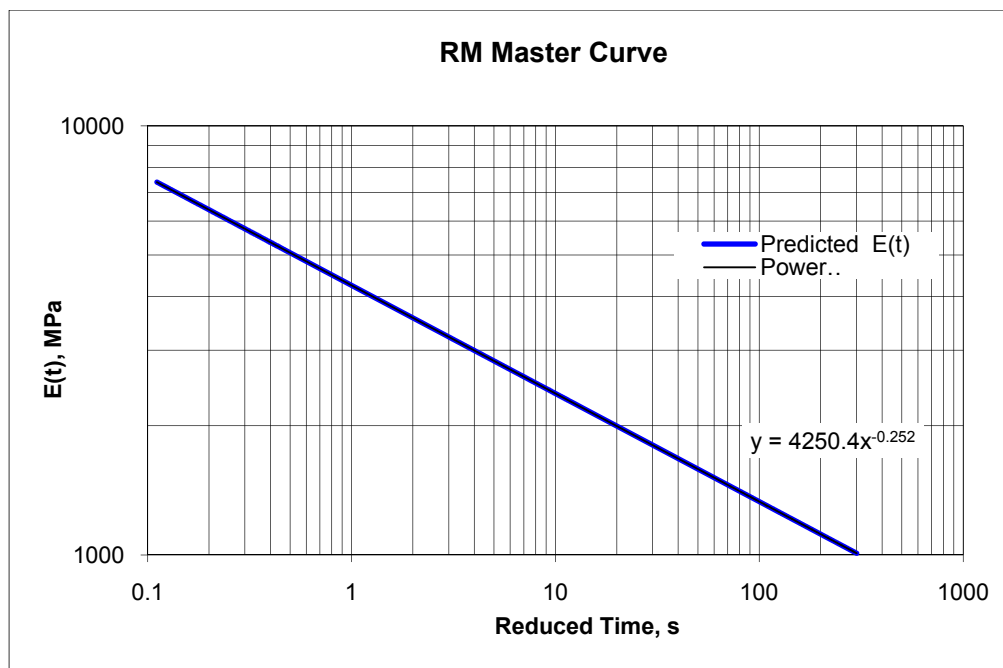


FIGURE 10. RM Master Curve Worksheet from VEC Master Spreadsheet.

The column containing the error between calculated and predicted  $E(t)$  is summed from the first row of data to row *LastRow30* and is recorded at the top of the

spreadsheet (FIGURE 10). The subroutine opens the SOLVER application in Excel in order to solve for the fitting parameters  $E_I$ ,  $m$ , and the values of  $a_T$  corresponding to 50°F (10°C) and 86°F (30°C). SOLVER is set to minimize the sum of the error by changing the values of the fitting parameters. The final results are the values of  $E_I$  and  $m$  for the material tested as well as a RM master curve (FIGURE 11) which is plotted in the RM master curve worksheet.



**FIGURE 11.** RM Master Curve.

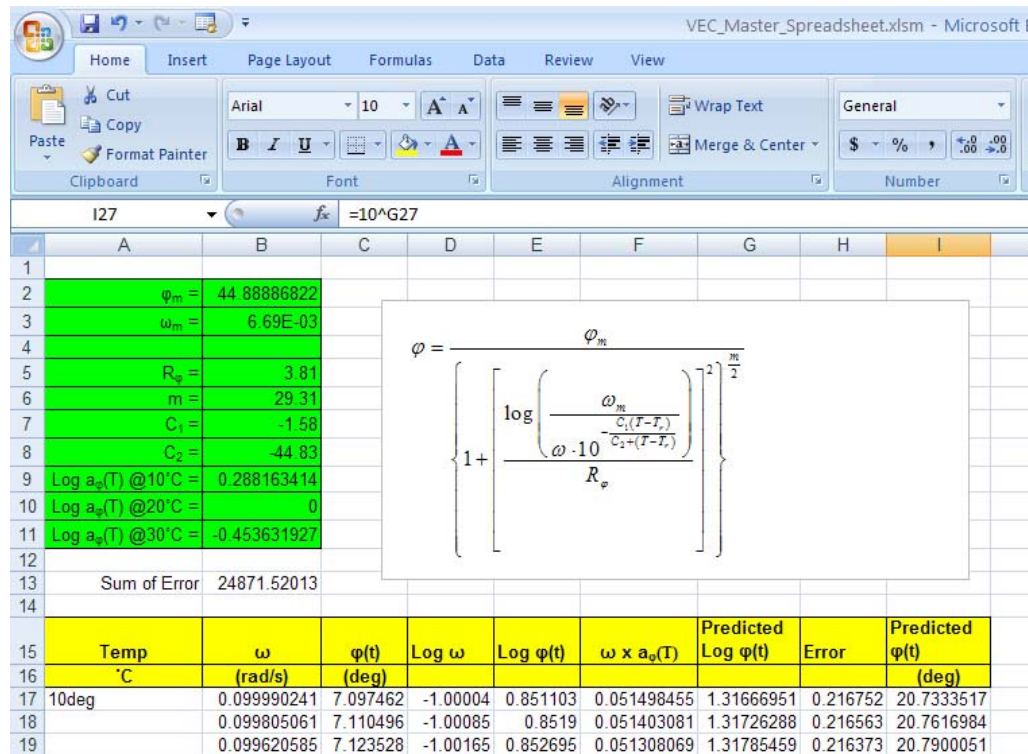
### *PhaseMasterCurve Subroutine*

To create a phase angle master curve for the current data, previous values of temperature,  $\omega$ , and  $\phi(\omega)$  are first removed by the subroutine. The  $\omega$  and corresponding  $\phi(\omega)$  values from the 50°F (10°C) calculations worksheets are copied and inserted into

the phase angle master curve worksheet, beginning with the  $\omega$  value corresponding to the testing time of five seconds. In order to properly insert the 68°F (20°C)  $\omega$  and  $\varphi(\omega)$  values, the final row of the 50°F (10°C) data is located and the value is stored as the variable *LastRow10*. The 68°F (20°C)  $\omega$  and  $\varphi(\omega)$  values are then copied from their respective calculations worksheet and inserted into the phase angle master curve worksheet beginning at row *LastRow10* + 1. The last row number of this new set of data is recorded as *LastRow20*. The process is repeated for the 86°F (30°C) data with the last row number recorded as *LastRow30*.

Formula cells are extended or deleted as described in previous sections. However, because each temperature will have a different value of  $a_\varphi(T)$  for calculating the time-temperature superposition shifted  $\varphi(\omega)$ , the formulas must be adjusted. Using *LastRow10*, *LastRow20*, and *LastRow30* to locate the beginning and end of each temperature data range, the formulas are adjusted to use the appropriate values of  $a_\varphi(T)$ , which are located at the top of the spreadsheet as seen in FIGURE 12.

The column containing the error between calculated and predicted  $\varphi(\omega)$  is summed from the first row of data to row *LastRow30* and is recorded at the top of the spreadsheet (FIGURE 12). The subroutine opens the SOLVER application in Excel in order to solve for the fitting parameters  $\varphi_m$ ,  $\omega_m$ ,  $C_1$ ,  $C_2$ ,  $R_\varphi$ , and  $m$ . SOLVER is set to minimize the sum of the error by changing the values of the fitting parameters. The final result is a phase angle master curve which is plotted in the phase angle master curve worksheet.



**FIGURE 12.** Phase Angle Master Curve Worksheet from VEC Master Spreadsheet.

### VEC Analysis Macro Summary

The VEC analysis macro combined all of the above subroutines into one continuous macro. A summary of the VEC analysis macro is shown in FIGURE 13 and FIGURE 14 with a copy of the code for this macro contained in Appendix A. The development of this macro considerably reduces the time required to perform the analysis of the VEC data in order to determine  $E_b$ ,  $m$ , and  $\varphi$ . A typical analysis takes an estimated 2 hours when run manually. With the VEC analysis macro, the analysis can be completed in less than 5 minutes. It also reduces the chances for the introduction of

human error by performing all of the importing, copying, pasting, and calculating electronically and with minimum human interaction.

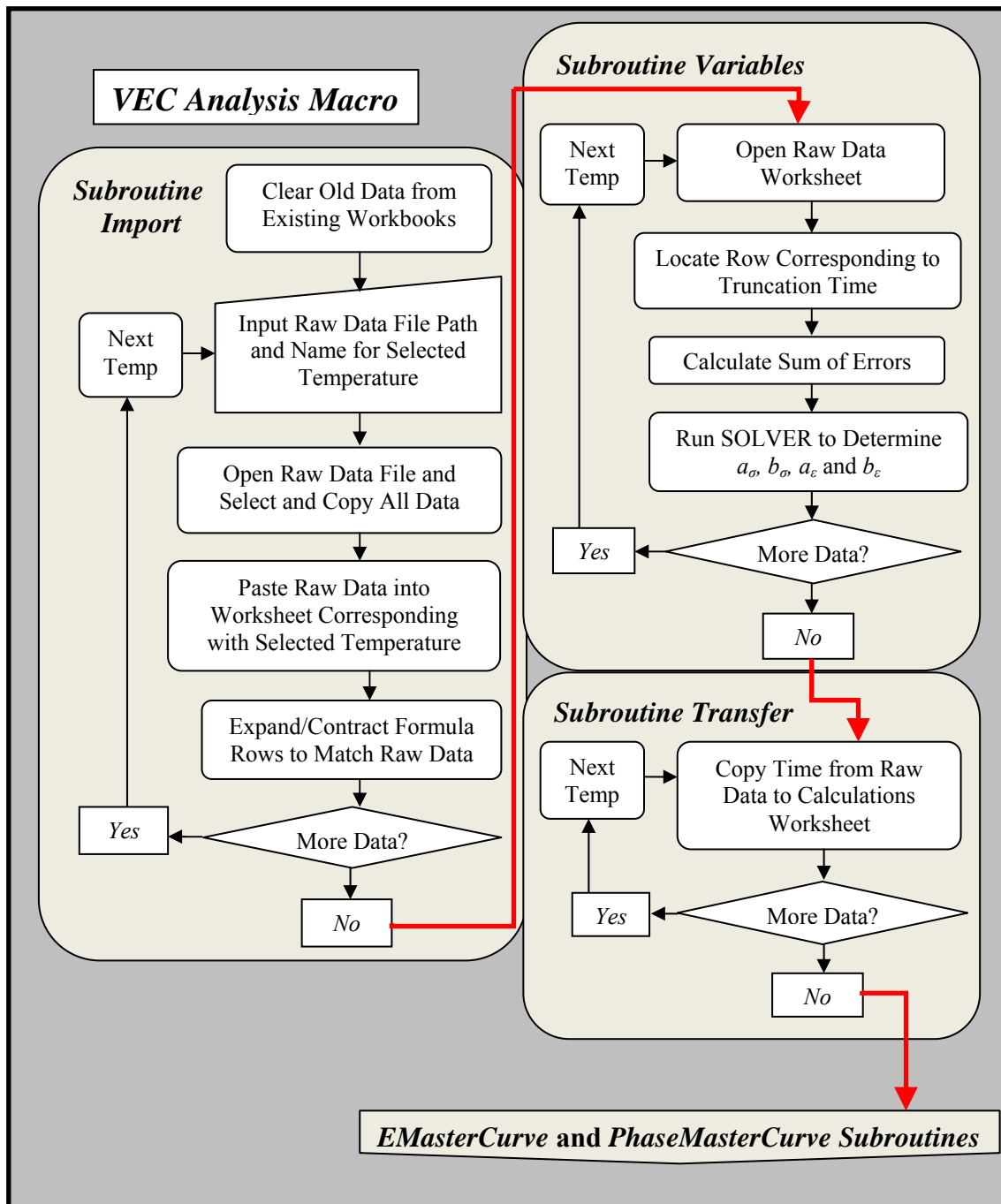
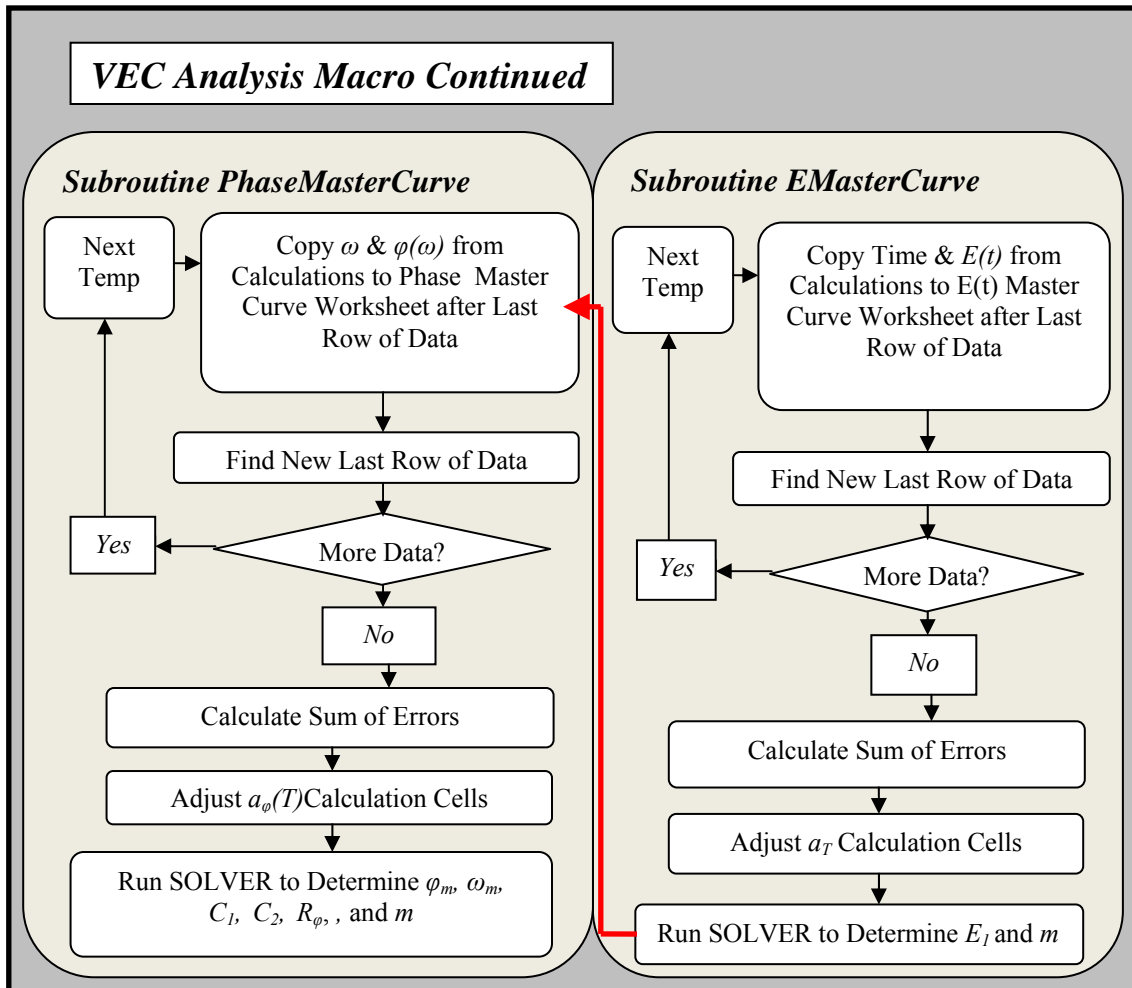


FIGURE 13. VEC Analysis Macro – Part One.



**FIGURE 14.** VEC Analysis Macro – Part Two.

While the VEC analysis macro helps to reduce error and analysis time, it is still recommended that the user carefully review and evaluate the results. Errors in data collection, such as improperly functioning LVDT's or an improperly organized data file, are overlooked by the macro and may cause the results to be erroneous.

## RDT\* ANALYSIS MACRO

In order to simplify the analysis process associated with the RDT\* test results, another macro was written which imports and analyzes data to determine  $W_{RI}$ ,  $a$ , and  $b$  from Equations 81 and 84. These values are then used to determine  $\bar{c}(N)$  and Paris's Law fracture coefficients  $A$  and  $n$ . Two spreadsheets were created which separate the evaluation of the 80  $\mu\epsilon$  analysis from the 350  $\mu\epsilon$  analysis. Both spreadsheets and macros are essentially the same with the exception that the 350  $\mu\epsilon$  spreadsheet contains the final analysis and calculations to determine  $a$  and  $b$  from Equation 84 by making use of the  $E_I$  and  $\phi$  values from the VEC test results or the average undamaged tensile modulus and phase angle ( $E_{VE}$ ,  $\phi_{VE}$ ) results from the 80  $\mu\epsilon$  RDT\* analysis to solve Equation 81. Because of the similarity of the two spreadsheets, only the 350  $\mu\epsilon$  spreadsheet will be described. To facilitate the tracking and analysis of the data, the spreadsheet is divided into three main sections.

The first section, defined as the raw data worksheets, contains the raw data for ten cycles surrounding the 1<sup>st</sup>, 50<sup>th</sup>, 100<sup>th</sup>, 250<sup>th</sup>, 500<sup>th</sup>, 750<sup>th</sup>, and 1000<sup>th</sup> cycles (the 80  $\mu\epsilon$  spreadsheet does not contain the 750<sup>th</sup> and 1000<sup>th</sup> cycle worksheets). Their purpose is to provide a specific section where the raw load and displacement data can be imported as well as formulas for calculating the measured stress, measured strain for each LVDT, and the average measured strain.

The second section, or the cycle calculations worksheets, contains the bulk of the calculations for determining  $W_{RI}$ . Calculation sheets are included for each of the above mentioned cycles. The first three columns contain time, average measured strain, and



measured stress for eleven cycles surrounding the sheet defined cycle. For example, the 50<sup>th</sup> cycle worksheet would contain the time, stress, and strain data for the 50<sup>th</sup> through the 61<sup>st</sup> load cycles of the RDT\* test.

The next nine columns contain specific points extracted from the first three columns of data. Ten cycles are represented in these columns with the maximum and minimum stress, tensile stress just preceding zero stress, compressive stress just following zero stress, minimum and maximum strain, and each of their associated times listed for each cycle.

The next set of columns contains the formulas and calculated values for ten cycles of  $T$ ,  $T_c$ , and  $T_t$  from FIGURE 6 as well as corresponding values of  $\sigma_{0t}$ ,  $\sigma_{st}$ ,  $\sigma_{0c}$ , and  $\varepsilon_0$  from Equations 64 through 70. Cells containing formulas for  $\varphi_t$  and  $\varphi_c$  for each of the ten cycles are also included. With these variables determined, the calculation of  $W_{RI}$  can be made by applying Equation 81. The formula for Equation 81 is included for each of the ten cycles. This value is averaged over the ten cycles for a final  $W_{RI}$  value.

The final section contains one worksheet: the DPSE chart worksheet. This worksheet contains the average  $W_{RI}$  values from each of the seven different cycle calculations worksheets. These values are plotted and fit with a linear equation to determine the  $a$  and  $b$  values from Equation 84.

With the master spreadsheets organized, macros were developed to import, transfer, and calculate data where necessary.

### **RDT\* Analysis Macro Process Description**

Several different automated processes were required to simplify the RDT\* analysis. In order to best accomplish this task, the RDT\* analysis macro was divided into three smaller subroutines. These subroutines were then compiled into the overall RDT\* analysis macro. Subroutines were named based on the functions they performed. For the RDT\* analysis macro, the subroutines were called Import, Transfer, and Analysis.

#### ***Import Subroutine***

The purpose of the Import subroutine is to import data from the raw data files into the raw data section of the master spreadsheets. The process is more complex than that contained in the VEC analysis macro because several sections of data representing different cycles in the RDT\* test need to be pulled from one data file and imported into the different raw data worksheets of the RDT\* analysis spreadsheet. Each set of cycles must be individually identified and imported.

In order to ensure that the data included in the analysis is only from the current test, the subroutine clears any old data contained in the raw data columns. The user is then asked to provide the file path for raw data file. In order for the subroutine to work correctly, the raw data file must be in Microsoft Excel 2007 format with the filename *specimen.xlsx*. The *specimen.xlsx* file contains the data for both the 80  $\mu\text{e}$  test and the 350  $\mu\text{e}$  test, since both are recorded during the same RDT\* test. The subroutine opens the raw data file and searches the Axial Count column for the row containing the first

point of the 502<sup>nd</sup> cycle (1<sup>st</sup> cycle if using the 80  $\mu\epsilon$  spreadsheet). The row value is stored as *FirstRow*. The subroutine then searches for the last point of the 515<sup>th</sup> cycle. The number representing this row is stored as *LastRow*. All data between rows *FirstRow* and *LastRow* are then copied and imported into the 1<sup>st</sup> cycle raw data worksheet of the master spreadsheet. The raw data spreadsheets contain several formulas which must be applied to each row of imported data. Because it is unknown whether or not the previous data file analyzed was longer or shorter than the current one, the subroutine determines the location of the final row of recently imported data. It then locates the last row of formulas. The formula columns are then extended or deleted to correspond with the final row of the raw data columns.

The process is repeated following the pattern shown in TABLE 7 until all of the required data is copied from the raw data file and imported into the master spreadsheet. The raw data file is then closed by the subroutine in order to avoid changes being made to the original data.

**TABLE 7.** RDT\* Data Import Correlations.

Axial Count (From Raw Data File)	RDT* Test Cycles	Representative 350 $\mu\epsilon$ Cycles	Master Spreadsheet Worksheet Description
1001 – 1033	502 – 515	1 – 13	1 <sup>st</sup>
1099 – 1131	550 – 565	50 – 65	50 <sup>th</sup>
1199 – 1231	600 – 615	100 – 115	100 <sup>th</sup>
1499 – 1531	750 – 765	250 – 265	250 <sup>th</sup>
1999 – 2031	1000 – 1015	500 – 515	500 <sup>th</sup>
2499 – 2531	1250 – 1265	750 – 765	750 <sup>th</sup>
2969 – 3000	1485 – 1500	985 – 1000	1000 <sup>th</sup>

### ***Transfer Subroutine***

With values for the average measured strain and applied stress determined for each range of load cycles, these values, along with the recorded testing times, now have to be transferred to their respective calculations worksheets where average values for  $W_{RI}$  are calculated. This simple subroutine simply clears the columns where time, strain, and stress data that may have existed from previous samples. Then the time, average measured strain, and stress columns from the raw data worksheets are copied and inserted into the calculations worksheets. The raw data is carefully selected to ensure that the first row of data is the beginning of the first cycle required.

### ***Analysis Subroutine***

The analysis subroutine sorts through the data supplied by the Transfer subroutine for the values required for calculation of the variables necessary to determine

$W_{RI}$ . This is accomplished by first opening the first calculation worksheet. The first value of stress is then stored as the variables *maxstress*, *minstress*, *zerostress*, and *onestress*. The first value of strain is stored as *maxstrain* and *minstrain*. The time associated with these values is stored as *timestart*. The subroutine then compares these values with the next row of data. If the value of *maxstress* is less than or equal to the stress value in the following row, *maxstress* is replaced with the new value. The time at this point is recorded as *tmaxstres*. Otherwise, these values remain unchanged. If the value of *minstress* is greater than or equal to the stress value in the following row, *minstress* is replaced with the new value. The time at this point is recorded as *tminstres*. Otherwise, these values also remain unchanged. *maxstrain* and *minstrain* follow the same respective procedures with their values being replaced if the following strain value is less than or equal to or greater than or equal to the current value, respectively. The time associated with *maxstrain* is recorded as *tmaxstrai* with *tminstrai* being recorded as the time associated with *minstrain*.

The subroutine then performs a check on the first and second values of stress. If the first value is less than zero and the second value is greater than zero, then the first is recorded as *zerostres* and the second is recorded as *onestress*. The times associated with these values are also recorded as *tzerostre* and *tonestres*, respectively.

The process is then repeated, moving to the second and third rows of data and so forth until it reaches the row where the stress changes from tension to compression. The time associated with the final tensile stress is recorded as *timeend*. This completes the first cycle. The recorded values are transferred to the extracted data cells associated with the first cycle. With these values in place, the spreadsheet uses preset formulas to calculate of  $T$ ,  $T_c$ ,  $T_t$  as well as corresponding values of  $\sigma_{0t}$ ,  $\sigma_{st}$ ,  $\sigma_{0c}$ , and  $\epsilon_0$  from Equations 64 through 70. Equation 63 is used to calculate  $\varphi_t$  and  $\varphi_c$ , which then allows for the calculation of  $W_{RI}$  for the first cycle.

The subroutine then moves to the first point in the next cycle and repeats the process. This is repeated until 10 cycles of data have been extracted and calculated.  $W_{RI}$  is averaged from these 10 cycles to represent the first cycle of the RDT\* test.

The process is repeated for each of the six remaining calculations worksheets. Once each worksheet is completed, the subroutine opens the DSPE Chart worksheet and runs the SOLVER application to solve for values of  $a$  and  $b$  from Equation 84.

### ***CopyAve Subroutine***

Because the 350  $\mu\epsilon$  analysis requires  $E_{VE}$  and  $\phi_{VE}$ , an additional subroutine was created to copy these values, which are calculated in the 80  $\mu\epsilon$  spreadsheet, into the 350  $\mu\epsilon$ .  $E_I$  and  $\phi$  from the VEC test can also be used in the 350  $\mu\epsilon$  spreadsheet, but were not included in the analysis at this time.

### **RDT\* Analysis Macro Summary**

As with the VEC analysis macro, the RDT\* analysis macro combines all of the above subroutines into one continuous macro. A summary of the RDT\* analysis macro is shown in FIGURE 15 with a copy of the code for the 350  $\mu\epsilon$  macro contained in Appendix A. The development of this macro considerably reduces the time required to perform the analysis of the RDT\* data in order to determine  $b$ . To run these processes manually would take an estimated 8 hours. With the RDT\* analysis macro, the analysis can be completed in less than 3 minutes. It also reduces the chances for the introduction of human error by performing all of the importing, searching, copying, pasting, and calculating electronically and with minimum human interaction.

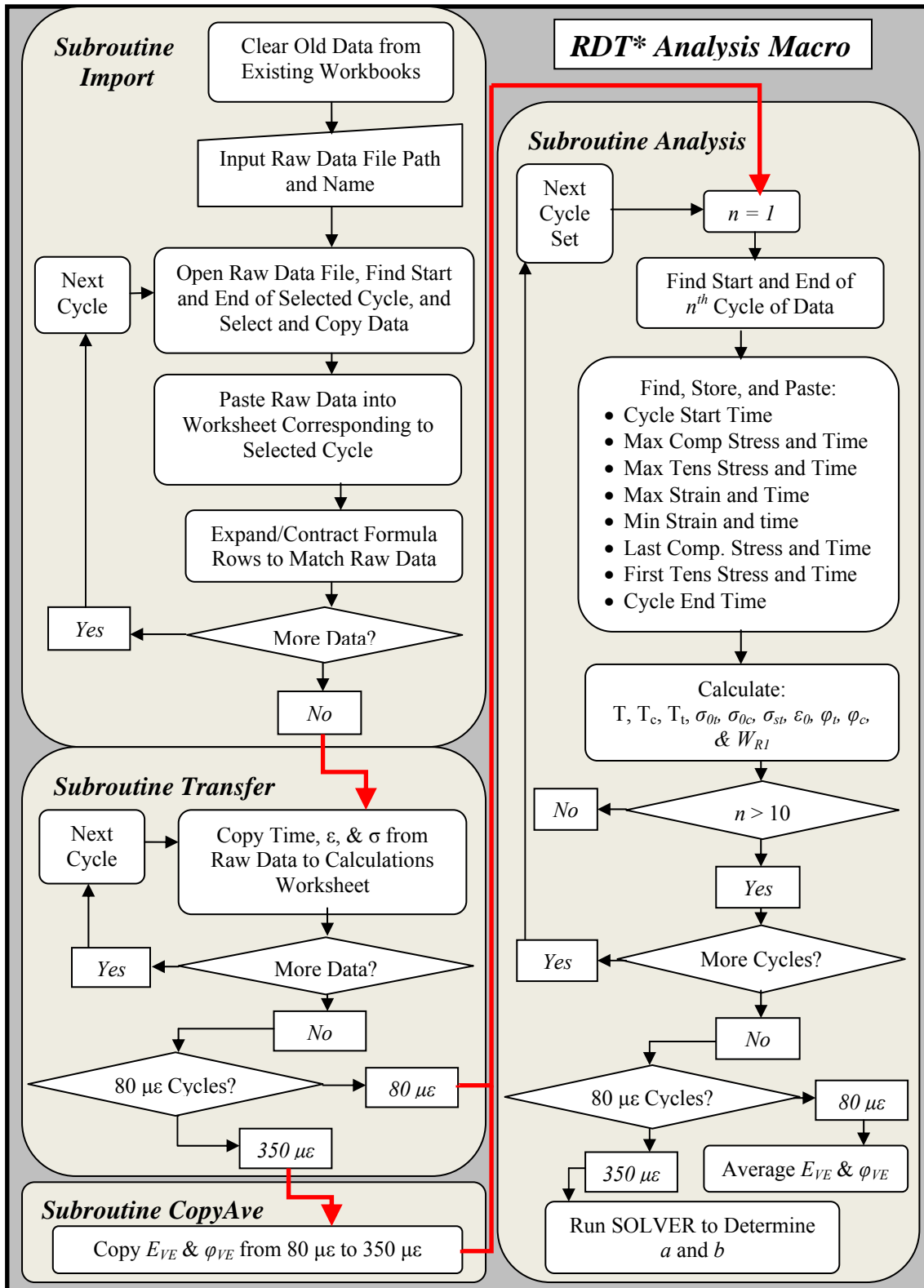


FIGURE 15. RDT\* Analysis Macro.



While the RDT\* analysis macro helps to reduce error and analysis time, it is still recommended that the user carefully review and evaluate the results. Errors in data collection, such as improperly functioning LVDT's or an improperly organized data file, are overlooked by the macro and may cause the results to be erroneous.

The RDT\* macro also uses the 80  $\mu\epsilon$  spreadsheet to correctly calculate values in the 350  $\mu\epsilon$  spreadsheet. It is recommended that the CopyAve subroutine be adjusted to copy  $E_I$  and  $\phi$  from the VEC analysis spreadsheet instead of the  $E_{VE}$  and  $\phi_{VE}$  values from the 80  $\mu\epsilon$  spreadsheet.

Finally, because the RDT\* analysis spreadsheet frequently uses averages in making calculations, occasional outliers can be found in the data that have to be manually eliminated. The macro could be adjusted to seek out and eliminate these values from the calculations.

With the development of the analysis macros for the VEC and RDT\* tests, several samples could be fabricated and tested in order to analyze the testing methods described in earlier sections. With the development of the macros, analysis of the test data takes considerably less time, making it more feasible to test and compare the results of many samples.

## **ANALYSIS OF VEC AND RDT\* TESTING METHODS**

In order to verify the application of the VEC and RDT\* tests, 14 samples were fabricated, tested, analyzed, and compared. Samples were fabricated at optimum, optimum +0.5%, and optimum -0.5% binder contents with air voids varying from low to medium to high. This was done in order to ensure the adequacy of the tests to produce the desired results. The materials and methods used for fabricating the samples are described. Successes, issues, and recommendations for both the VEC and RDT\* tests are also described.

### **MATERIAL SELECTION AND PREPARATION**

LMLC samples were fabricated based on a TxDOT Type C mix previously used in the Laredo District for US Route 277. A TxDOT Type C mix is a dense graded HMA mix that follows the gradation shown in TABLE 8 and is used as a course surface mix. Binders used must be performance graded (PG) binders (21). The following sections describe the properties associated with this particular mix.

**TABLE 8.** TxDOT Type C Master Gradation Bands (% Passing by Weight or Volume) (21).

Sieve Size		Type C
#	mm	Course Surface
1-1/2"	37.5	100.0
1"	25.0	100.0
3/4"	19.0	95 - 100
3/8"	9.5	70 - 85
No. 4	4.75	43 - 63
No. 8	2.36	32 - 44
No. 30	0.600	14 - 28
No.50	0.300	7 - 21
No. 200	0.075	2 - 7

### Aggregate Gradation

Aggregates were selected based on the Laredo, US Route 277 mix design (LRD Mix) comprised of a blend of four different aggregate gradations. Three of the aggregates consist of limestone from the South Texas Aggregates Inc., Sabinal Quarry located in Uvalde County, Texas. They include a course limestone aggregate, a blend of Type D and Type F limestone aggregates, and manufactured sand. The fourth aggregate used in the blend is manufactured sand from the Vulcan Materials Company, Knippa Quarry, also located in Uvalde County, Texas. The bin fractions and gradations of each blend are shown in TABLE 9.

**TABLE 9.** LRD Mix Aggregate Gradation Blend.

		Material 1		Material 2		Material 3		Material 4		
Aggregate Source:		South Texas Aggregate		South Texas Aggregate		South Texas Aggregate		Vulcan Materials		
Aggregate Quarry:		Sabinal		Sabinal		Sabinal		Knippa		
Description:		Course Limestone Aggregate		Type D/F Blend		Manufactured Sand		Manufactured Sand		Comb Total
Percent Used:		21	%	31	%	29	%	19	%	100
Sieve Size		Cum. % Pass	Wt. Cum. % Pass	Cum. % Pass	Wt. Cum. % Pass	Cum. % Pass	Wt. Cum. % Pass	Cum. % Pass	Wt. Cum. % Pass	Cum. % Pass
#	mm									
1"	25.0	100.0	21.0	100.0	31.0	100.0	29.0	100.0	19.0	100.0
3/4"	19.0	100.0	21.0	100.0	31.0	100.0	29.0	100.0	19.0	100.0
3/8"	9.5	6.2	1.3	96.6	29.9	100.0	29.0	100.0	19.0	79.2
# 4	4.75	1.1	0.2	37.4	11.6	99.9	29.0	99.7	18.9	59.7
# 8	2.36	0.8	0.2	5.1	1.6	83.6	24.2	85.0	16.2	42.1
# 30	0.600	0.6	0.1	2.0	0.6	46.1	13.4	24.4	4.6	18.8
# 50	0.300	0.4	0.1	1.6	0.5	33.9	9.8	11.3	2.1	12.6
# 200	0.075	0.2	0.0	1.0	0.3	19.1	5.5	1.3	0.2	6.1

Samples of the aggregates were blended, and a wet sieve analysis was performed.

The final gradation was adjusted to account for any extra fines discovered during the wet-sieve analysis and is shown in TABLE 10.

**TABLE 10.** LRD Mix Adjusted Aggregate Gradation Based on Wet-Sieve Analysis.

Sieve Size		Cumulative % Passing	Specification Limits		Cumulative % Retained	Individual % Retained
#	mm		Low	High		
1"	25.0	100.0	100	100	0.0	0
3/4"	19.0	100.0	95	100	0.0	0.0
3/8"	9.5	79.2	70	85	20.8	20.8
No. 4	4.75	59.7	43	63	40.3	19.5
No. 8	2.36	41.6	32	44	58.4	18.1
No. 30	0.600	17.7	14	28	82.3	23.9
No.50	0.300	11.0	7	21	89.0	6.7
No. 200	0.075	3.3	2	7	96.7	7.7

### Binder Type and Content

A Valero Asphalt binder graded as PG 70-22 was selected based on the binder type used for US Route 277. This was done in order to mimic field conditions as closely as possible. An optimum asphalt content of 4.5% was selected based on the original design.

### Mixing, Molding, and Compaction

Prior to mixing, aggregates were placed in an oven at the mixing temperature of 149°C (300°F) and were left overnight in order to remove any moisture. The binder was also heated to the same mixing temperature for 2 hours just prior to mixing. Mixing for the 14 samples was completed according to the binder contents and maximum specific gravities listed in TABLE 11. The mixture was then short term oven aged at the molding temperature of 135°C (275°F) for four hours. This short term oven aging is

intended to represent the aging that takes place during the mixing, transporting, and placing of HMA in the field.

**TABLE 11.** Binder Content,  $G_{mm}$ , and Air Voids for LRD Mix Samples.

# of Samples	Binder Content		$G_{mm}$	AV Content	
2	Optimum	4.5%	2.540	High	> 7%
2	Optimum	4.5%	2.540	Medium	5% - 7%
2	Opt +0.5%	5.0%	2.523	High	> 7%
2	Opt +0.5%	5.0%	2.523	Medium	5% - 7%
2	Opt +0.5%	5.0%	2.523	Low	< 5%
2	Opt -0.5%	4.0%	2.557	High	> 7%
2	Opt -0.5%	4.0%	2.557	Low	< 5%

Samples were molded and compacted using the Super Gyrotory Compacter (SGC) shown in FIGURE 16 to a 6 inch (152 mm) diameter by 6 inch (152 mm) height in order to meet a specified air voids content.



**FIGURE 16.** Super Gyrotory Compactor (SGC).

### **Air Voids Content**

The initial air voids content found in the 6 inch (152 mm) diameter by 6 inch (152 mm) high samples was slightly higher than those shown in TABLE 11 due to the conditions imposed by the SGC mold. Material on the boundaries cannot be compacted the same as that in the center of the mold. In order to remedy this problem, samples were molded at a higher air void content and then cored to a 4 inch (102 mm) diameter. The sample then had one inch (25 mm) trimmed from each end to produce the final 4 inch (102 mm) diameter by 4 inch (102 mm) high sample with the correct low, medium, or high range of air voids. The coring and trimming of the LMLC samples provided samples with a more even distribution of air voids, as would be found in the field (22).

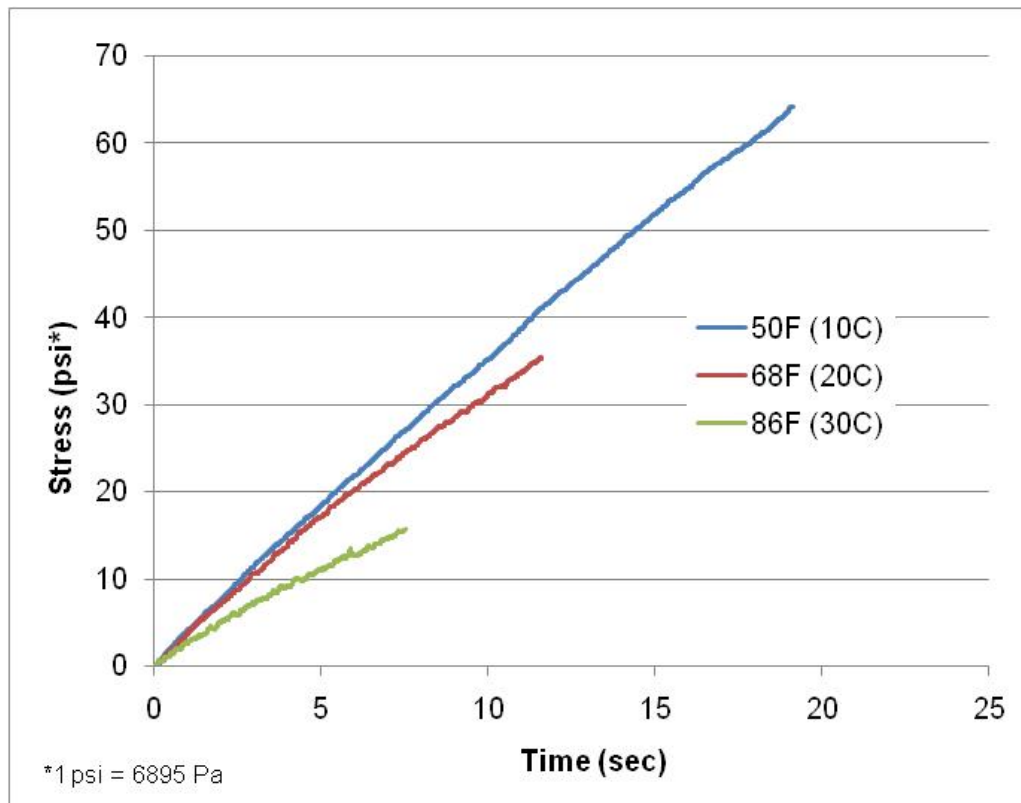
## **VEC TEST ANALYSIS**

With samples of various binder and air void contents prepared, testing was performed with the intent of evaluating the effectiveness of the VEC test. Tests performed on the samples revealed portions of the VEC test which were successful as well as exposing issues that require resolution. These successes, issues, and recommendations for changes with respect to the VEC test are discussed in the following sections.

### **VEC Test Successes**

With a few exceptions, all samples tested using the VEC test followed the generally expected trends. The Materials Testing System (MTS) machine was capable of applying the controlled monotonically increasing load at the predefined strain rate of 0.01 inches per minute (0.254 mm/min). A plot of the increasing stress with respect to time is shown in FIGURE 17. FIGURE 17 shows that the applied loading was relatively free of noise and continued at a steady rate until completion of the test. The stress levels at higher temperatures are less than those at lower temperatures, as would be expected. It can also be seen that the test is quick, with the longest test lasting approximately 20 seconds.

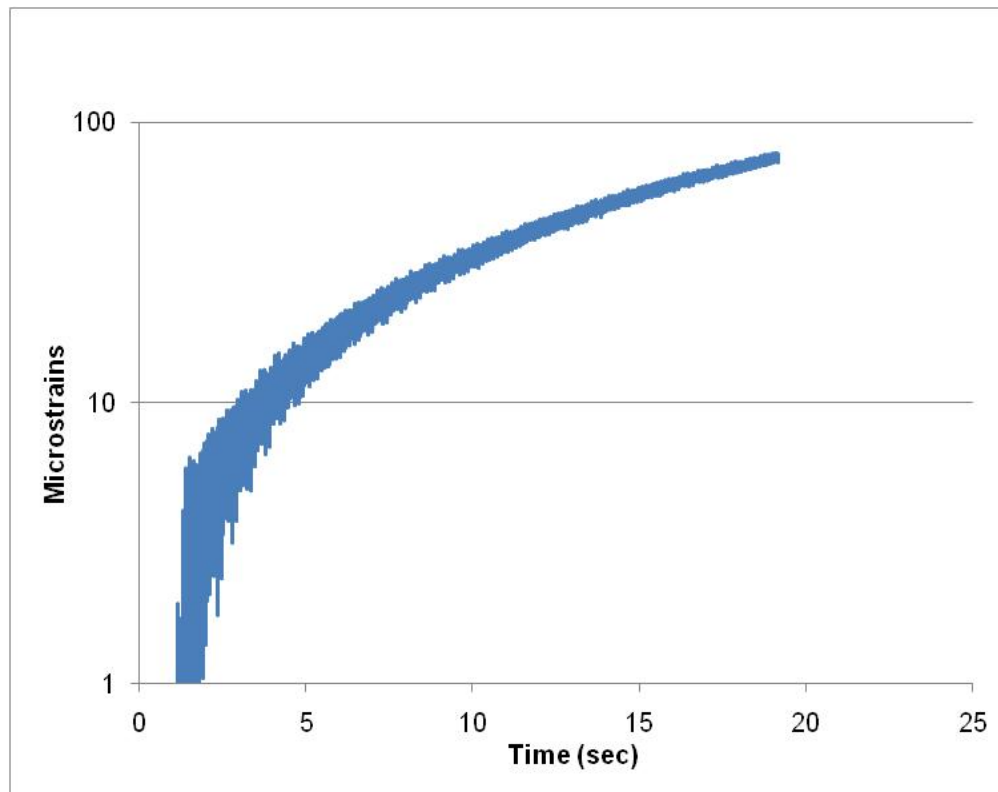




**FIGURE 17.** Typical Applied Stresses During VEC Test.

A plot of the average strain for a sample tested at 50°F (10°C) is shown in FIGURE 18. The strain levels gradually increase towards 100  $\mu\epsilon$  as planned. Note the large amount of variability in the strain levels prior to the 5 second point. This variability necessitated the truncation of the first 5 seconds of data for the 50°F (10°C) test prior to calculating the relaxation modulus and the development of the RM mastercurve. Similar responses can be seen for the 68°F (20°C) and 86°F (30°C) tests, necessitating the 3 second and 2 second truncations, respectively.

Perhaps one of the greatest benefits of running the VEC test is that it is designed to collect data without causing damage. If a test doesn't appear to follow expected trends, the test can be rerun after allowing the sample to rest for a short period of time.



**FIGURE 18.** 50°F (10°C) Average Strain Response from VEC Test.

Calculated values of  $E_1$  and  $m$  for each of the 14 samples are listed in TABLE 12. Upon first glance, the results shown appear to fall within a reasonable range. However, no clear correlation could be made between these values and the different binder and air voids contents. A thorough review of the test data gives insight into some of the issues that need to be resolved before reliable results can be obtained.

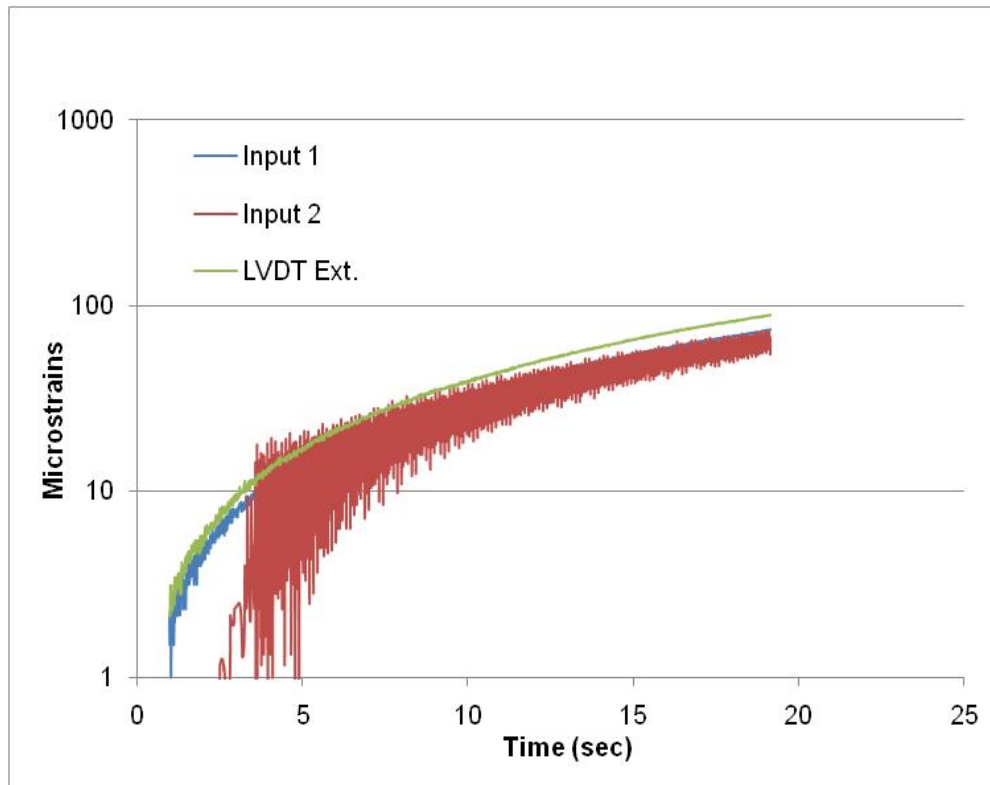
**TABLE 12.**  $E_I$  and  $m$  Values from VEC Test.

Sample #	Binder Content Opt, +0.5%, -0.5%	Air Content L, M, H	AV %	$E_I$		$m$ ---
				MPa	psi	
1-3	-0.5%	L	3.4%	4186	6.07.E+05	0.217
1-4	-0.5%	L	3.2%	3846	5.58.E+05	0.200
2-3	-0.5%	H	7.9%	5625	8.16.E+05	0.565
2-4	-0.5%	H	7.9%	5226	7.58.E+05	0.434
3-3	+0.5%	M	5.9%	1825	2.65.E+05	0.559
3-4	+0.5%	M	5.8%	2694	3.91.E+05	0.308
4-3	+0.5%	H	8.7%	3458	5.01.E+05	0.529
4-4	+0.5%	H	9.0%	3512	5.09.E+05	0.568
5-3	+0.5%	L	3.0%	2488	3.61.E+05	0.179
5-4	+0.5%	L	3.2%	3382	4.90.E+05	0.241
6-3	Optimum	M	5.9%	2901	4.21.E+05	0.235
6-4	Optimum	M	6.3%	2754	3.99.E+05	0.212
7-3	Optimum	H	9.4%	2941	4.26.E+05	0.286
7-4	Optimum	H	8.8%	2321	3.37.E+05	0.260

### VEC Test Issues

Throughout testing and analysis, several issues arose which affected the outcome of the VEC test results. First, in several of the tests one of the LVDT's recorded a considerable amount of noise. An example of this type of LVDT malfunction is shown in FIGURE 19. As can be seen, the LVDT's represented by Input 1 and LVDT Ext plot a smooth, upward trending line. The Input 2 LVDT, however, fluctuates so significantly that it is impossible to identify what the sample is actually experiencing. The LVDT interference from Input 2 makes it impossible to calculate an average strain level with any degree of confidence. By changing LVDT's, Input 2 was identified as a damaged

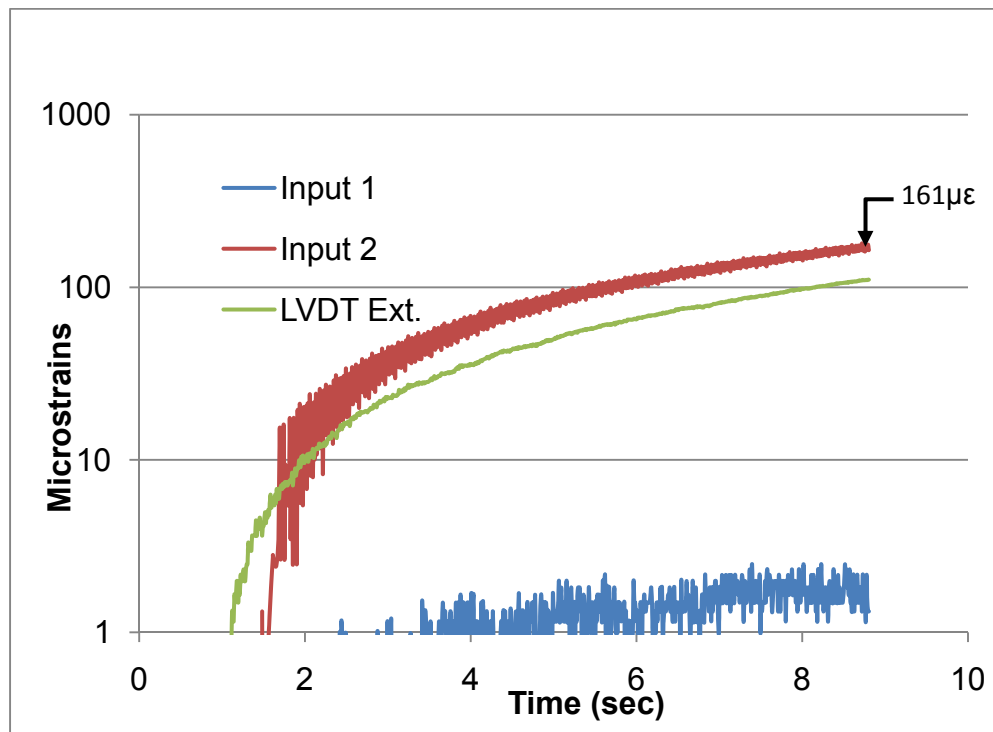
LVDT and was replaced. If the LVDT's are not carefully checked prior to testing, test data may not be usable and the test will need to be repeated.



**FIGURE 19.** VEC Test Indicating LVDT Noise.

FIGURE 20 identifies the next issue that arose when running the VEC test. The VEC test is run to a maximum strain of  $100 \mu\epsilon$ . By staying below this point, the sample remains undamaged and can be either retested in the VEC test or used for the RDT\* test. Currently, the stopping point of the VEC test is controlled by the user. A selected LVDT reading is monitored until it reaches the  $100 \mu\epsilon$  limit. However, the sample exhibits slightly different strain rates throughout its cross-section. One side of the sample may have a higher stiffness than another. If the user monitors the LVDT

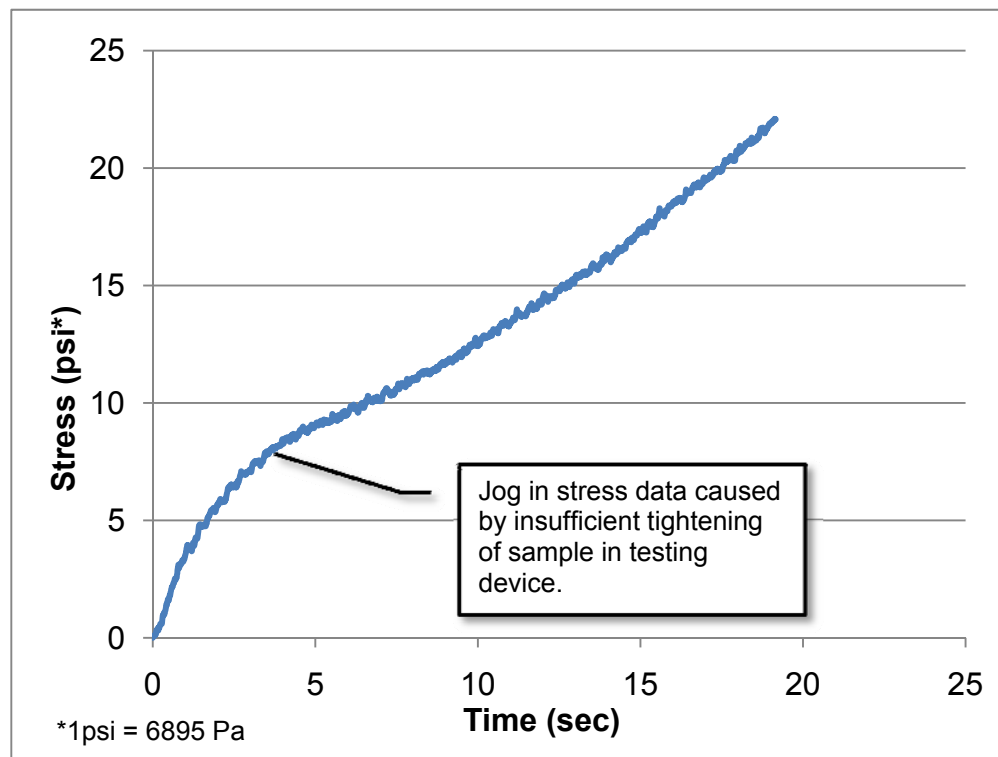
associated with the stiff side of the sample in order to control the completion of the test, it is likely that the less stiff sides will exceed the  $100 \mu\epsilon$  limit. In FIGURE 20, LVDT Ext. was used to control the test completion. It can be seen that Input 2 was placed on a less stiff area of the sample than was LVDT Ext. The result is that Input 2 exceeded the  $100 \mu\epsilon$  limit by approximately  $65 \mu\epsilon$ . Because the VEC test is used to calculate the undamaged properties of the material, damaging the sample during testing makes the data unreliable for accurate analysis.



**FIGURE 20.** VEC Test Exceeding  $100 \mu\epsilon$ .

In addition to exceeding the maximum  $100 \mu\epsilon$  limit, FIGURE 20 also shows another issue that arose during testing. The sample was fitted with an LVDT bracelet

which measures the horizontal displacement during testing. These data can be used to calculate Poisson's ratio, but they are not used for this study. For the test associated with FIGURE 20, the vertical LVDT labeled Input 1 was hung up on the LVDT bracelet. This rendered the data from Input 1 useless.

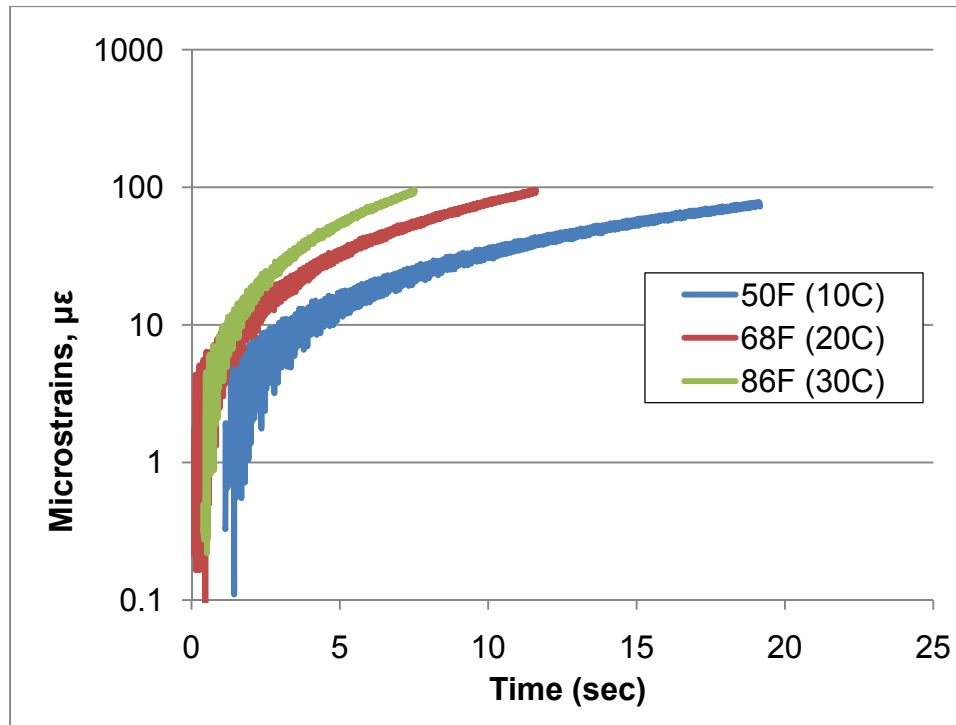


**FIGURE 21.** VEC Test Insufficient Sample Tightening.

Occasionally, the sample was not sufficiently tightened when placed in the MTS testing machine. In this case, the load would cause the tightening threads to slip which

produced the jog in the stress data that is shown in FIGURE 21. The sample would have to be allowed to rest, reinserted, and retested before reliable data could be obtained.

The final issue associated with the VEC test is related to the rate at which the sample is tested. The testing rate is set at 0.01 inches per minute (0.254 mm/min) and is controlled by machine displacement. While the machine can successfully match this rate, the samples behave differently for different temperatures. FIGURE 22 shows how the change in temperature affects the sample strain rate. At higher temperatures, such as 86°F (30°C) the strain rate experienced by the sample is significantly higher than that experienced at 50°F (10°C). This results in a reduction of the total testing time at higher temperatures. For the sample shown in FIGURE 22, the 50°F (10°C) test took approximately 20 seconds while the 86°F (30°C) test only lasted 8 seconds. A reduction in testing time also reduces the number of data points collected. This reduction in data points does not allow for sufficient data to perform the necessary calculations accurately.



**FIGURE 22.** VEC Test Average Microstrains Recorded for Same Sample at Three Different Testing Temperatures.

The majority of the data collected did not provide the expected results due to the issues described in this section. Changes must be made to the VEC testing procedure in order to ensure that accurate and reliable data is collected. Only by collecting accurate data can an accurate analysis be performed.

### **VEC Test Recommendations**

In order to resolve the issues associated with the VEC test, several recommendations have been made.

First, all LVDT's must be properly calibrated before testing and monitored regularly during testing. If LVDT's begin to exhibit fluctuations exceeding 10 μɛ, they



should be immediately replaced and the sample retested. A careful check of the LVDT's before beginning the test should also be made to ensure that they are not in contact with anything that will inhibit their movement. The sample should also be securely tightened so that there is no movement of the sample or unwanted displacement in the attaching fixtures. If the test results show a jog in the applied stress, the sample should be removed, allowed to rest, and then retested.

It has been shown that the test can produce strain levels above  $100 \mu\epsilon$  depending on the placement of the LVDT's. Above  $100 \mu\epsilon$  the sample may experience damage. This response is less likely to happen during the  $50^{\circ}\text{F}$  ( $10^{\circ}\text{C}$ ) test due to the higher overall stiffness of the sample. However, the  $50^{\circ}\text{F}$  ( $10^{\circ}\text{C}$ ) test should still reveal which side of the sample is the stiffest and which is the softest. The LVDT on the soft side can be located after careful evaluation of the  $50^{\circ}\text{F}$  ( $10^{\circ}\text{C}$ ) data. The  $68^{\circ}\text{F}$  ( $20^{\circ}\text{C}$ ) and  $86^{\circ}\text{F}$  ( $30^{\circ}\text{C}$ ) tests should be terminated based on the strain levels associated with this LVDT on the soft side identified from the  $50^{\circ}\text{F}$  ( $10^{\circ}\text{C}$ ) data. This will reduce the likelihood of exceeding the  $100 \mu\epsilon$  limits at the higher temperatures and thus reduce the chances of damaging the sample. It is also recommended that an evaluation of the testing software be made to determine if the termination of the test can be LVDT controlled.

Finally, it is recommended that the VEC test loading rate be changed from 0.01 inches per minute (0.254 mm/min) to 0.004 inches per minute (0.102 mm/min). This will extend the testing time as well as the number of data points collected for the  $86^{\circ}\text{F}$  ( $30^{\circ}\text{C}$ ) test. If this does not produce nearly 20 seconds worth of data at  $86^{\circ}\text{F}$  ( $30^{\circ}\text{C}$ ), the

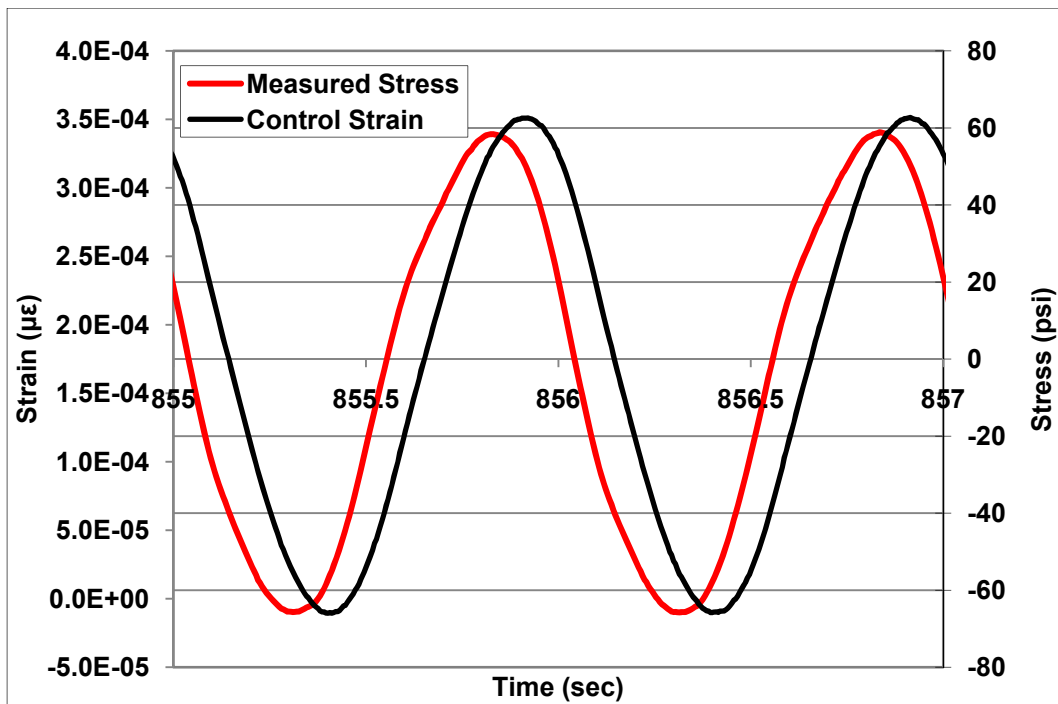
loading rate should be further reduced until sufficient data can be collected to provide an adequate analysis.

### **RDT\* TEST ANALYSIS**

RDT\* tests were performed on the samples at 68°F (20°C) following completion of the VEC tests at 50°F (10°C), 68°F (20°C), and 86°F (30°C). These RDT\* tests were run with the intent of evaluating the effectiveness of the testing protocol. Tests performed on the samples revealed portions of the RDT\* test which were successful and exposed issues that require resolution. These successes, issues, and recommendations for changes with respect to the RDT\* test are discussed in the following sections.

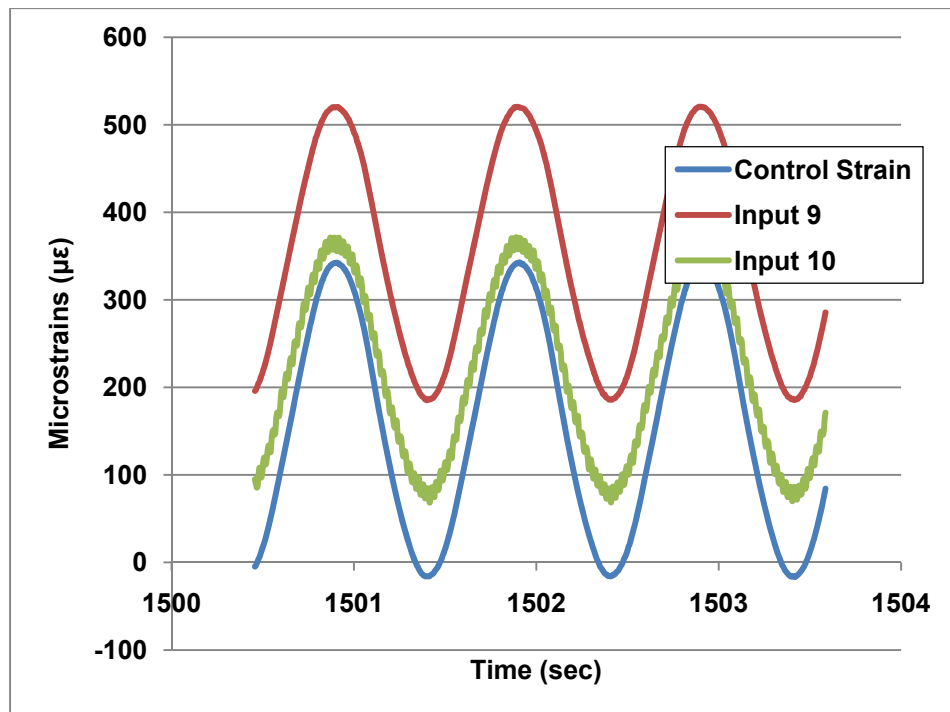
#### **RDT\* Test Successes**

The RDT\* tests ran to completion for all but one of the 14 samples tested. FIGURE 23 shows that the MTS testing machine successfully controlled the loading to the required 1 Hz frequency and the 80  $\mu\epsilon$ /350  $\mu\epsilon$  limits. It also shows the strain lagging behind the stress as expected.



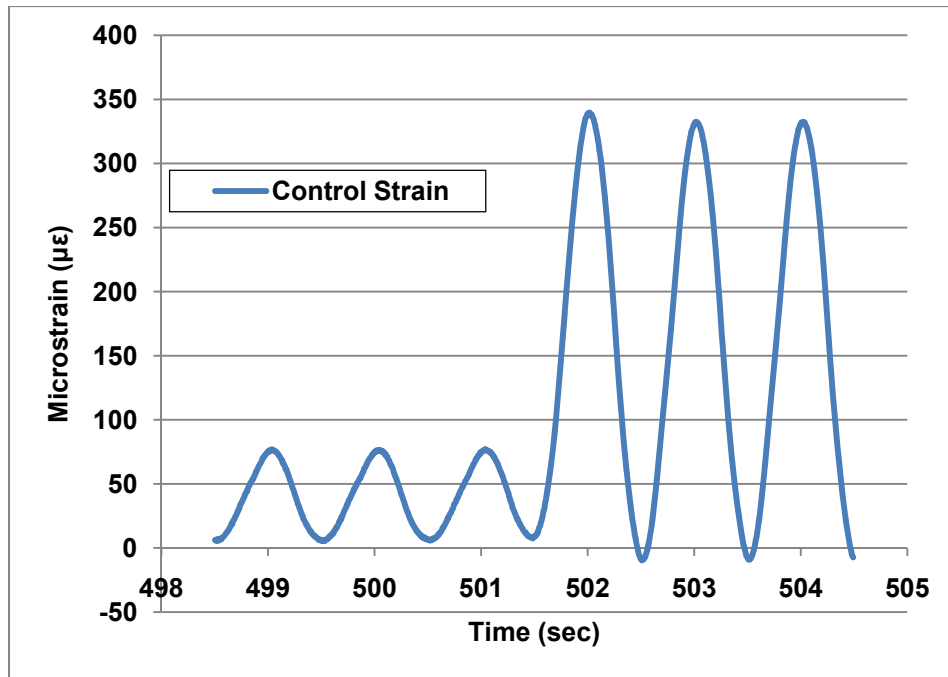
**FIGURE 23.** Typical RDT\* Test Applied Stress and Resulting Strain.

While the plot of the controlling LVDT consistently stays between zero and 350  $\mu\epsilon$ , the other two LVDT plots begin to drift as shown in FIGURE 24. As the sample experiences damage under the repeated loading, the uncontrolled LVDT's fail to completely recover. This drifting is an indication that damage is occurring in the sample. Because the 350  $\mu\epsilon$  RDT\* test is used to determine the damaged properties of the sample, FIGURE 24 shows that the test is performing as planned and expected.



**FIGURE 24.** Drifting LVDT's in RDT\* Test.

Another concern expressed before running the RDT\* test was that the MTS machine would not be able to successfully and smoothly switch from the 80  $\mu\epsilon$  limit to the 350  $\mu\epsilon$  limit. If the MTS machine could not make a smooth transition, it was feared that the sample would be either damaged to a point that it would not provide usable data or that it would be completely destroyed. However, FIGURE 25 shows that the MTS machine could successfully make the immediate transition required.



**FIGURE 25.** RDT\* Test 80  $\mu\epsilon$  to 350  $\mu\epsilon$  transition.

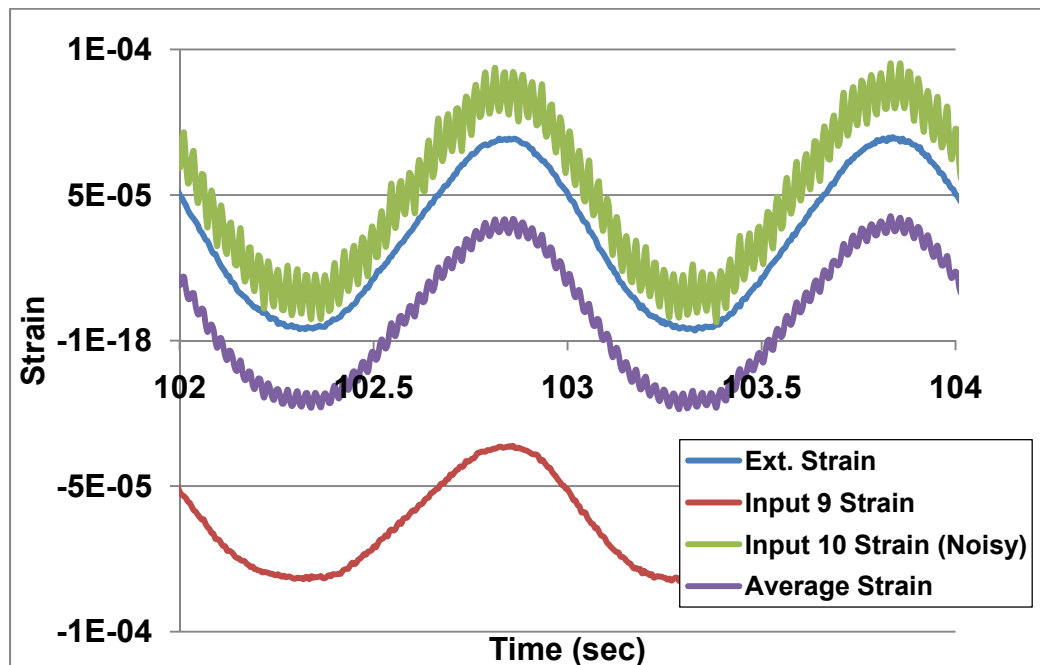
The RDT\* test appeared to be most successful for the stiffer mixes. While all of the tests but one ran to completion, only two of the tests provided data that was accurate enough to use in the CMSE\* method. These included the two mixes that had low air voids and low binder contents, and therefore, were the stiffer mixtures.

### **RDT\* Test Issues**

By examining, reviewing, and evaluating data from the less successful tests; several issues were identified as possible reasons for inadequate or poor quality data collection.

As with the VEC test, damaged LVDT's recorded sufficient noise to affect the analysis and overall results. This noise, as shown in FIGURE 26, makes it difficult to

average the three LVDT readings into one consistent and smooth average. When the averaged data is not smoothed, it is difficult to pick the peaks and valleys of the strain response necessary for effective evaluation of  $W_{RI}$ . When using the macro developed for analysis of the data, these fluctuations cause the macro to find the maximum and minimum points in the noise rather than the maximum and minimum of the strain response. The use of these short “cycles” rather than the actual strain cycle causes inaccurate calculation of  $\phi$ ,  $E_N$ , and, ultimately,  $W_{RI}$ .



**FIGURE 26.** RDT\* Test Noisy LVDT and Effects on Average.

The next issue discovered during the analysis of the RDT\* test data was the effects of stiff side LVDT control versus soft side LVDT control. Because the MTS machine is controlled by an LVDT attached to the sample, the applied load, as well as

the strain experienced by the other two LVDT's, depends on the controlling LVDT. The location of the controlling LVDT was randomly selected. If the controlling LVDT was placed on the stiffest side of the sample, the sample would experience a net tensile strain as shown by the other two LVDT's. The resulting fracture damage would then be the result of tensile stresses that the sample experienced. However, if the controlling LVDT was placed on the soft side of the sample, the other two LVDT's show that the sample undergoes a net compressive strain. This type of response can be seen in FIGURE 27. Because the RDT\* test is utilized as a direct tension test to determine the tensile properties of the material, net compressive strains do not provide the data necessary to make an accurate analysis of fatigue resistance. Unfortunately, all but one of the RDT\* tests that were completed had the controlling LVDT located on a side other than the stiffest side. Therefore, for most of these results, this resulted in one, and sometimes two, of the three LVDT readings drifting negative. FIGURE 27 is a good example of the LVDT being placed on the softest side of the sample. The controlling LVDT holds the strain level at its location within the zero to 350  $\mu\epsilon$  limits. The other two LVDT's show their respective sample sides drifting further and further into compression until both experience a net compressive strain throughout the entire cycle. When this occurs, the resulting data is unusable.

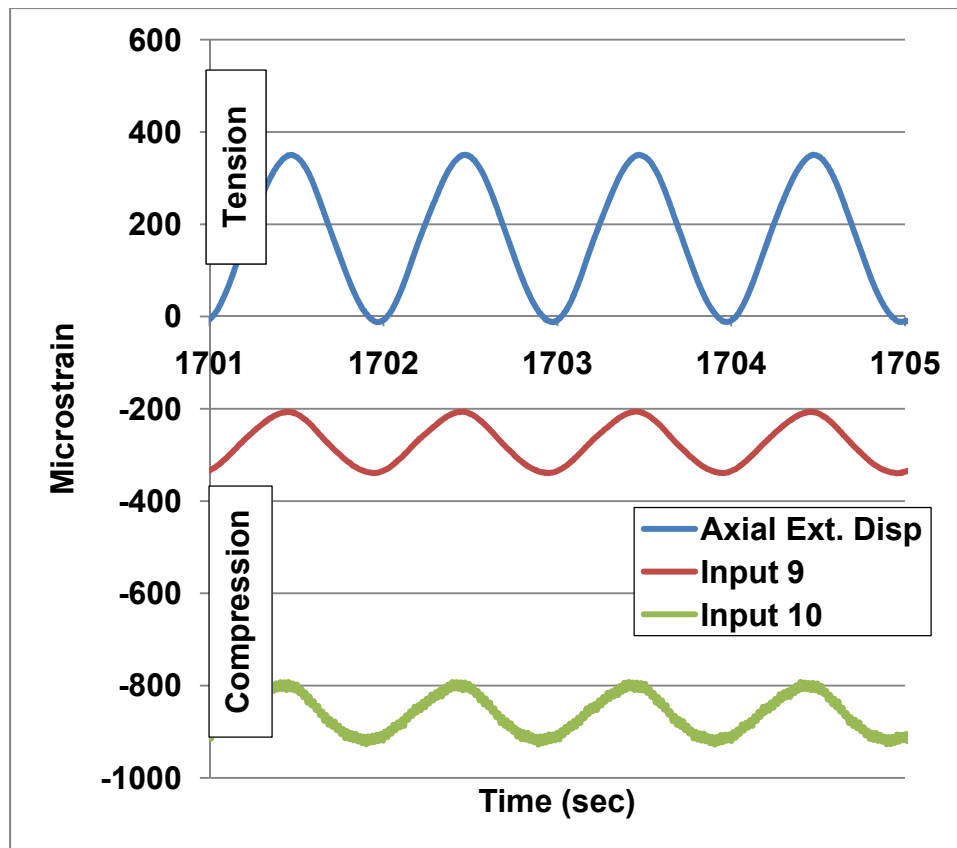
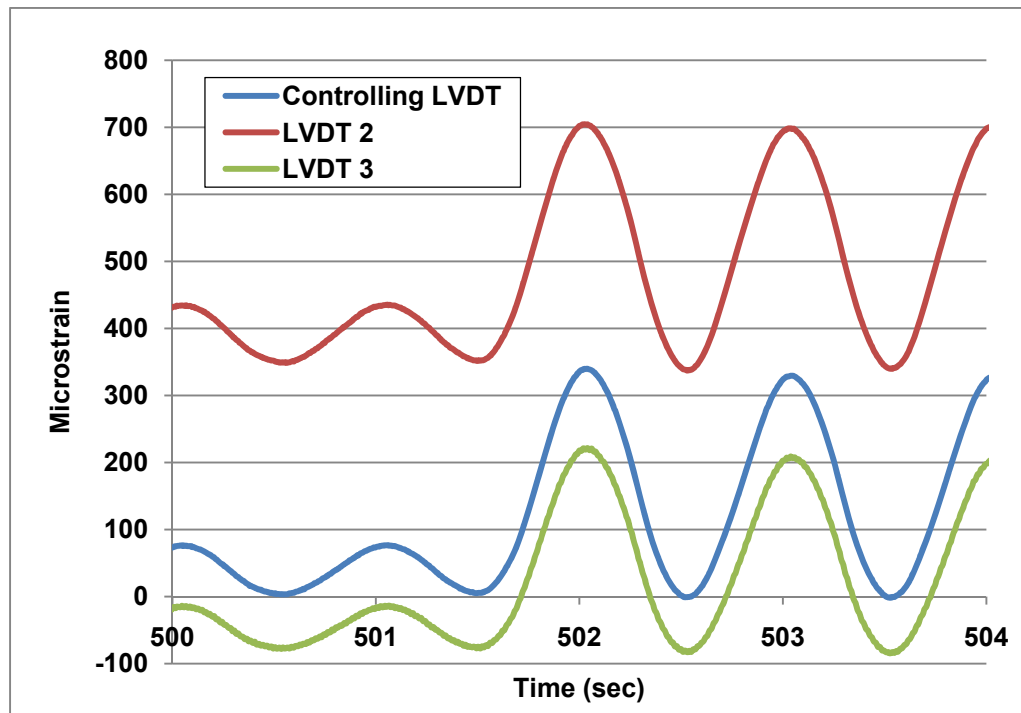


FIGURE 27. RDT\* Test Soft Side LVDT Placement and Results.

Perhaps the issue of greatest importance and impact has to do with the strain levels used during the test. The  $80 \mu\epsilon$  test is intended to be run in an undamaged state. However, because of the issue previously mentioned with respect to the LVDT placement on stiff versus soft sides of the sample, if the controlling LVDT experiences a maximum of  $80 \mu\epsilon$ , then the softer sides of the sample will likely experience a higher strain. If the strain is sufficient to cause damage, then the LVDT data will begin to drift. FIGURE 28 shows the end of the  $80 \mu\epsilon$  cycles and the beginning of the  $350 \mu\epsilon$  cycles. At the end of the  $80 \mu\epsilon$  cycles, the uncontrolled LVDT 2 readings are at strain levels



exceeding  $400 \mu\epsilon$  and are considerably higher than the controlling LVDT. This indicates that damage has already begun to occur and is rapidly progressing.



**FIGURE 28.** RDT\* Test Sample Damage During  $80 \mu\epsilon$  Cycles.

Another indication of damage during the  $80 \mu\epsilon$  cycles is reflected in the change in  $\phi$ . According to Luo et al. (20), when a viscoelastic material experiences loading in an undamaged condition,  $\phi_t$  and  $\phi_c$  should be statistically the same. TABLE 13 contains all of the two sided test statistics for each representative cycle for the  $80 \mu\epsilon$  RDT\* test performed on each sample. During the first cycle, only 50% of the tests fall within the range of significant evidence that the values of  $\phi_t$  and  $\phi_c$  are equal. Beyond this point the percentage of equivalency drops. This suggests two things. First, that the sample is

being damaged as the test proceeds through the 500 cycles of 80  $\mu\epsilon$ . It also suggests that some of the samples may have been damaged during the VEC test, which precedes the RDT\* Test. In the case of sample 7-4, the difference in strain between the controlling and non-controlling LVDT's was so great that the sample prematurely failed, splitting the sample in two.

**TABLE 13.** Two Sided t-Test Results for 80  $\mu\epsilon$  RDT\* Test.

Sample Number	Cycle									
	1st		50th		100th		250th		500th	
	t Stat	Equal ?	t Stat	Equal ?	t Stat	Equal ?	t Stat	Equal ?	t Stat	Equal ?
1-3	-3.84	N	-4.30	N	-9.95	N	-4.74	N	-3.75	N
1-4	-1.53	Y	-4.22	N	-3.34	N	-3.34	N	-4.55	N
2-3	-2.45	N	-1.54	Y	-2.27	N	-0.39	Y	-1.89	Y
2-4	-3.06	N	-4.74	N	-7.31	N	-7.06	N	-4.84	N
3-3	-0.10	Y	-3.34	N	-3.72	N	-1.72	Y	-2.70	N
3-4	-1.53	Y	-4.80	N	-1.75	Y	-1.92	Y	-1.64	Y
4-3	0.87	Y	6.72	N	6.05	N	2.54	N	3.98	N
4-4	-5.36	N	-2.43	N	-4.35	N	-0.63	Y	-0.62	Y
5-3	-0.39	Y	0.18	Y	4.97	N	4.79	N	0.54	Y
5-4	-3.13	N	-0.31	Y	-1.68	Y	-3.04	N	-1.73	Y
6-3	-3.14	N	-6.75	N	-6.17	N	-3.82	N	-6.05	N
6-4	-2.74	N	-4.43	N	-7.77	N	-8.41	N	-5.52	N
7-3	0.15	Y	-3.50	N	-1.80	Y	-1.40	Y	-2.66	N
7-4	-0.82	Y	N/A	N/A	N/A	N/A	N/A	N/A	N/A	N/A

Degrees of Freedom = 18     $\alpha = 0.05$

Sample Size n = 10

For two sided t-test, reject equivalency if  $|t| > t(0.025, 18) = 2.101$

If damage is occurring during the 80  $\mu\epsilon$  cycles, then the data obtained from this portion of the test is unreliable for further use. Also, if the damage and strain difference between controlling and non-controlling LVDT's can be so great as to destroy a sample, then it is reasonable to assume that when samples are tested at the 350  $\mu\epsilon$  level, the likelihood of total failure will be much greater.

The majority of the data collected did not provide the expected results due to the above mentioned issues. Changes must be made to the RDT\* testing procedure in order to ensure that accurate and reliable data is collected. Only by collecting accurate data can an accurate analysis be performed.

#### **RDT\* Test Recommendations**

In order to resolve the above mentioned issues, the following recommendations are made.

First, all LVDT's must be properly calibrated before testing and monitored regularly during the undamaged testing cycles. If LVDT's begin to exhibit fluctuations exceeding 5  $\mu\epsilon$  during the undamaged testing cycles, they should be immediately replaced, the sample allowed to rest, and the test be restarted. Once the damaged testing cycles begin, the test must run to completion. Damaged samples cannot be retested, so careful attention to the LVDT response during the undamaged stage is critical. A careful check of the LVDT's before beginning the test should also be made to ensure that they are not in contact with anything that will inhibit their movement.

Second, in order to ensure that the sample is being tested in tension, the controlling LVDT should be placed on the stiff side of the sample. This can be determined either during the undamaged RDT\* test cycles or from the VEC test results. It is preferential that the determination be made during the VEC test, so that the RDT\* test can run uninterrupted through all cycles. When the controlling LVDT is placed on the stiff side of the sample, the response of the non-controlling LVDT's should follow an upward trend during the damage cycles.

Finally, in order to prevent damage to the sample during the undamaged test cycles and to prevent total failure during the damaged cycles, it is recommended that the sample be tested at lower strain levels than those previously described. If the undamaged cycles are controlled at  $20 \mu\epsilon$  on the stiff side of the sample, it is less likely that the softer sides of the sample will go beyond  $80 \mu\epsilon$  and will, therefore, remain undamaged. During the damage cycles, reducing the strain level to  $175 \mu\epsilon$  on the controlling LVDT side will still provide data that represents a damaged sample, but will be less likely to extend the soft sides of the sample to total failure before the test is completed.

## **TEST METHOD ANALYSIS SUMMARY**

Preliminary results from the VEC and RDT\* tests indicate that the tests generally function as expected. However, only some of the data obtained could be successfully applied to the CMSE\* method of fatigue analysis. In order to ensure that the tests

provide good data, changes should be made according to the recommendation made above and listed in TABLE 14.

**TABLE 14.** VEC and RDT\* Test Issues and Recommendations.

<b>Test</b>	<b>Issue</b>	<b>Recommendation</b>
VEC	Noise in Data	Pre-test and change out bad LVDT's.
	Load is not Monotonically Increasing	Remove unwanted fixture displacement by tightening sample in testing fixture.
	Excessive Strain Response	Monitor LVDT on soft side of sample.
		Terminate test by using LVDT control.
	Short Testing Time	Lower loading rate to 0.004 in/min. (0.102 mm/min).
RDT*	Noise in Data	Pre-test and change out bad LVDT's.
	Sample Experiences Damage in Compression	Place controlling LVDT on stiff side of sample.
	Damage Sample During Non-Damage Cycles	Lower strain level from 80 $\mu\epsilon$ to 30 $\mu\epsilon$ .
	Total Sample Failure	Lower strain level from 350 $\mu\epsilon$ to 175 $\mu\epsilon$ .

## IMPLEMENTATION OF TEST RECOMMENDATIONS

A new sample was fabricated and tested using the testing recommendations listed in the previous section. The materials selected for the sample as well as the updated VEC and RDT\* results will be discussed in the following sections.

### MATERIAL SELECTION AND PREPARATION

The LMLC sample was fabricated based on a TxDOT Type D mix previously used in the Childress District for US Route 83. A TxDOT Type D mix is a dense graded HMA mix that follows the gradation shown in TABLE 15 and is used as a fine surface mix. The following sections describe the properties associated with this particular mix.

**TABLE 15.** TxDOT Type D Master Gradation Bands (% Passing by Weight or Volume) (21).

Sieve Size		Type D
#	mm	Fine Surface
3/4"	19.0	100.0
1/2"	12.5	98 - 100
3/8"	9.5	85 - 100
No. 4	4.75	50 - 70
No. 8	2.36	35 - 46
No. 30	0.600	15 - 29
No.50	0.300	7 - 20
No. 200	0.075	2 - 7

## Aggregate Gradation

Aggregates selected based on the Childress, US Route 83 mix design (CHS Mix) included a blend of three different aggregate gradations with the addition of lime as an antistripping agent. Three of the aggregates consist of granite from the Martin Marietta Quarry located in Snyder, Kiowa County, Oklahoma. They include course granite aggregate and crushed screenings passing the #4 (4.75 mm) sieve. The bin fractions and gradations of each blend are shown in TABLE 16. The 2% lime comes from Texas Lime in Cleburne, Texas.

**TABLE 16. CHS Mix Aggregate Gradation Blend.**

		Material 1		Material 2		Material 3				
Aggregate Source:		Snyder, OK		Snyder, OK		Snyder, OK				
Aggregate Quarry:		Martin Marietta		Martin Marietta		Martin Marietta				
Description:		Course Granite Aggregate		#4 Crushed Screenings		Crushed Screenings		Lime		Comb Total
Percent Used:		40	%	25	%	33	%	2	%	100
Sieve Size		Cum. % Pass	Wt. Cum. % Pass	Cum. % Pass	Wt. Cum. % Pass	Cum. % Pass	Wt. Cum. % Pass	Cum. % Pass	Wt. Cum. % Pass	Cum. % Pass
#	mm									
3/4"	19.0	100.0	40.0	100.0	25.0	100.0	33.0	100.0	2.0	100.0
1/2"	12.5	97.5	39.0	100.0	25.0	100.0	33.0	100.0	2.0	99.0
3/8"	9.5	71.5	28.6	100.0	25.0	100.0	33.0	100.0	2.0	88.6
# 4	4.75	12.9	5.2	96.8	24.2	95.6	31.5	100.0	2.0	62.9
# 8	2.36	4.6	1.8	73.1	18.3	62.6	20.7	100.0	2.0	42.8
# 30	0.600	2.0	0.8	35.5	8.9	20.0	6.6	100.0	2.0	18.3
# 50	0.300	1.4	0.6	23.0	5.8	9.5	3.1	100.0	2.0	11.4
# 200	0.075	0.7	0.3	9.9	2.5	2.2	0.7	100.0	2.0	5.5

Samples of the aggregates were blended, and a wet sieve analysis was performed. The final gradation was adjusted to account for any extra fines discovered during the wet-sieve analysis and is shown in TABLE 17.

**TABLE 17. CHS Mix Adjusted Aggregate Gradation Based on Wet-Sieve Analysis.**

Sieve Size		Cumulative % Passing	Specification Limits		Cumulative % Retained	Individual % Retained
#	mm		Low	High		
3/4"	19.0	100.0	100	100	0.0	0.0
1/2"	12.5	99.0	98	100	1.0	1.0
3/8"	9.5	88.6	85	100	11.4	10.4
No. 4	4.75	62.9	50	70	37.1	25.7
No. 8	2.36	42.9	35	46	57.1	20.1
No. 30	0.600	18.4	15	29	81.7	24.5
No.50	0.300	11.1	7	20	89.0	7.3
No. 200	0.075	5.2	2	7	94.9	5.9

### **Binder Type and Content**

A SemMaterials binder graded as PG 70-28 was selected based on the binder type used for US Route 83. This was done in order to mimic field conditions as closely as possible. An optimum asphalt content +0.5% equal to 5.8% was used based on the original design.

### **Mixing, Molding, Compaction, and Air Voids Content**

This sample was mixed, molded, and compacted as described in the previous section with respect to the mixing, molding, and compaction of the LRD LMLC samples. Samples were also cored and trimmed to the 4 inch (102 mm) diameter by 4

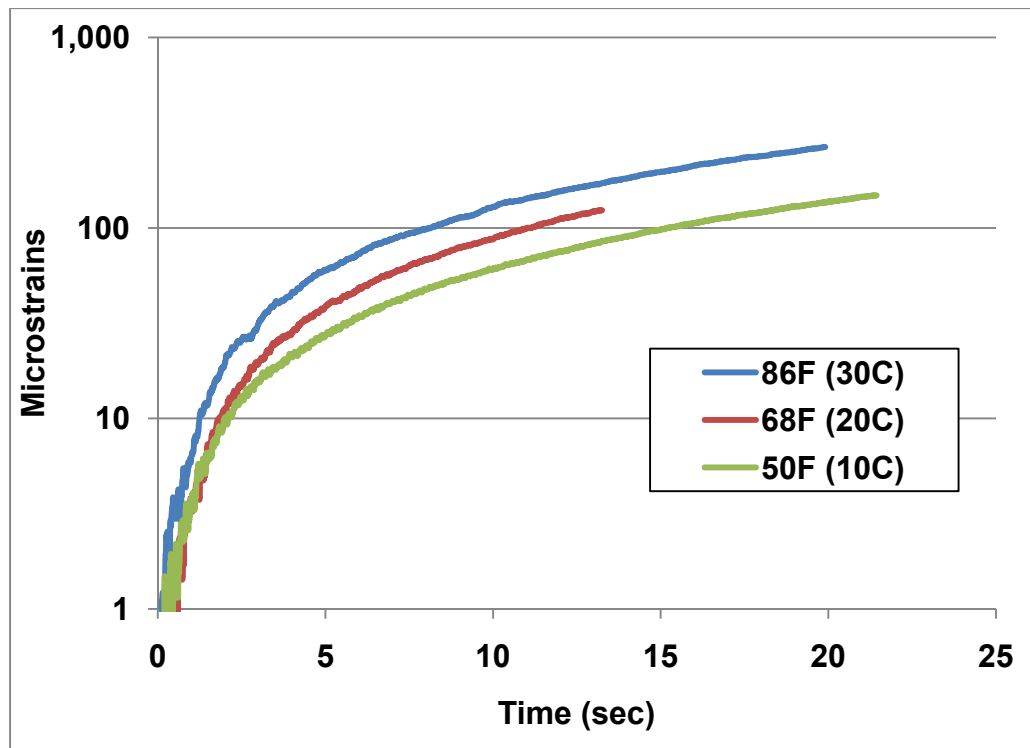


inch (102 mm) high sample size in order to provide more evenly distributed air voids. The air voids content for this particular sample was 7.7%.

### **IMPLEMENTATION OF VEC TEST RECOMMENDATIONS**

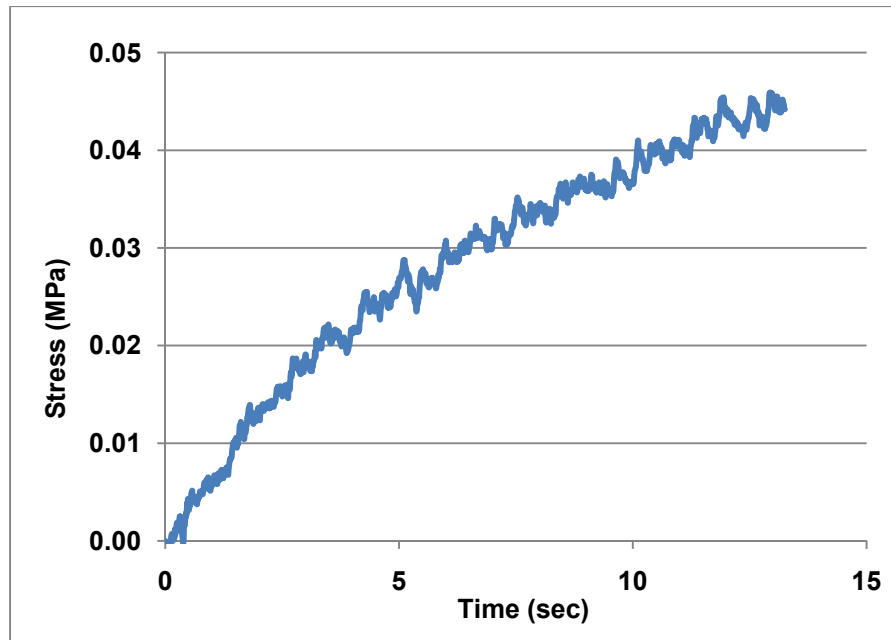
Some of the test recommendations discussed in the previous section were implemented while performing the VEC test for the CHS LMLC sample. All LVDT's were checked, and noisy LVDT's were replaced. The loading rate was changed from 0.01 inches per minute (0.254 mm/min) to 0.004 inches per minute (0.102 mm/min).

As can be seen in FIGURE 29, the reduced loading rate allowed more data to be collected at the 86°F (30°C) testing temperature. This provided more data from which a more accurate analysis could be performed. FIGURE 29 also shows that the reduced rate eliminated much of the preliminary noise that could be seen in previous tests. This may eliminate the need to truncate the data at the 5 second, 3 second, and 2 second points for the 50°F (10°C), 68°F (20°C), and 86°F (30°C) temperatures, respectively. It can also be seen from FIGURE 29 that the soft side LVDT identified from the 50°F (10°C) test was not used to stop the VEC test at the other test temperatures. This resulted in the average microstrains for 86°F (30°C) being considerably higher than the 100  $\mu\epsilon$  limit, which may have caused damage to the sample.



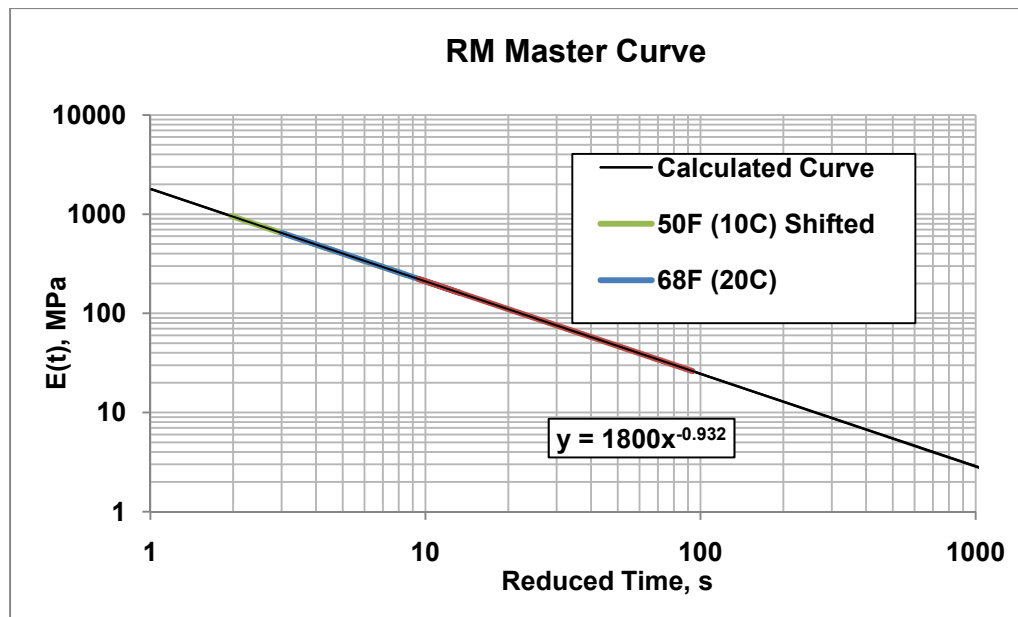
**FIGURE 29.** VEC Test Results with Implemented Recommendations.

While the applied stress shown in FIGURE 30 exhibits slightly more noise than that obtained from the previous test procedure, it still provides usable results and trends as expected.



**FIGURE 30.** Applied Stress from VEC Test with Implemented Recommendations.

Using the data from the CHS samples VEC test, a RM master curve was created and is show in FIGURE 31. The values of  $E_I$  and  $m$  for this sample were 261,068 psi (1800 MPa) and 0.932, respectively, which fall within the expected range for HMA.



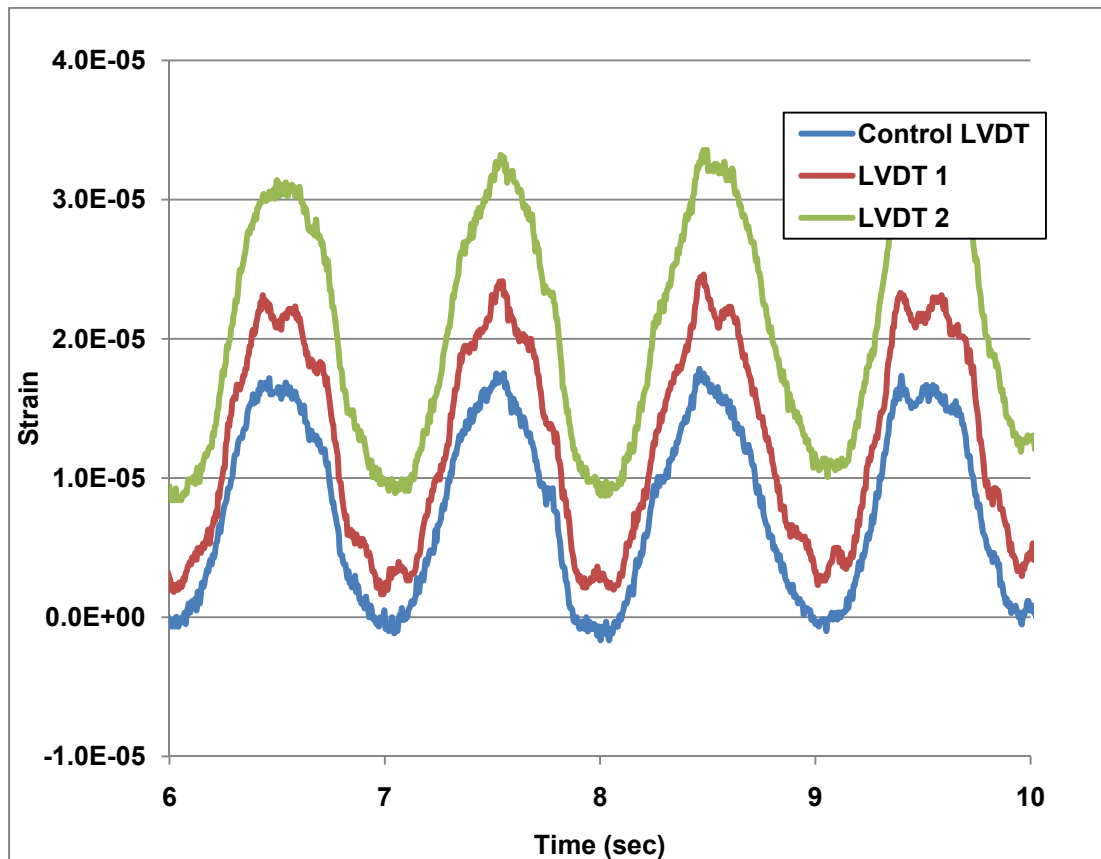
**FIGURE 31.** RM Master Curve from VEC Test with Implemented Recommendations.

### IMPLEMENTATION OF RDT\* TEST RECOMMENDATIONS

Some of the test recommendations discussed in the previous section were implemented while performing the RDT\* test for the CHS LMLC sample. All LVDT's were checked, and noisy LVDT's were replaced. Monitoring of the LVDT's took place during the undamaged cycles of the test to ensure that the test was proceeding as expected and the LVDT's were functioning properly. Strain levels for the undamaged and damaged cycles were reduced to  $20 \mu\epsilon$  and  $175 \mu\epsilon$ , respectively.

FIGURE 32 shows the strain response for the  $20 \mu\epsilon$ , undamaged cycles. The LVDT's exhibit a small amount of noise, which may be caused by the MTS machine attempting to control the testing at such a low strain level. There is a small upward trend in the data indicating that the sample is still experiencing or has experienced some

damage. This may be the result of the damage caused during the VEC test. However, the upward trend is only slight and strain levels remain relatively low.



**FIGURE 32.**  $20 \mu\epsilon$  Response from RDT\* Test with Implemented Recommendations.

A review of the average phase angles from each of the five representative cycles shows that the tensile and compressive phase angles are statistically the same with the exception of the 100<sup>th</sup> cycle, as indicated in TABLE 18. The 100<sup>th</sup> cycle just falls outside the limits for the two sided t-test. From this it can be assumed that the sample is

undamaged and that the slight upward trend is not significant enough to affect the results.

**TABLE 18.** Two Sided t-Test Results for the 20  $\mu\epsilon$  RDT\* Test.

Sample Number	Cycle									
	1st		50th		100th		250th		500th	
	t Stat	Equal ?	t Stat	Equal ?	t Stat	Equal ?	t Stat	Equal ?	t Stat	Equal ?
CHS	-0.71	Y	-0.37	Y	-2.14	N	0.17	Y	0.01	Y

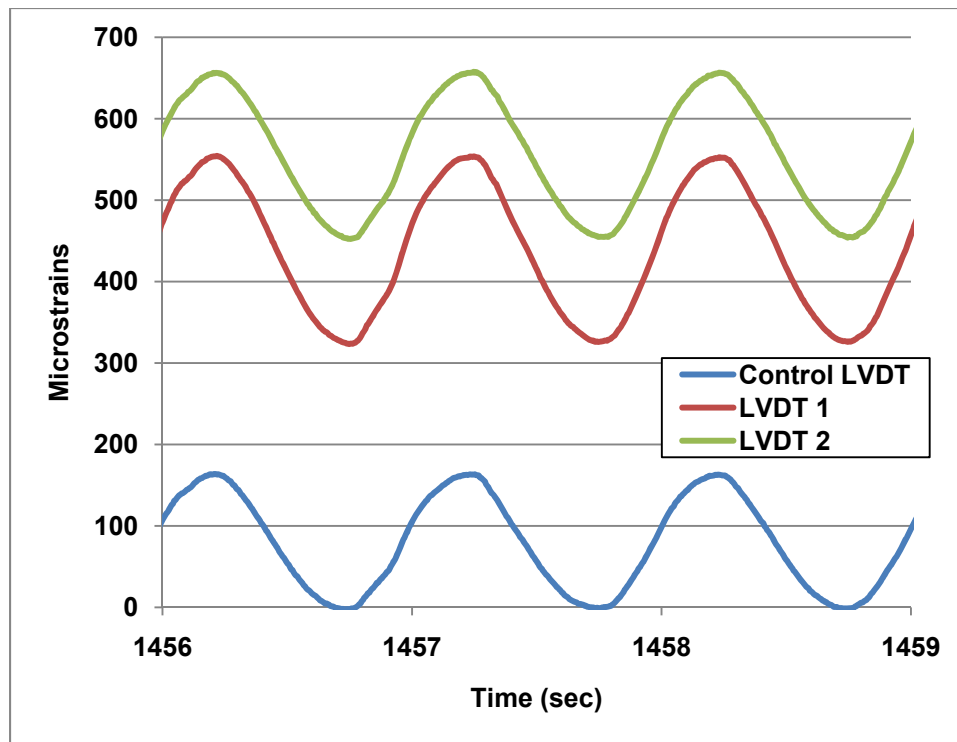
Degrees of Freedom = 18     $\alpha = 0.05$

Sample Size n = 10

For two sided t-test, reject equivalency if  $|t| > t(0.025, 18) = 2.101$

Another indication of the accuracy and reliability of both the RDT\* and VEC tests when the recommendations are applied is found in the fact that  $E_{VE}$  from the RDT\* test for the CHS sample is nearly the same as  $E_I$  from the VEC test.  $E_I$  and  $E_{VE}$  are both representative of the undamaged RM for the sample. As shown in the previous section,  $E_I$  from the VEC test was 261,068 psi (1800 MPa) and  $E_{VE}$ , as calculated from the results of the updated RDT\* test, was 258,321 psi (1781 MPa).

The results of the 175  $\mu\epsilon$  cycles also provided satisfactory results. Tensile data was obtained by ensuring that the controlling LVDT was placed on the stiffest side of the sample. With the controlling LVDT in the correct place, the response of the other two LVDT's followed the expected upward trend as shown in FIGURE 33. By setting the controlling LVDT strain limit to 175  $\mu\epsilon$ , the sample did not fail when the softer sides of the sample experienced much greater strains than the controlling side.



**FIGURE 33.** 175  $\mu\epsilon$  Response from RDT\* Test with Implemented Recommendations.

Because the damaged cycles of the test remained in tension, sufficient quality data was collected to be able to calculate  $W_{RI}$  for each cycle by using Equation 81. With  $W_{RI}$  from each cycle,  $b$  can be determined by applying Equation 84. For the CHS sample the value of  $b$  was found to be  $5.53 \times 10^{-3}$ , which is similar to those found in studies performed by Walubita (7) and Mercado (23).

### IMPLEMENTATION OF RECOMMENDATIONS SUMMARY

By applying the recommended changes to the VEC and RDT\* test which were listed in the previous section, a higher quality data set was obtained. The lower rate of testing for the VEC test allowed more data to be collected and also unexpectedly

smoothed out the strain response. The VEC test still needs to be run with either the testing equipment controlling the termination of the test or with the technician observing the soft side LVDT in order to stop the test at the appropriate strain level without causing damage.

The RDT\* test was greatly improved by applying the recommendations. The 20  $\mu\epsilon$  cycles provided data sufficient to calculate the undamaged properties of the HMA. However, there was some noise that may be able to be removed by slightly increasing the strain limit to 30  $\mu\epsilon$ . The 175  $\mu\epsilon$  cycles showed damage occurring in tension rather than in compression due to the application of the controlling LVDT on the stiff side of the sample. The sample experienced the required damage without being destroyed.

With the application of these changes, quality data can be collected which can be used to make the calculations required for the CMSE\* method.



## CONCLUSION

The CMSE method of design requires that the HMA material be tested using the Relaxation Modulus (RM) and Repeated Direct Tension (RDT) tests to determine the material properties required for accurate calculations. However, these tests exhibit some flaws that make the testing time consuming and the provide results which are highly variable (14, 20). Because of these issues, the RM and RDT tests were replaced by the VEC and RDT\* tests.

### VEC TEST

The VEC test has been developed by Luo and Lytton to replace the RM test (14). The VEC test provides the following benefits over the RM test.

- The VEC test takes approximately 20 seconds to run the test for each of the three testing temperatures of 50°F (10°C), 68°F (20°C), and 86°F (30°C) as compared to approximately 25 minutes of testing time for each of the three temperatures for the RM Test (7, 14).
- The VEC test can be run independent of any other tests, while the RM test requires the TS test to set the allowable strain levels (7, 14).
- The VEC test is relatively easy to control, while the RM test is difficult to run without causing damage (14).

While the VEC test is an improvement over the RM test, it still has some issues that require resolution. These issues were found during the testing of 14 LRD samples and are listed below.

- Noise was found in the output data, caused by bad LVDT's.
- The loading rate was much too quick for higher temperatures, causing insufficient data to be collected for proper analysis.
- The controlling LVDT was selected randomly, which allowed the sample to experience high levels of strain when selected on the stiff side of the sample. This may cause damage in the sample when tested.

The following recommendations were made and tested on one CHS sample in order to improve the VEC test.

- Check and monitor LVDT's during testing and replace bad LVDT's immediately.
- Change VEC loading rate from 0.01 inches per minute (0.254 mm/min) to 0.004 inches per minute (0.102 mm/min)
- Monitor the LVDT placed on the soft side of the sample for the 68°F (20°C) and 86°F (30°C) tests as determined during the 50°F (10°C) test.

Results of the VEC test that incorporated these changes provided more reliable data that followed expected trends without noise. Because of the change in loading rate, the test was able to run longer for the higher temperatures and provided more data for analysis. Application of the developed VEC macro to the new data provided fast and accurate development of the RM master curve for the CHS sample.

## **RDT\* TEST**

The RDT\* test, as developed by Luo et al. (20), replaced the original RDT test.

The RDT\* test provides the following benefits over the RDT test.

- The RDT\* test can be run independent of any other tests, while the RDT test requires the TS test to set the allowable strain levels (7, 2014).
- The RDT\* test removes the 0.9 second rest period from the RDT test which prevents unwanted healing from occurring (7, 20).
- Analysis of RDT\* data accounts for the short compressive phase of the test and separates compression and tension results, while the RDT test analysis assumes that the compressive and tensile phases are the same (7, 20).
- The RDT\* test includes a 500 cycle low strain test period for determining undamaged properties of the material (20).

While the RDT\* test is an improvement over the RDT test, it still has some issues that require resolution. These issues were found during the testing of 14 samples and are listed below.

- Noise was found in the output data, caused by bad LVDT's.
- The controlling strain levels of 80  $\mu\epsilon$  and 350  $\mu\epsilon$  proved to be too high for accurate testing. Damage was found during the 80  $\mu\epsilon$  test cycles which did not allow for accurate determination of undamaged properties. The cycles associated with the 350  $\mu\epsilon$  level could potentially cause premature failure of the sample.
- The controlling LVDT was selected randomly, which allowed the sample to experience overall compression when placed on the soft side of the sample. This

compressive damage did not allow for accurate determination of the tensile properties of the material.

The following recommendations were made and tested on one sample in order to improve the RDT\* test.

- Check and monitor LVDT's during the undamaged testing cycles and replace bad LVDT's immediately.
- Change RDT\* strain levels from 80  $\mu\epsilon$  and 350  $\mu\epsilon$  to 20  $\mu\epsilon$  and 175  $\mu\epsilon$  for undamaged and damaged cycles, respectively.
- Place the controlling LVDT on the stiff side of the sample as determined from the results of the VEC test.

Results from the RDT\* test that incorporated these changes provided accurate and usable data. The CHS sample did not experience significant damage during the 20  $\mu\epsilon$  cycles, and the 175  $\mu\epsilon$  cycles ran to completion without causing the sample to fail. Correct placement of the LVDT's resulted in accurate tensile data which was quickly and efficiently analyzed using the RDT\* macro to determine fracture DPSE and *b*.

Analysis of the undamaged, 20  $\mu\epsilon$  cycles using the RDT\* macro provided an undamaged modulus of 258,321 psi (1781 MPa). The corresponding modulus from the VEC test results was 261,068 psi (1800 MPa). These values are extremely close, as would be expected. This shows that both tests are reliable and provide accurate material characteristics which can be used in the CMSE\* equations.

## **FUTURE RESEARCH**

With the VEC and RDT\* test recommendations implemented, accurate tests can now be run to determine the material properties required for the CMSE\* analysis. However, these recommendations have only been applied to one sample. Further testing is required to establish a consistent record of accurate data collection.

Along with extending the data collection, the material properties determined from these tests should be inserted into the CMSE\* equations and compared with results obtained from the CMSE methodology. The equations described and listed in this thesis should be tested and applied to verify that all of the material properties required can be accurately determined from the test data obtained from the VEC and RDT\* tests.

## REFERENCES

1. Highway Statistics 2007. *Public Road Length – 2007 Miles by Type of Surface and Ownership/Functional System National System*. U.S. Department of Transportation. Federal Highway Administration. Table HM-12. October 2008. <http://www.fhwa.dot.gov/policyinformation/statistics/2007/hm12.cfm>
2. Highway Statistics 2007. *State Highway Agency Capital Outlay – 2007*. U.S. Department of Transportation. Federal Highway Administration. Table SF-12A. October 2008. <http://www.fhwa.dot.gov/policyinformation/statistics/2007/sf12a.cfm>
3. Roberts, F. L., P. S. Kadhal, E. R. Brown, D. Lee, and T. W. Kennedy. *Hot Mix Asphalt Materials, Mixture Design, and Construction, 2nd Edition*. National Asphalt Pavement Association Research and Education Foundation, Lanham, Maryland, 1996.
4. Huang, B., X. Shu, and Y. Tang. *Comparison of Semi-Circular Bending and Indirect Tensile Strength Tests for HMA Mixtures* Geo-Frontiers 2005, Austin, Texas, January 24–26, 2005, ASCE GSP-130.
5. Tayebali, A. A., J. A. Deacon, and C. L. Monismith. Development and Evaluation of Dynamic Flexural Beam Fatigue Test System. In *Transportation Research Record: Journal of the Transportation Research Board, No. 1545*, Transportation Research Board of the National Academies, Washington, D.C., 1996, pp. 89-97.

6. Matthews, J. M., C. L. Monismith, and J. Craus. Investigation of Laboratory Fatigue Testing Procedures for Asphalt Aggregate Mixtures. *Journal of Transportation Engineering*, Vol. 119, No. 4, 1993, pp. 634-654.
7. Walubita, L. F. Comparison of Fatigue Analysis Approaches for Prediction Fatigue Lives of Hot-Mix Asphalt Concrete (HMAC) Mixtures. Doctoral Dissertation. Texas A&M University, College Station, Texas, 2006.
8. Paris, P., and F. Erdogan. A Critical Analysis of Crack Propagation Laws. *Journal of Basic Engineering*, Vol. 85, 1963, pp. 528-534.
9. Schapery, R. A. Correspondence Principles and a Generalized J-integral for Large Deformation and Fracture Analysis of Viscoelastic Media. *International Journal of Fracture*, Vol. 25, 1984, pp. 195-223.
10. Si, Z. Characterization of Microdamage and Healing of Asphalt Concrete Mixtures. Doctoral Dissertation, Texas A&M University, College Station, Texas, 2001.
11. Cheng, D. Surface Free Energy of Asphalt-Aggregate System and Performance Analysis of Asphalt Concrete Based on Surface Energy. Doctoral Dissertation, Texas A&M University, College Station, Texas, 2002.
12. Marek, C. R., and M. Herrin. Tensile behavior and failure characteristics of asphalt cements in thin films. *Proceedings of the Association of Asphalt Paving Technologists*, AAPT, Atlanta, February 26-28, Vol. 37, 1968, pp. 386-421.

13. Lytton, R. L., Uzan, J., Fernando, E.G, Roque, R., Hiltunen, D., and Stoffels, S. *Development and validation of performance prediction models and specifications for asphalt binders and paving mixes*, Report SHRP-A-357, Strategic Highway Research Program, National Research Council, Washington, D.C., 1993.
14. Luo, R., R. L. Lytton, Characterization of the Tensile Viscoelastic Properties of an Undamaged Asphalt Mixture. *Journal of Transportation Engineering*, (7/3/2009), 10.1061/(ASCE)TE.1943-5436.0000083.
15. Cleveland, G. S., R. L. Lytton, and J. W. Button. Using pseudo-strain damage theory to characterize reinforcing benefits of geosynthetic materials in asphalt concrete overlays. In *Transportation Research Record: Journal of the Transportation Research Board, No. 1849*, Transportation Research Board of the National Academies, Washington D.C., 2003, pp. 202-211.
16. Findley, W. N., J. S. Lai, and K. Onaran. *Creep and Relaxation of Nonlinear Viscoelastic Materials with an Introduction to Linear Viscoelasticity*. Dover Publication, Inc., Mineola, New York, 1989.
17. Gross, B. *Mathematical Structure of the Theories of Viscoelasticity*. Hermann & Cie, Paris, 1953.
18. Williams, M. L., R. F. Landel, and J. D. Ferry. The Temperature Dependence of Relaxation Mechanisms in Amorphous Polymers and Other Glass-Forming Liquids. *Journal of the American Chemical Society*, Vol. 77, No. 14, 1955, pp. 3701 – 3707.



19. Bahia, H. U., D. I. Hanson, M. Zeng, H. Zhai, M. A. Khatri, and R. M. Anderson. *Characterization of Modified Asphalt Binders in Superpave Mix Design*, Report 459, National Cooperative Highway Research Program (NCHRP), Transportation Research Board, National Research Council, Washington, D.C., 2001.
20. Luo, X., A. Epps Martin, R. Luo, R. L. Lytton, C. J. Glover. *Aging Experiment Design Including Revised CMSE\* Testing Protocols and Analysis to Characterize Mixture Fatigue Resistance*. Publication FHWA-DTFH61-07H-0009, Federal Highway Administration, U.S. Department of Transportation, McLean, Virginia, 2008.
21. *Item 340 Dense-Graded Hot-Mix Asphalt (Method)*. Standard Specifications for Construction and Maintenance of Highways, Streets, and Bridges. Texas Department of Transportation, Austin, Texas, 2004, pp. 265 – 278.
22. Mercado, E. A. *Influence of Fundamental Material Properties and Air Void Structure on Moisture Damage of Asphalt Mixes*. Doctoral Dissertation. Texas A&M University, College Station, Texas, 2007.

## APPENDIX A

### VEC ANALYSIS MACRO CODE

#### Sub VEC\_Analysis()

```
Call Import
Call Variables
Call Transfer
Call EMasterCurve
Call PhaseMasterCurve
```

#### End Sub

#### Sub Import()

```
Dim i As Integer
Dim j As Integer
Dim k As Integer
Dim l As Integer
Dim temp As Integer
Dim s10cRaw As String
Dim s20cRaw As String
Dim s30cRaw As String
Dim main As String
Dim Raw10c As Workbook
Dim Raw20c As Workbook
Dim Raw30c As Workbook
```

```
For i = 1 To 3
```

```
    temp = i * 10
```

```
    Sheets("specimen " & temp & "deg").Range("A1:k1").EntireColumn.Clear 'Clears contents of first 11
columns for new input
```

```
Next i
```

```
main = ActiveWorkbook.Name
```

```
s10cRaw = InputBox("Enter the file path and name for 10 degree raw data.")
```

```
Workbooks.Open Filename:=s10cRaw 'Open 10deg raw data file
```

```
Workbooks("specimen").Sheets("specimen").Range("A1:K1").EntireColumn.Copy 'Copy raw data
```

```
Workbooks(main).Sheets("specimen 10deg").Range("a1").PasteSpecial 'Paste raw data in main
calculation file
```

```
Windows("specimen.xls").Activate 'Close raw data file
```

```
ActiveWindow.Close
```

```
Sheets("specimen 10deg").Activate 'Find last cell of raw data
```

```
    j = 14
```

```
    k = 14
```

```
    Do While Not IsEmpty(ActiveSheet.Rows(j).Cells(1))
```

```

    j = j + 1
Loop
LastRowRaw = j - 1
Do While Not IsEmpty(ActiveSheet.Rows(k).Cells(12))
    k = k + 1
Loop
LastRowCalc = k - 1                'set last row to equal second to last row
If LastRowRaw < LastRowCalc Then    'Clear calculation cells beyond last row
data row
    Range("L" & LastRowRaw + 1 & ":AG" & LastRowCalc).Clear

    ElseIf LastRowRaw > LastRowCalc Then    'Copy calculation cells to end of raw
data
    Range("L" & LastRowCalc & ":AG" & LastRowCalc).Copy
    Range("L" & LastRowCalc + 1 & ":I" & LastRowRaw).PasteSpecial

Else
End If

s20cRaw = InputBox("Enter the file path and name for 20 degree raw data.")
Workbooks.Open Filename:=s20cRaw
Workbooks("specimen").Sheets("specimen").Range("A1:K1").EntireColumn.Copy
Workbooks(main).Sheets("specimen 20deg").Range("a1").PasteSpecial
Windows("specimen.xls").Activate
ActiveWindow.Close
Sheets("specimen 20deg").Activate    'Find last cell of raw data
j = 14
k = 14
Do While Not IsEmpty(ActiveSheet.Rows(j).Cells(1))
    j = j + 1
Loop
LastRowRaw = j - 1
Do While Not IsEmpty(ActiveSheet.Rows(k).Cells(12))
    k = k + 1
Loop
LastRowCalc = k - 1                'set last row to equal second to last row
If LastRowRaw < LastRowCalc Then    'Clear calculation cells beyond last raw
data row
    Range("L" & LastRowRaw + 1 & ":AG" & LastRowCalc).Clear

    ElseIf LastRowRaw > LastRowCalc Then    'Copy calculation cells to end of raw
data
    Range("L" & LastRowCalc & ":AG" & LastRowCalc).Copy
    Range("L" & LastRowCalc + 1 & ":I" & LastRowRaw).PasteSpecial

Else
End If

s30cRaw = InputBox("Enter the file path and name for 30 degree raw data.")
Workbooks.Open Filename:=s30cRaw
Workbooks("specimen").Sheets("specimen").Range("A1:K1").EntireColumn.Copy
Workbooks(main).Sheets("specimen 30deg").Range("a1").PasteSpecial

```

```

Windows("specimen.xls").Activate
ActiveWindow.Close
Sheets("specimen 30deg").Activate           'Find last cell of raw data
  j = 14
  k = 14
  Do While Not IsEmpty(ActiveSheet.Rows(j).Cells(1))
    j = j + 1
  Loop
  LastRowRaw = j - 1
  Do While Not IsEmpty(ActiveSheet.Rows(k).Cells(12))
    k = k + 1
  Loop
  LastRowCalc = k - 1                       'set last row to equal second to last row
  If LastRowRaw < LastRowCalc Then          'Clear calculation cells beyond last row
data row
    Range("L" & LastRowRaw + 1 & ":AG" & LastRowCalc).Clear

  ElseIf LastRowRaw > LastRowCalc Then     'Copy calculation cells to end of raw
data
    Range("L" & LastRowCalc & ":AG" & LastRowCalc).Copy
    Range("L" & LastRowCalc + 1 & ":I" & LastRowRaw).PasteSpecial

  Else
  End If

End Sub

Sub Variables()

Dim t5sec As Integer
Dim tEnd As Integer

Application.DisplayAlerts = False

Sheets("specimen 10deg").Activate          'Run solver for 10 deg data

i = 14
j = 15

Do While Cells(i, 12) < 5                   'Find row for time = 5 seconds
  i = i + 1
  t5sec = i - 1
Loop

Do While Not IsEmpty(ActiveSheet.Rows(j).Cells(12)) 'Find last row of data
  j = j + 1
  tEnd = j - 1
Loop

Range("Y4").Select                         'Solve for a & b for strain
  ActiveCell.Formula = "=SUM(AF" & t5sec & ":AF" & tEnd & ")"
Range("Y5").Select

```

```
ActiveCell.FormulaR1C1 = "=PEARSON(R[" & t5sec - 5 & "]C[3]:R[" & tEnd - 5 & "]C[3],R[" &
t5sec - 5 & "]C[-1]:R[" & tEnd - 5 & "]C[-1])"
```

```
SolverOk SetCell:="$Y$4", MaxMinVal:=2, ValueOf:="0", ByChange:="$Y$2:$Y$3"
```

```
SolverSolve
```

```
Range("v4").Select 'Solve for a & b for stress
```

```
ActiveCell.Formula = "=SUM(AE" & t5sec & ":AE" & tEnd & ")"
```

```
Range("v5").Select
```

```
ActiveCell.FormulaR1C1 = "=PEARSON(R[" & t5sec - 5 & "]C[5]:R[" & tEnd - 5 & "]C[5],R[" &
t5sec - 5 & "]C[4]:R[" & tEnd - 5 & "]C[4])"
```

```
SolverOk SetCell:="$v$4", MaxMinVal:=2, ValueOf:="0", ByChange:="$v$2:$v$3"
```

```
SolverSolve
```

```
Range("ab4").Select 'Solve for a & b for radial strain
```

```
ActiveCell.Formula = "=SUM(AG" & t5sec & ":AG" & tEnd & ")"
```

```
Range("ab5").Select
```

```
ActiveCell.FormulaR1C1 = "=PEARSON(R[" & t5sec - 5 & "]C[-3]:R[" & tEnd - 5 & "]C[-3],R[" &
t5sec - 5 & "]C[1]:R[" & tEnd - 5 & "]C[1])"
```

```
SolverOk SetCell:="$ab$4", MaxMinVal:=2, ValueOf:="0", ByChange:="$ab$2:$ab$3"
```

```
SolverSolve
```

```
Sheets("specimen 20deg").Activate 'Run solver for 20 deg data
```

```
i = 14
```

```
j = 15
```

```
Do While Cells(i, 12) < 3 'Find row for time = 3 seconds
```

```
 i = i + 1
```

```
 t3sec = i - 1
```

```
Loop
```

```
Do While Not IsEmpty(ActiveSheet.Rows(j).Cells(12)) 'Find last row of data
```

```
 j = j + 1
```

```
 tEnd = j - 1
```

```
Loop
```

```
Range("Y4").Select 'Solve for a & b for strain
```

```
ActiveCell.Formula = "=SUM(AF" & t3sec & ":AF" & tEnd & ")"
```

```
Range("Y5").Select
```

```
ActiveCell.FormulaR1C1 = "=PEARSON(R[" & t3sec - 5 & "]C[3]:R[" & tEnd - 5 & "]C[3],R[" &
t3sec - 5 & "]C[-1]:R[" & tEnd - 5 & "]C[-1])"
```

```
SolverOk SetCell:="$Y$4", MaxMinVal:=2, ValueOf:="0", ByChange:="$Y$2:$Y$3"
```

```
SolverSolve
```

```
Range("v4").Select 'Solve for a & b for stress
```

```
ActiveCell.Formula = "=SUM(AE" & t3sec & ":AE" & tEnd & ")"
```

```
Range("v5").Select
```

```
ActiveCell.FormulaR1C1 = "=PEARSON(R[" & t3sec - 5 & "]C[5]:R[" & tEnd - 5 & "]C[5],R[" &
t3sec - 5 & "]C[4]:R[" & tEnd - 5 & "]C[4])"
```

```
SolverOk SetCell:="$v$4", MaxMinVal:=2, ValueOf:="0", ByChange:="$v$2:$v$3"
```

```
SolverSolve
```

```

Range("ab4").Select           'Solve for a & b for radial strain
    ActiveCell.Formula = "=SUM(AG" & t3sec & ":AG" & tEnd & ")"
Range("ab5").Select
    ActiveCell.FormulaR1C1 = "=PEARSON(R[" & t3sec - 5 & "]C[-3]:R[" & tEnd - 5 & "]C[-3],R[" &
t3sec - 5 & "]C[1]:R[" & tEnd - 5 & "]C[1])"
    SolverOk SetCell:="$ab$4", MaxMinVal:=2, ValueOf:="0", ByChange:="$ab$2:$ab$3"
    SolverSolve

Sheets("specimen 30deg").Activate           'Run solver for 30 deg data

i = 14
j = 15

Do While Cells(i, 12) < 2           'Find row for time = 2 seconds
    i = i + 1
    t2sec = i - 1
Loop

Do While Not IsEmpty(ActiveSheet.Rows(j).Cells(12))   'Find last row of data
    j = j + 1
    tEnd = j - 1
Loop

Range("Y4").Select           'Solve for a & b for strain
    ActiveCell.Formula = "=SUM(AF" & t2sec & ":AF" & tEnd & ")"
Range("Y5").Select
    ActiveCell.FormulaR1C1 = "=PEARSON(R[" & t2sec - 5 & "]C[3]:R[" & tEnd - 5 & "]C[3],R[" &
t2sec - 5 & "]C[-1]:R[" & tEnd - 5 & "]C[-1])"
    SolverOk SetCell:="$Y$4", MaxMinVal:=2, ValueOf:="0", ByChange:="$Y$2:$Y$3"
    SolverSolve

Range("v4").Select           'Solve for a & b for stress
    ActiveCell.Formula = "=SUM(AE" & t2sec & ":AE" & tEnd & ")"
Range("v5").Select
    ActiveCell.FormulaR1C1 = "=PEARSON(R[" & t2sec - 5 & "]C[5]:R[" & tEnd - 5 & "]C[5],R[" &
t2sec - 5 & "]C[4]:R[" & tEnd - 5 & "]C[4])"
    SolverOk SetCell:="$v$4", MaxMinVal:=2, ValueOf:="0", ByChange:="$v$2:$v$3"
    SolverSolve

Range("ab4").Select           'Solve for a & b for radial strain
    ActiveCell.Formula = "=SUM(AG" & t2sec & ":AG" & tEnd & ")"
Range("ab5").Select
    ActiveCell.FormulaR1C1 = "=PEARSON(R[" & t2sec - 5 & "]C[-3]:R[" & tEnd - 5 & "]C[-3],R[" &
t2sec - 5 & "]C[1]:R[" & tEnd - 5 & "]C[1])"
    SolverOk SetCell:="$ab$4", MaxMinVal:=2, ValueOf:="0", ByChange:="$ab$2:$ab$3"
    SolverSolve

```

```
Application.DisplayAlerts = True
```

**End Sub**

**Sub Transfer()**

Dim LastRowCalc As Integer

Dim LastRowRaw As Integer

Application.DisplayAlerts = False

'Copy zeroed time data for 10 degree data

Sheets("Calculations 10deg").Range("a1").EntireColumn.Clear

Sheets("specimen 10deg").Range("L1").EntireColumn.Copy

'Paste zeroed time data in corresponding calculation file

Sheets("Calculations 10deg").Range("a1").PasteSpecial Paste:=xlPasteValues, Operation:=xlNone,  
SkipBlanks \_

:=False, Transpose:=False

'Find last cell of calculations data

Sheets("Calculations 10deg").Activate

j = 14

k = 14

Do While Not IsEmpty(ActiveSheet.Rows(j).Cells(1))

j = j + 1

Loop

LastRowRaw = j - 1

Do While Not IsEmpty(ActiveSheet.Rows(k).Cells(2))

k = k + 1

Loop

LastRowCalc = k - 1

'set last row to equal second to last row

If LastRowRaw < LastRowCalc Then

'Clear calculation cells beyond last row

data row

Range("B" & LastRowRaw + 1 & ":" & LastRowCalc).Clear

ElseIf LastRowRaw > LastRowCalc Then

'Copy calculation cells to end of raw

data

Range("B" & LastRowCalc & ":" & LastRowCalc).Copy

Range("B" & LastRowCalc + 1 & ":" & LastRowRaw).PasteSpecial

Else

End If

'Copy zeroed time data for 20 degree data

Sheets("Calculations 20deg").Range("a1").EntireColumn.Clear

Sheets("specimen 20deg").Range("L1").EntireColumn.Copy

'Paste zeroed time data in corresponding calculation file

Sheets("Calculations 20deg").Range("a1").PasteSpecial Paste:=xlPasteValues, Operation:=xlNone,  
SkipBlanks \_

:=False, Transpose:=False

'Find last cell of calculations data

Sheets("Calculations 20deg").Activate

j = 14

```

k = 14
Do While Not IsEmpty(ActiveSheet.Rows(j).Cells(1))
  j = j + 1
Loop
LastRowRaw = j - 1
Do While Not IsEmpty(ActiveSheet.Rows(k).Cells(2))
  k = k + 1
Loop
LastRowCalc = k - 1                                'set last row to equal second to last row
If LastRowRaw < LastRowCalc Then                    'Clear calculation cells beyond last raw
data row
  Range("B" & LastRowRaw + 1 & ":O" & LastRowCalc).Clear

  ElseIf LastRowRaw > LastRowCalc Then              'Copy calculation cells to end of raw
data
  Range("B" & LastRowCalc & ":O" & LastRowCalc).Copy
  Range("B" & LastRowCalc + 1 & ":O" & LastRowRaw).PasteSpecial

  Else
  End If

'Copy zeroed time data for 30 degree data
Sheets("Calculations 30deg").Range("a1").EntireColumn.Clear
Sheets("specimen 30deg").Range("L1").EntireColumn.Copy

'Paste zeroed time data in corresponding calculation file
Sheets("Calculations 30deg").Range("a1").PasteSpecial Paste:=xlPasteValues, Operation:=xlNone,
SkipBlanks _
:=False, Transpose:=False

'Find last cell of calculations data
Sheets("Calculations 30deg").Activate
j = 14
k = 14
Do While Not IsEmpty(ActiveSheet.Rows(j).Cells(1))
  j = j + 1
Loop
LastRowRaw = j - 1
Do While Not IsEmpty(ActiveSheet.Rows(k).Cells(2))
  k = k + 1
Loop
LastRowCalc = k - 1                                'set last row to equal second to last row
If LastRowRaw < LastRowCalc Then                    'Clear calculation cells beyond last raw
data row
  Range("B" & LastRowRaw + 1 & ":O" & LastRowCalc).Clear

  ElseIf LastRowRaw > LastRowCalc Then              'Copy calculation cells to end of raw
data
  Range("B" & LastRowCalc & ":O" & LastRowCalc).Copy
  Range("B" & LastRowCalc + 1 & ":O" & LastRowRaw).PasteSpecial

  Else

```



```

    End If

Application.DisplayAlerts = True

End Sub

Sub EMasterCurve()

Dim LastRow As Integer

Application.DisplayAlerts = False

Sheets("E(t) Master Curve").Activate

j = 15
Do While Not IsEmpty(ActiveSheet.Rows(j).Cells(2))
    j = j + 1
Loop
LastRow = j - 1

Range("A15:C" & LastRow).Clear

'Transfer 10deg data to E(t) Master Curve Sheet
Sheets("Calculations 10deg").Activate

i = 14
Do While Cells(i, 1) < 5                'Find row for time = 5 seconds
    i = i + 1
    t5sec = i
Loop

j = 14
Do While Not IsEmpty(ActiveSheet.Rows(j).Cells(1))    'Find last row of data
    j = j + 1
    LastRow = j - 1
Loop

Range("A" & t5sec & ":B" & LastRow).Copy

Sheets("E(t) Master Curve").Activate
Range("b15").PasteSpecial Paste:=xlPasteValues, Operation:=xlNone, SkipBlanks_
:=False, Transpose:=False

Range("a15").Select
ActiveCell.FormulaR1C1 = "10deg"
LastRow10 = LastRow - t5sec + 15

'Transfer 20deg data to E(t) Master Curve Sheet
Sheets("Calculations 20deg").Activate

i = 14
Do While Cells(i, 1) < 3                'Find row for time = 3 seconds

```

```

    i = i + 1
    t3sec = i
Loop

j = 14
Do While Not IsEmpty(ActiveSheet.Rows(j).Cells(1))    'Find last row of data
    j = j + 1
    LastRow = j - 1
Loop

Range("A" & t3sec & ":B" & LastRow).Copy

Sheets("E(t) Master Curve").Activate
Range("b" & LastRow10 + 1).PasteSpecial Paste:=xlPasteValues, Operation:=xlNone, SkipBlanks _
:=False, Transpose:=False

Range("a" & LastRow10 + 1).Select
ActiveCell.FormulaR1C1 = "20deg"
LastRow20 = LastRow10 + LastRow - t3sec

'Transfer 30deg data to E(t) Master Curve Sheet
Sheets("Calculations 30deg").Activate

i = 14
Do While Cells(i, 1) < 2                                'Find row for time = 2 seconds
    i = i + 1
    t2sec = i
Loop

j = 14
Do While Not IsEmpty(ActiveSheet.Rows(j).Cells(1))    'Find last row of data
    j = j + 1
    LastRow = j - 1
Loop

Range("A" & t2sec & ":B" & LastRow).Copy

Sheets("E(t) Master Curve").Activate
Range("b" & LastRow20 + 1).PasteSpecial Paste:=xlPasteValues, Operation:=xlNone, SkipBlanks _
:=False, Transpose:=False

Range("a" & LastRow20 + 1).Select
ActiveCell.FormulaR1C1 = "30deg"
LastRow30 = LastRow20 + LastRow - t2sec + 1

'Extend and correct calculations
Range("d15:h15").Copy
Range("d16:h" & LastRow30).PasteSpecial

Range("F" & LastRow10 + 1).Select
ActiveCell.Formula = "=B" & LastRow10 + 1 & "/10^$B$8"

```

```

Range("f" & LastRow10 + 1).Copy
Range("f" & LastRow10 + 2 & ":f" & LastRow20).PasteSpecial

Range("F" & LastRow20 + 1).Select
ActiveCell.Formula = "=B" & LastRow20 + 1 & "/10^$B$9"
Range("f" & LastRow20 + 1).Copy
Range("f" & LastRow20 + 2 & ":f" & LastRow30).PasteSpecial

'Run Solver to determine E1 and m
Range("B11").Select
ActiveCell.Formula = "=sum(h15:h" & LastRow30 & ")"
SolverOk SetCell:="$B$11", MaxMinVal:=2, ValueOf:="0", ByChange:="$B$4,$B$5,$B$7,$B$9"
    SolverSolve

Application.DisplayAlerts = True

End Sub

Sub PhaseMasterCurve()

Dim LastRow As Integer

Application.DisplayAlerts = False

Sheets("Phase(t) Master Curve").Activate

j = 17
Do While Not IsEmpty(ActiveSheet.Rows(j).Cells(2))
    j = j + 1
Loop
LastRow = j - 1

Range("A17:C" & LastRow).Clear

'Transfer 10deg data to Phase(t) Master Curve Sheet
Sheets("Calculations 10deg").Activate

i = 14
Do While Cells(i, 1) < 5                'Find row for time = 5 seconds
    i = i + 1
    t5sec = i
Loop

j = 14
Do While Not IsEmpty(ActiveSheet.Rows(j).Cells(1))    'Find last row of data
    j = j + 1
    LastRow = j - 1
Loop

Range("C" & t5sec & ":C" & LastRow).Copy

Sheets("Phase(t) Master Curve").Activate

```

```

Range("b17").PasteSpecial Paste:=xlPasteValues, Operation:=xlNone, SkipBlanks _
:=False, Transpose:=False

Sheets("Calculations 10deg").Activate

Range("H" & t5sec & ":H" & LastRow).Copy

Sheets("Phase(t) Master Curve").Activate
Range("C17").PasteSpecial Paste:=xlPasteValues, Operation:=xlNone, SkipBlanks _
:=False, Transpose:=False

Range("a17").Select
ActiveCell.FormulaR1C1 = "10deg"
LastRow10 = LastRow - t5sec + 17

'Transfer 20deg data to E(t) Master Curve Sheet
Sheets("Calculations 20deg").Activate

i = 14
Do While Cells(i, 1) < 3           'Find row for time = 3 seconds
    i = i + 1
    t3sec = i
Loop

j = 14
Do While Not IsEmpty(ActiveSheet.Rows(j).Cells(1)) 'Find last row of data
    j = j + 1
    LastRow = j - 1
Loop

Range("C" & t3sec & ":C" & LastRow).Copy

Sheets("Phase(t) Master Curve").Activate
Range("b" & LastRow10 + 1).PasteSpecial Paste:=xlPasteValues, Operation:=xlNone, SkipBlanks _
:=False, Transpose:=False

Sheets("Calculations 20deg").Activate

Range("H" & t3sec & ":H" & LastRow).Copy

Sheets("Phase(t) Master Curve").Activate
Range("C" & LastRow10 + 1).PasteSpecial Paste:=xlPasteValues, Operation:=xlNone, SkipBlanks _
:=False, Transpose:=False

Range("a" & LastRow10 + 1).Select
ActiveCell.FormulaR1C1 = "20deg"
LastRow20 = LastRow10 + LastRow - t3sec

'Transfer 30deg data to E(t) Master Curve Sheet
Sheets("Calculations 30deg").Activate

i = 14

```

```

Do While Cells(i, 1) < 2          'Find row for time = 2 seconds
    i = i + 1
    t2sec = i
Loop

j = 14
Do While Not IsEmpty(ActiveSheet.Rows(j).Cells(1))    'Find last row of data
    j = j + 1
    LastRow = j - 1
Loop

Range("C" & t2sec & ":C" & LastRow).Copy

Sheets("Phase(t) Master Curve").Activate
Range("b" & LastRow20 + 1).PasteSpecial Paste:=xlPasteValues, Operation:=xlNone, SkipBlanks _
:=False, Transpose:=False

Sheets("Calculations 30deg").Activate

Range("H" & t2sec & ":H" & LastRow).Copy

Sheets("Phase(t) Master Curve").Activate
Range("C" & LastRow20 + 1).PasteSpecial Paste:=xlPasteValues, Operation:=xlNone, SkipBlanks _
:=False, Transpose:=False

Range("a" & LastRow20 + 1).Select
ActiveCell.FormulaR1C1 = "30deg"
LastRow30 = LastRow20 + LastRow - t2sec + 1

'Extend and correct calculations
Range("d17:i17").Copy
Range("d17:i" & LastRow30).PasteSpecial

Range("F" & LastRow10 + 1).Select
ActiveCell.Formula = "=B" & LastRow10 + 1 & "*10^$B$10"
Range("f" & LastRow10 + 1).Copy
Range("f" & LastRow10 + 2 & ":f" & LastRow20).PasteSpecial

Range("F" & LastRow20 + 1).Select
ActiveCell.Formula = "=B" & LastRow20 + 1 & "*10^$B$11"
Range("f" & LastRow20 + 1).Copy
Range("f" & LastRow20 + 2 & ":f" & LastRow30).PasteSpecial

'Run Solver to determine PhaseMax, OmegaMax, Rphase, m, C1, and C2
Range("B13").Select
ActiveCell.Formula = "=sum(h17:h" & LastRow30 & ")"
SolverOk SetCell:="$B$13", MaxMinVal:=2, ValueOf:="0", ByChange:="$B$2,$B$3,$B$5,$B$6$,
B$7,$B$8"
    SolverSolve

```

Application.DisplayAlerts = True

**End Sub**

### **350 $\mu\epsilon$ RDT\* ANALYSIS MACRO CODE**

**Sub RDTAnalysis()**

Call Import  
Call Transfer  
Call CopyAve  
Call Analysis

**End Sub**

**Sub Import()**

Dim i As Integer  
Dim j As Long  
Dim k As Long  
Dim l As Long  
Dim sRDTRaw As String  
Dim main As String  
Dim Raw10c As Workbook

Workbooks("RDT_Worksheet_350microstrain.xls").Activate Sheets("1th Raw Data").Range("A1:k1").EntireColumn.Clear columns for new input	'Clears contents of first 11
Sheets("50th Raw Data").Range("A1:k1").EntireColumn.Clear columns for new input	'Clears contents of first 11
Sheets("100th Raw Data").Range("A1:k1").EntireColumn.Clear columns for new input	'Clears contents of first 11
Sheets("250th Raw Data").Range("A1:k1").EntireColumn.Clear columns for new input	'Clears contents of first 11
Sheets("500th Raw Data").Range("A1:k1").EntireColumn.Clear columns for new input	'Clears contents of first 11
Sheets("750th Raw Data").Range("A1:k1").EntireColumn.Clear columns for new input	'Clears contents of first 11
Sheets("1000th Raw Data").Range("A1:k1").EntireColumn.Clear columns for new input	'Clears contents of first 11

'Copy raw data from original file into RDT\_Worksheet file while separating data into  
'respective worksheets corresponding to 1st, 50th, 100th, 250th, and 500th cycles.

main = ActiveWorkbook.Name

```

sRDTRaw = InputBox("Enter the file path for RDT raw data.")
Workbooks.Open Filename:=sRDTRaw & "\specimen.xlsx"
For i = 1 To 7
  If i = 1 Then
    j = 1002
    k = 1033
    num = 1
  ElseIf i = 2 Then
    j = 1100
    k = 1131
    num = 50
  ElseIf i = 3 Then
    j = 1200
    k = 1231
    num = 100
  ElseIf i = 4 Then
    j = 1500
    k = 1531
    num = 250
  ElseIf i = 5 Then
    j = 2000
    k = 2031
    num = 500
  ElseIf i = 6 Then
    j = 2500
    k = 2531
    num = 750
  ElseIf i = 7 Then
    j = 2970
    k = 3000
    num = 1000
  End If

  l = 13
  Workbooks("specimen.xlsx").Activate

  Do While Cells(l, 8) < j
    l = l + 1
  Loop
  FirstRow = l
  l = 13
  Do While Cells(l, 8) < k
    l = l + 1
  Loop
  LastRow = l - 1
  Range("A1:K12").Copy
  Workbooks("RDT_Worksheet_350microstrain.xls").Activate
  Sheets(num & "th Raw Data").Range("A1").PasteSpecial
  Workbooks("specimen.xlsx").Activate
  Sheets("specimen").Range("A" & FirstRow & ":H" & LastRow).Copy
  Workbooks("RDT_Worksheet_350microstrain.xls").Sheets(num & "th Raw
Data").Range("A13").PasteSpecial

```

```

Workbooks("RDT_Worksheet_350microstrain.xls").Sheets(num & "th Raw Data").Activate
'Find last cell of raw data
j = 13
k = 13
Do While Not IsEmpty(ActiveSheet.Rows(j).Cells(1))
    j = j + 1
Loop
LastRowRaw = j - 1
Do While Not IsEmpty(ActiveSheet.Rows(k).Cells(12))
    k = k + 1
Loop
LastRowCalc = k - 1                                'set last row to equal second to last row
If LastRowRaw < LastRowCalc Then                    'Clear calculation cells beyond last raw
data row
    Range("L" & LastRowRaw + 1 & ":T" & LastRowCalc).Clear

    ElseIf LastRowRaw > LastRowCalc Then            'Copy calculation cells to end of raw
data
    Range("L" & LastRowCalc & ":T" & LastRowCalc).Copy
    Range("L" & LastRowCalc + 1 & ":I" & LastRowRaw).PasteSpecial

Else
End If
Next i

Workbooks("specimen.xlsx").Close

```

**End Sub**

**Sub Transfer()**

```

Dim l As Long
Dim x As Double
Dim y As Double
Dim FirstRowNeg As Long
Dim LastRowPos As Long

'Copy 10 cycles from raw data sheets to calculation sheet beginning with the
'first full compression (negative) cycle.
For i = 1 To 7
    If i = 1 Then
        num = 1
    ElseIf i = 2 Then
        num = 50
    ElseIf i = 3 Then
        num = 100
    ElseIf i = 4 Then
        num = 250
    ElseIf i = 5 Then
        num = 500
    ElseIf i = 6 Then

```



```

    num = 750
  ElseIf i = 7 Then
    num = 1000
  End If

  Sheets(num & "th").Activate
  l = 3
  Do While Not Cells(l, 1) = ""
    l = l + 1
  Loop
  Range("A3:C" & l).Clear

  Sheets(num & "th Raw Data").Activate

  l = 13
  x = Cells(l, 17).Value
  y = Cells(l + 1, 17).Value

  Do While Not (x > 0 And y < 0)      'Find row corresponding to beginning of first cycle
    l = l + 1
    x = Cells(l, 17).Value
    y = Cells(l + 1, 17).Value
  Loop
  FirstRowNeg = l + 1
  For q = 1 To 11                    'Find row corresponding to end of 11th cycle
    l = l + 1
    x = Cells(l, 17).Value
    y = Cells(l + 1, 17).Value
    Do While Not (x > 0 And y < 0)
      l = l + 1
      x = Cells(l, 17).Value
      y = Cells(l + 1, 17).Value
    Loop
  Next q
  LastRowPos = l

  'Copy 11 cycles of time to calculation sheets
  Sheets(num & "th Raw Data").Range("L" & FirstRowNeg & ":L" & LastRowPos).Copy
  Sheets(num & "th").Activate
  Sheets(num & "th").Range("A3").PasteSpecial Paste:=xlPasteValues, Operation:=xlNone, SkipBlanks _
    :=False, Transpose:=False

  'Copy 11 cycles of stress and strain to calculation sheets
  Sheets(num & "th Raw Data").Activate
  Sheets(num & "th Raw Data").Range("P" & FirstRowNeg & ":Q" & LastRowPos).Copy
  Sheets(num & "th").Activate
  Sheets(num & "th").Range("B3").PasteSpecial Paste:=xlPasteValues, Operation:=xlNone, SkipBlanks _
    :=False, Transpose:=False

Next i      'Repeat process for each of the cycle ranges

```

**End Sub**

**Sub Analysis()**

```
Dim sheet As Worksheet
Set sheet = ThisWorkbook.ActiveSheet
```

```
Dim change As Double
Dim maxstress As Double
Dim minstress As Double
Dim onestress As Double
Dim zerostres As Double
Dim maxstrain As Double
Dim minstrain As Double
Dim tmaxstres As Double
Dim tminstres As Double
Dim tmaxstrai As Double
Dim tminstrai As Double
Dim tonestres As Double
Dim tzerostre As Double
```

```
For i = 1 To 7
```

```
  If i = 1 Then
```

```
    num = 1
```

```
  ElseIf i = 2 Then
```

```
    num = 50
```

```
  ElseIf i = 3 Then
```

```
    num = 100
```

```
  ElseIf i = 4 Then
```

```
    num = 250
```

```
  ElseIf i = 5 Then
```

```
    num = 500
```

```
  ElseIf i = 6 Then
```

```
    num = 750
```

```
  ElseIf i = 7 Then
```

```
    num = 1000
```

```
  End If
```

```
  Sheets(num & "th").Activate
```

```
  Set sheet = ThisWorkbook.ActiveSheet
```

```
  l = 2
```

```
  For j = 1 To 10 'cycle from 1 to 10
```

```
    l = l + 1
```

```
    maxstress = sheet.Cells(l, 3).Value 'maximum compressive stress
```

```
    minstress = sheet.Cells(l, 3).Value 'maximum tensile stress
```

```
    maxstrain = sheet.Cells(l, 2).Value 'maximum strain
```

```
    minstrain = sheet.Cells(l, 2).Value 'minimum strain
```

```
    zerostress = sheet.Cells(l, 3).Value 'point of stress just before zero (mid-cycle)
```

```
    onestress = sheet.Cells(l, 3).Value 'point of stress just after zero (mid-cycle)
```

```
    timestart = sheet.Cells(l, 1).Value 'time at start of cycle
```

```
    x = Cells(l, 3).Value
```

```
y = Cells(l + 1, 3).Value
```

```
Do While Not (x > 0 And y < 0)
```

```
  If maxstress <= sheet.Cells(l + 1, 3).Value Then
    maxstress = sheet.Cells(l + 1, 3).Value
    tmaxstres = Cells(l + 1, 1).Value
  End If
```

```
  If minstress >= sheet.Cells(l + 1, 3).Value Then
    minstress = sheet.Cells(l + 1, 3).Value
    tminstres = sheet.Cells(l + 1, 1).Value
  End If
```

```
  If maxstrain <= sheet.Cells(l + 1, 2).Value Then
    maxstrain = sheet.Cells(l + 1, 2).Value
    tmaxstrai = sheet.Cells(l + 1, 1).Value
  End If
```

```
  If minstrain >= sheet.Cells(l + 1, 2).Value Then
    minstrain = sheet.Cells(l + 1, 2).Value
    tminstrai = sheet.Cells(l + 1, 1).Value
  End If
```

```
  If x < 0 And y > 0 Then
    zerostres = sheet.Cells(l, 3).Value
    tzerostre = sheet.Cells(l, 1).Value
    onestress = sheet.Cells(l + 1, 3).Value
    tonestres = sheet.Cells(l + 1, 1).Value
  End If
```

```
  l = l + 1
  x = sheet.Cells(l, 3).Value
  y = sheet.Cells(l + 1, 3).Value
```

```
Loop
```

```
timeend = sheet.Cells(l, 1) 'time at end of cycle
```

```
sheet.Cells(j + 2, 5) = maxstress 'maximum tension stress
sheet.Cells(j + 2, 6) = tmaxstres ' time corresponding to maximum tension stress
sheet.Cells(j + 2, 7) = minstress * (-1) 'maximum compressive stress
sheet.Cells(j + 2, 8) = tminstres 'time corresponding to maximum compressive stress
sheet.Cells(j + 13, 5) = maxstrain 'maximum tension strain
sheet.Cells(j + 13, 6) = tmaxstrai ' time corresponding to maximum tension strain
sheet.Cells(j + 13, 7) = minstrain * (-1) 'maximum compressive strain
sheet.Cells(j + 13, 8) = tminstrai 'time corresponding to maximum compressive strain
sheet.Cells(j + 2, 9) = zerostres
sheet.Cells(j + 2, 10) = tzerostre 'time corresponding to end of tension stress
sheet.Cells(j + 2, 11) = onestress
sheet.Cells(j + 2, 12) = tonestres 'time corresponding to begin of compressive stress
sheet.Cells(j + 2, 18) = (tonestres - timestart) 'computing Tc
sheet.Cells(j + 2, 16) = (timeend - tonestres) 'computing Tt
```

```
Next j
```

```

sheet.Range("A1:C1").EntireColumn.Copy
sheet.Range("AD1").PasteSpecial
Next i

```

```

Sheets("DPSE Chart").Activate
SolverOk SetCell:="$F$14", MaxMinVal:=2, ValueOf:="0", ByChange:="$C$2,$C$3"
SolverSolve

```

**End Sub**

**Sub CopyAve()**

'Copy averages from 80 microstrain file to 350 microstrain file

```

s80micro = InputBox("Enter the file path for RDT_Worksheet_80microstrain.xls")
Workbooks.Open Filename:=s80micro & "\RDT_Worksheet_80microstrain.xls"
Sheets("Averages").Select
Range("C8").Select
Selection.Copy
Windows("RDT_Worksheet_350microstrain.xls").Activate
Sheets("1th").Select
Range("P14").Select
Selection.PasteSpecial Paste:=xlPasteValues, Operation:=xlNone, SkipBlanks _
:=False, Transpose:=False

```

```

Windows("RDT_Worksheet_80microstrain.xls").Activate
Range("D8").Select
Application.CutCopyMode = False
Selection.Copy
Windows("RDT_Worksheet_350microstrain.xls").Activate
Range("P15").Select
Selection.PasteSpecial Paste:=xlPasteValues, Operation:=xlNone, SkipBlanks _
:=False, Transpose:=False

```

```

Windows("RDT_Worksheet_80microstrain.xls").Activate
Range("E8").Select
Application.CutCopyMode = False
Selection.Copy
Windows("RDT_Worksheet_350microstrain.xls").Activate
Range("R14").Select
Selection.PasteSpecial Paste:=xlPasteValues, Operation:=xlNone, SkipBlanks _
:=False, Transpose:=False

```

```

Windows("RDT_Worksheet_80microstrain.xls").Activate
Range("F8").Select
Application.CutCopyMode = False
Selection.Copy
Windows("RDT_Worksheet_350microstrain.xls").Activate
Range("R15").Select
Selection.PasteSpecial Paste:=xlPasteValues, Operation:=xlNone, SkipBlanks _
:=False, Transpose:=False

```

```
Windows("RDT_Worksheet_80microstrain.xls").Close
```

```
End Sub
```

## VITA

James Jefferies Lawrence received his B.S. degree in civil engineering from Utah State University in 1999. Following graduation, he worked for the Utah Department of Transportation (UDOT) for six years where he gained experience in materials, maintenance, construction, and roadway design. The majority of his time with UDOT was spent in roadway design where he worked on several projects including Redwood Road and 700 East in Salt Lake City, UT and SR-36 in Tooele County, UT. While employed with UDOT, James obtained his Professional Civil Engineer license in the State of Utah.

James left UDOT in 2005 to take a position in Tooele County, UT as the Tooele County Engineer. As the County Engineer, James was responsible for the Roads, Planning and Zoning, Building Inspection, Trails, and GIS Divisions. In December of 2007, James left Tooele County to pursue his M.S. and Ph.D. degrees from Texas A&M University in College Station, TX. He graduated with his M.S. degree in civil engineering from Texas A&M in December 2009. His research interest is in hot mix asphalt pavement materials with emphasis in fatigue, aging, and X-ray CT material analysis.

James can be reached at: Texas A&M University, Texas Transportation Institute, Materials and Pavement Division, 3135 TAMU (501J, CE/TTI Building), College Station, TX 77843-3135. His e-mail address is: [j-lawrence@ttimail.tamu.edu](mailto:j-lawrence@ttimail.tamu.edu).